Mechanisms of recognition of HIV-infected cells by CD8+ T cells that mediate effective antiviral responses

Mechanisms of recognition of HIV-infected cells by $CD8^+$ T cells that mediate effective antiviral responses

A dissertation presented

by

Pedro Alberto Lamothe Molina

to

The Committee on Higher Degrees in Biological Sciences in Public Health

in partial fulfillment of the requirements

for the degree of

Doctor of Philosophy

in the subject of

Biological Sciences in Public Health

Harvard University

Cambridge, Massachusetts

May, 2017

Advisor: Professor Bruce D. Walker Pedro Alberto Lamothe Molina

Mechanisms of recognition of HIV-infected cells by CD8$^+$ T cells that mediate effective antiviral responses

ABSTRACT

CD8$^+$ T cells are a major defense against viruses by killing infected cells, and unraveling the molecular mechanisms involved in their control of HIV-1 infection is thus a topic of paramount importance for developing therapeutic strategies. Conventional CD8$^+$ T cells recognize infected cells by T cell receptor (TCR) engagement of cognate viral peptides presented on human leukocyte antigen (HLA) class I molecules. Control of HIV-1 infection is associated with "protective" HLA alleles but the causality behind this association is not completely understood. Protective HLA molecules often present conserved viral epitopes, suggesting that specificity is an important mechanism for this protection, but there is also evidence that CD8$^+$ T cells, restricted by protective alleles, respond with higher functionality. To investigate peptide-independent effects of HLA, we examined recognition of the Gag peptide QASQEVKNW (QW9) that is presented by the protective HLA-B*57:01 and the non-protective HLA-B*53:01 molecules. We found that CD8$^+$ T cell responses from HIV-infected persons recognizing QW9 differ functionally but not quantitatively in the context of these two disparate restricting HLA molecules. Using x-ray crystallography and molecular dynamics simulation, we structurally identified an unusual mode of distinctive QW9 peptide presentation by the two HLA molecules. The unique observation is that the central peptide residue K7 can assume either a buried conformation in the peptide-binding groove or an exposed one. These data give insight on the role that protective HLA alleles play in HIV control.

The lack of effective HIV control by conventional CD8$^+$ T cells in most infected persons led us to investigate whether there are alternative ways to mobilize CD8$^+$ T cells to recognize and kill virus-

infected cells, which could potentially be utilized in translational medical applications. Although $CD8^+$ T cell recognition of virus-infected cells is characteristically restricted by HLA class I, we demonstrated the presence of HLA class II-restricted $CD8^+$ T cell responses with antiviral properties in a small subset of HIV-infected individuals. In these cases, class II-restricted $CD8^+$ T cells underwent clonal expansion and mediated killing of HIV-infected cells. In one instance, these cells comprised 12% of circulating $CD8^+$ T cells, and exhibited two distinct co-expressed TCRα chains, with only one contributing to binding of the class II HLA-peptide complex. These data indicate that class II-restricted $CD8^+$ T cell responses can exist in a chronic human viral infection, and may contribute to immune control.

Finally, we explored an HLA-independent mode of $CD8^+$ T cell recognition using chimeric antigen receptors (CARs). CARs are synthetic proteins expressed on genetically-modified T cells (CAR T cells) to redirect their specificity to a desired antigen. Unlike TCRs that bind viral peptides presented on HLA, we designed HIV-specific CARs to detect viral Env antigens expressed on the surface of infected cells. Previous attempts to use CAR T cells against HIV relied on CD4 as the chimeric receptor, but this rendered cells expressing them susceptible to HIV infection. Basing CAR construct design on anti-HIV broadly neutralizing antibodies (bNAbs), we generated CAR T cells capable of binding to multiple strains of HIV Env and showing HIV-specific activation. We proved that, unlike other designs based on the CD4 molecule, bNAb-based CARs do not induce infectability of the CAR T cells. We conclude that using bNAbs as the basis for the design of anti-HIV CARs is a promising approach allowing for HIV-specific recognition of multiple strains without increasing susceptibility to infection. This approach, having an HLA-independent mode of recognition, makes a potential therapeutic application more broadly applicable.

Together these studies provide additional perspectives on immune control of HIV infection, and have implications for preventive vaccines, immunotherapy and cure strategies.

TABLE OF CONTENTS

DEDICATION

I dedicate this dissertation to my father, Dr. Pedro Lamothe-Cervera to whom I owe everything I am today and to my wife, life partner, best friend, and soul mate Daniela Hernandez-Sariñana.

ACKNOWLEDGEMENTS

The journey as a graduate student has definitely not been an easy one, having had many overwhelming and even frustrating moments. Nevertheless, my time at Harvard University has overall been an incredible experience and some of the best years of my life.

Doing a Ph.D. is about contributing to science and this dissertation presents the work I have done as a graduate student. But, doing a Ph.D. is also about learning and I think I have come a long way. When started the program almost five years ago, I had very little lab experience and I could not have gotten to this point without the immeasurable help from many great people I have been fortunate to interact with along the way.

It has been a great honor for me to work under Professor Bruce Walker's supervision as my Dissertation Advisor. I have learned an inconceivable amount from him, directly through his leadership but also indirectly. He has become one of the most important role models and he has taught me what I should aim to achieve. Professor Walker continuously encourages collaboration; he has a natural ability to bring people to efficiently work together fomenting diversity and inclusion in his laboratory. This has allowed me to learn from other lab members and has given me the opportunity to contribute to several projects. Working in the Walker laboratory has been vastly gratifying by learning how to apply basic immunology towards fighting the HIV pandemic. I will forever be grateful to my mentor Professor Bruce Walker for his guidance and support.

The scientific guidance that I have received from my Dissertation Advisory and Defense Committee Members Professor Tun-Hou Lee, Professor Max Essex, Professor Dan Barouch,

Professor Kai Wucherpfennig, Dr. Douglas Kwon, Professor Anne Goldfeld, and Professor Phyllis Kanki has been instrumental for my development as a researcher.

One of the most important things about acquiring knowledge is passing along what you have learned. When I started my Ph.D., I knew I wanted to be involved in teaching and mentoring. I am honored to have helped mentor two students through the Ragon Institute Summer Student Program. I also want to thank Professor Shiv Pillai for inviting me to be a Teaching Fellow in his very famous Cellular and Molecular Immunology class at Harvard and for all his academic advice.

Collaboration has been one of the most important features of my PhD. All my collaborators are acknowledged in the appropriate chapters of this dissertation. However, I have immense gratitude towards two people who have been fundamental. Priya Jani, my technician, has been involved in almost every experiment. She has participated in countless ways, from the experimental design and implementation to the data interpretation. She is already a great scientist with a bright academic future. Dr. Srinika Ranasinghe started the HLA Class II-restricted $CD8^+$ T cell project presented in Chapter 2 of this dissertation and invited me to participate in this ambitious endeavor. We made a great team and became close friends while working together. Additionally, I would like to thank all the members of the Walker laboratory and Ragon Institute including the Virology Core, Flow Cytometry Core, and Processing Lab. Last but certainly not least, I deeply acknowledge the courage and selflessness of the human blood donors that have made this research possible.

Sometimes, doing a Ph.D. can also be about having a good time. Some of the best memories of my graduate school years are alongside my friends. Things I will never forget: going on bike rides with Crystal Rawlings and her feeding me with chocolate and treats made with “dirt”, Ryan Park always pushing me to be better and do more rigorous science, and the lengthy scientific

discussions in “Spanglish” with my Latin American friends Dr. Wilfredo Garcia-Beltran and Dr. Yovana Pacheco that led to fruitful collaborations. Being an international student makes the whole Ph.D. experience even more challenging but my Mexican friends in Boston (A.K.A. Los Topos), Enrique, Luly, Hiram, Florencia, Hori, Mabel, Eduardo, Anna, Agus, Ari, Gaby, Alex, and Wanda have made me feel like being at home in a foreign country. There is no way I could have survived graduate school without my dog Simon who always made me feel better after a difficult day in the lab and who gives me more joy and laughter than anyone else.

The financial support that I have been incredibly fortunate to receive from Howard Hughes Medical Institute International Student Research Fellowship, CONACYT (National Council of Science and Technology, Mexico), and “Fundación México en Harvard” has permitted me to focus on science without distractions or restrictions.

I have always admired former Dean of the Harvard T.H. Chan School of Public Health Julio Frenk, I want to thank him for his contributions to the School and for his personal support. The Biological Sciences in Public Health Ph.D. Program Directors, Professor Marianne Wessling-Resnick and Professor Brendan Manning as well as Program Coordinators, Deirdre Duckett and Holly Southern have helped me tremendously in many aspects throughout my Ph.D.

Most importantly, I want to thank my family: my father Dr. Pedro Lamothe-Cervera, my wife Daniela, my mother Blanca, my brothers Paul and Daniel, my twin sisters Nery and Mara, and their mother Mara for their unconditional love and support that are the fuel for my enthusiasm and determination.

GLOSSARY OF TERMS

ADCC: Antibody-dependent cellular cytotoxicity

AIDS: acquired immunodeficiency syndrome

APC: allophycocyanin

ART: antiretroviral therapy

BCL: Epstein–Barr virus-transformed B cell line

bNAb: broadly neutralizing antibodies

CAR T cells: T cells genetically modified to express chimeric antigen receptors

CAR: Chimeric antigen receptor

CDR3: complementarity-determining region 3

CFSE: carboxyfluorescein diacetate succinimidyl ester

CMV: cytomegalovirus

CRISPR: clustered regularly interspaced short palindromic repeats

CTL: cytotoxic T lymphocyte cell

EBV: Epstein–Barr virus

Fab: antigen-binding fragment of an antibody

FACS: fluorescence-activated cell sorting

Fc: crystallizable fragment of an antibody.

FEP: free energy perturbation

FPKM: fragments per kilobase million

Gag: Group-specific antigen, composes the core structural proteins of HIV

GWAS: genome-wide association study

HDAC: histone deacetylase

HIV: human immunodeficiency virus

HIV controllers: Individual who control viral replication without the need of antiretroviral therapy

HLA: human leukocyte antigen

IFN-γ: interferon γ

iono: ionomycin

LCL: mouse lymphoblastoid cell lines

MD: molecular dynamics

MDM: Monocyte-derived macrophages

MHC: major histocompatibility complex

MIP-1β: macrophage inflammatory protein 1β

MPER: membrane proximal external region

NK cell: natural killer cell

PBMC: peripheral blood mononuclear cells

PE: phycoerythrin

PHA: phytohaemagglutinin

PMA: phorbol 12-myristate 13-acetate

scFv: single chain variable fragment

scRNA-seq: single-cell RNA sequencing

SIV: simian immunodeficiency virus

TCR: T cell receptor

TNF-α: tumor necrosis factor α

TPM: Transcripts per kilobase million

TRAV: Gene coding for TCR α variable

TRBV: Gene coding for TCR β variable

VSV-G: fusogenic envelope G glycoprotein of vesicular stomatitis virus

WT: wild-type

CHAPTER 1: INTRODUCTION

1.1 CURRENT CHALLENGES IN THE HIV IMMUNOLOGY FIELD

There are over 36 million people infected with human immunodeficiency virus type 1 (HIV-1) worldwide (UNAIDS World AIDS Day report 2013). Conquering the acquired immunodeficiency syndrome (AIDS) epidemic remains one of the most challenging public health issues of our time; there are currently no fully effective means of preventing or curing this disease, but these are urgently needed. Even though antiretroviral medications to successfully control viral replication now exist, and treatment has been extended to resource-constrained setting, these medications must be taken life-long, representing not only a substantial financial burden but are also associated with problems of adherence, the potential for development of drug resistance and toxicities [1, 2, 3]. It is thus very challenging to rely on antiretroviral treatment alone as the only method to combat the HIV pandemic effectively.

The ultimate challenge in the HIV field is to create a successful means to prevent infection. Despite significant advances in combination antiretroviral therapy (cART) to treat HIV, and progress in the development of prevention interventions [3, 4], an effective vaccine has remained elusive. Since there is no natural protective immune response against the virus, creating an effective vaccine has been very challenging. Successful vaccination will require the immune system to function better than it does in natural infection, in which the infection invariably becomes chronic [5]. Neutralizing antibodies, which are the basis for most licensed vaccines, are not readily induced in natural infection. Although about 50 percent of infected persons develop some ability to recognize multiple strains of virus [6], broadly neutralizing antibodies develop in only a small fraction of persons, and this typically takes three or more years of chronic infection to occur [7]. The structure of these rare antibodies is very complex and is associated with extensive somatic mutation involving both the heavy chain complementarity-determining region 3 (HCDR3) region as well as framework mutations [8]. Therefore, induction of effective neutralizing antibodies by an immunogen represents an enormous challenge. There have been several vaccine clinical trials to date but only one

(RV144 “Thailand” vaccine trial) has shown partial success in preventing infection [9]. None of these vaccines tested to date has induced broadly neutralizing antibodies.

Another challenge in the HIV field is that despite the ability of cART to reduce plasma viremia to undetectable levels, it does not lead to viral eradication in HIV-infected persons, committing them to life-long therapy. Cure of HIV or eradication of the viral reservoir represents an enormous challenge because HIV integrates into host genome and can remain latent, without expressing viral proteins, allowing infected cells to escape both immune surveillance and antiretroviral drugs [10, 11, 12, 13, 14] These latently infected cells, in which HIV is transcriptionally silent, do not express any viral proteins but contain a viral genome that can become transcriptionally active upon cellular activation, leading to production of new infectious particles [11 , 14, 15, 16, 17 , 18 , 19]. The elimination of this small but persistent HIV reservoir is a major obstacle to current cure efforts [20, 21, 22, 23]. Reactivation of these cells to become visible to the immune system has been attempted with histone deacetylase (HDAC) inhibitors, and other drugs, with some success [24, 25, 26, 27, 28]. However, if there is no effective immune response present to remove these reactivated cells, the virus would not be expected to be contained [29]. Indeed, it appears that the dominant cytotoxic T lymphocyte (CTL) response in persons who are candidates for cure strategies target epitopes that have already escaped through mutation [30]. Therefore, another challenge in the field is to induce immune responses that would effectively target HIV upon reactivation from the cellular reservoir. Understanding effective immune responses, particularly effective HIV-specific CTL responses, is thus of paramount importance.

In the absence of treatment, infected persons experience progressive $CD4^+$ T cell decline and gradual rise in viremia, associated with the development of opportunistic infections reflective of severe defects in cell mediated immunity. However, unlike these chronic progressors, there is a rare subpopulation (0.3-1.0%) of infected persons termed elite controllers who spontaneously

control viral replication to below the level of detection by standard assay of plasma viral load, and maintain stable $CD4^+$ T cell counts without the need of antiretroviral therapy. Another group, termed viremic controllers maintains viral loads below 2000 RNA copies/ml without the need for treatment. Both groups of HIV controllers are less likely to progress to AIDS (reviewed in [31, 32, 33]). The existence of such persons implies that the human immune system is potentially capable of durable control of HIV and prevention of HIV-associated disease. Although not able to eradicate infection, HIV controllers have a reduced viral reservoir [34], and are considered a model for functional cure of HIV infection [35]. Mechanisms contributing to this phenomenon indicate a dominant role for human leukocyte antigen (HLA) class I alleles in modulating control and that the proximate mediator of control is likely to be HIV-specific CTL [36, 37]. A better understanding of the mechanisms of control is likely to facilitate the development of immunotherapeutic interventions and have implications for the design of effective vaccines and cure strategies [38]. Since viral titers correlate with disease progression [39, 40] and also with increased transmissibility of infection [41], controlling viral load is not only critical for a better clinical outcome but also has a great significance from the global health point of view. To this end, understanding mechanisms of durable control of HIV remains a major priority.

1.2 HIV INFECTION

The first cases of AIDS were reported in 1981, and by 1983-1984 the viral etiology of this new disease had been established [42, 43, 44, 45, 46, 47]. HIV is a human retrovirus, and has a life cycle similar to animal retroviruses. To complete its viral replication and produce *de novo* viral particles, HIV must enter the cytoplasm of the host cell, reverse transcribe its viral RNA into cDNA using the reverse transcriptase enzyme present inside the virion particle, migrate to the nucleus, and integrate it into the host genome (reviewed by [48]). It then employs host cellular machinery to translate viral functional and structural proteins that will assemble on the cell membrane and give

rise to new infectious viral particles, establishing a productive infection. HIV preferentially infects $CD4^+$ T lymphocytes, particularly HIV-specific $CD4^+$ T cells [49] leading to their progressive decline and causing the immunosuppression associated with clinical AIDS. Without treatment, the vast majority of infected individuals progresses to acquired immunodeficiency syndrome (AIDS) and die from opportunistic infections [39].

The natural course of HIV infection consists of three stages: an early acute infection stage, a period of relative clinical latency, and an AIDS stage associated with severe opportunistic infections and cancers [50]. The acute infection stage is characterized by a rapid increase of viral load, associated with flu-like symptoms in the majority of patients (reviewed in [51]). Acute infection is associated with a decline in peripheral blood $CD4^+$ T cells which subsequently partially recover, but with marked and persistent loss of CD4 lymphocytes in tissues, particularly in the gut associated lymphoid tissue [52]. In this phase, viral load rises to a peak that is often 10 million viral particles per ml plasma [53, 54].

After this acute period, there is a relatively asymptomatic stage of clinical latency where the immune system appears to partially control the virus. At the beginning of this stage viral load drops to a quasi set point, and the peripheral $CD4^+$ T cell count stabilizes. The duration of this stage is variable among individuals, and is influenced not just by viral load but also $CD4^+$ T cell count [55]. Progression to AIDS can occur within six months of infection, whereas some persons have been infected and remain healthy after more than three decades without therapy [31, 56, 57]. Plasma viral load during the clinical latency phase directly correlates with progression to AIDS [40]. The AIDS stage is defined by a decline in $CD4^+$ T cell count to 200 cells/μL or less and characterized by a progressive rise in viral load, leading to opportunistic infections and death.

1.3 THE ROLE OF CD8$^+$ T CELLS IN HIV CONTROL

Antigen-specific CD8$^+$ T cells are a major defense mechanism against invading viruses by killing infected cells that harbor virus-derived, non-self-proteins. Activation of CD8$^+$ T cells involves recognition by the T cell receptor (TCR) of virus-derived peptides presented on the surface of infected cells by molecules of the major histocompatibility complex (MHC), named human leukocyte antigen (HLA) in humans [58]. Even though there is confirmation that in HIV infection the effect of CD8$^+$ T cells killing HIV-infected cells is one of the most important mechanisms for controlling viral load and disease progression, it remains unclear exactly what causes some HIV infected individuals to progress to AIDS and others to control infection without antiretroviral therapy (reviewed in [33]).

Virus-specific CD8$^+$ T-cell responses are thought to play a pivotal role in the long-term control in HIV controllers. The preponderance of evidence in both HIV infection and animal models of AIDS virus infections points to CD8$^+$ T cell mediated immune control as the main contributor [37, 59, 60, 61, 62, 63, 64, 65]. Studies of untreated hyperacute infection have shown that the rapidity of generation of HIV-1-specific CTLs and the relative level of these cells during acute HIV-1 infection is critical for viral control [53]. During the chronic phase of HIV infection, effective CD8$^+$ T cell responses have also been repeatedly linked to lower viral loads and better clinical outcome [66, 67, 68, 69, 70, 71, 72]. Numerous studies have shown that several functional properties of HIV-specific CD8$^+$ T cells in HIV controllers are critical to containing viral replication, including specificity for the structural protein Gag [64, 67, 73], polyfunctionality [74, 75, 76], avidity [74], *in-vitro* killing capacity [77], proliferation [61, 62, 78] and TCR usage [79, 80].

The importance of CTLs in controlling HIV is also suggested by the enrichment of certain protective HLA class I alleles. Some alleles are associated with HIV control, whereas others are associated with disease susceptibility (review by [81]). The above-mentioned HIV controllers are

enriched in expression of certain “protective” alleles such as HLA-B*57/5801 and B*27. By contrast, other persons who express disease susceptible alleles, including HLA-B*18/53, are much more likely to develop AIDS in the absence of ART. Notably, studies of HIV controllers expressing protective HLA-B*27 and B*57/5801 alleles have shown that $CD8^+$ T cell targeting of specific peptides in the structurally important Gag protein can result in the selection of viral escape mutants with reduced viral fitness, facilitating immune control [82, 83, 84, 85, 86].

The differential peptide presentation by HLA molecules is explained by host polymorphisms. The HLA genes are coded in the short arm of chromosome 6 and constitutes the most polymorphic coding region of the entire human genome [87]. Indeed, a genome-wide association study (GWAS) clearly demonstrated that specific amino acid variations in the peptide-binding groove are associated with host control of HIV-1 infection. This GWAS was performed in a multiethnic cohort of HIV-1 controllers and progressors in order to find the host genetic variants associated with controlling viral load and disease progression [70]. This study identified more than 300 genome-wide significant single nucleotide polymorphisms within the HLA and none elsewhere. Specific amino acids in the HLA-B peptide binding groove, as well as an independent HLA-C effect, were the most important modulators of viral control.

Chronic viral infections in mice and humans are modulated by CTL-mediated immune pressure, but the level of immune control is quite variable. This is particularly apparent with HIV-1, a chronic human viral infection that undergoes rapid sequence variation under CTL-mediated immune pressure (reviewed in [51]). Immune escape is impeded by the elicitation of a diverse T cell response consisting of multiple specificities [88, 89], but these can vary significantly in antiviral efficacy [67, 77, 79, 90]. Some induced responses effectively target both wild-type (WT) virus and naturally arising mutants, impeding the development of immune escape [79, 91, 92, 93]. Other responses are readily

detectable, but exhibit little antiviral function *in vitro*, and appear to exert little immune selection pressure *in vivo* [94].

Despite this significant association between HIV control and HLA, most people that have protective alleles do not effectively control the virus and progress to AIDS in the absence of antiretroviral therapy. The presence of protective HLA alleles is neither necessary nor sufficient to confer the ability to control HIV *in vivo*, as protective alleles can be observed in both elite controllers and chronic progressors. Previous reports have shown that CTL responses from controllers are functionally superior to those from chronic progressors targeting the same peptide-HLA, and are critical for HIV control [79]. Indeed, current models suggest that no single $CD8^+$ T cell function is uniquely associated with HIV controller status, but rather multiple functions of epitope-specific $CD8^+$ T cells contribute to immune control, with multivariate analysis revealing that proliferative capacity is the strongest single predictor of control [62]. During the course of HIV infection, progressive dysfunction of virus-specific $CD8^+$ T cells referred to as "immune exhaustion" and immune viral escape contribute to lack of control in most infected persons, resulting in progressive disease [33]. In particular, the expression of negative immunoregulatory molecules such as programmed cell death protein 1 (PD-1), lymphocyte-activation gene 3 (LAG-3), and T-cell immunoglobulin and mucin-domain containing-3 (TIM-3) reduce cytokine secretion and proliferative capacity, thus negatively impacting CTL-mediated control [95, 96, 97, 98, 99, 100]. The properties of effective $CD8^+$ T cell responses as still not fully understood, and thus far, control has not been reliably predicted by qualitative or quantitative features of these cells.

Finally, although $CD8^+$ T-cell responses are fundamental to control of viral replication, they are not effective at eradicating HIV infection once a productive infection is established. Therefore, unraveling the molecular mechanisms of host control of HIV-1 infection by cellular immunity is extremely important for eventually devising cure strategies. With this in mind, Chapter 2 of this

dissertation presents work with the objective of better understanding what is the role of protective HLA alleles in HIV control.

1.4 CLASSICAL $CD8^+$ T CELL RECOGNITION OF PEPTIDE-HLA CLASS I COMPLEXES

The first step in recognition of an infected cell is mediated by engagement of the TCR by cognate peptide-HLA complexes. CTL adhere tightly to the infected cell, with the formation of an immunological synapse at the site of contact between the TCR and the peptide-HLA complex. Once the TCR engages the ligand, the ζ-chain-associated protein kinase molecules are recruited to the TCR-CD3 site and activated, which initiates several signaling cascades that lead to the downstream activation of transcription factors that regulate T-cell activation and effector function (recently reviewed by [101]). The activated CTL release their granule contents by exocytosis, which induces cell death of the HIV-infected $CD4^+$ T cells, macrophages and dendritic cells. The two main types of granule protein released by activated CTL are perforin and granzymes (reviewed by [102]. Perforin forms a pore in the membrane of the target cell, which allows the granzymes to enter the infected cell. Granzymes are serine proteases that cleave the proteins inside the cell, shutting down the production of viral proteins, thus resulting in target cell death via apoptosis. In addition to degranulation of perforin and granzymes, CTL secrete cytokines such as IFN-γ and TNF-α, which have antiviral functions.

The dominant paradigm of T cell recognition maintains that $CD8^+$ T cells recognize viral peptides 8-11 amino acids in length bound to HLA class I molecules, whereas $CD4^+$ T cells recognize peptides of 12 or more amino acids restricted by HLA class II [58]. During thymic selection, double positive ($CD4^+CD8^+$) T cells undergo a maturation process where they are selected as either $CD8^+$ T cells or $CD4^+$ T cells depending on TCR binding to peptide complexed with HLA class I or class II, respectively.

An individual cell can express up to six different HLA class I alleles and each molecule of a given allele is estimated to potentially bind billions of distinct peptides [103]. Generating the repertoire of peptides and loading them onto HLA molecules and expressing them as peptide-HLA complexes on the cell surface is accomplished by the antigen processing and presentation pathway (reviewed by [104, 105]. In brief, classical HLA class I processing for CTL recognition starts with the intracellular degradation of virally derived protein products by the proteasome or immunoproteasome. Immunoproteasomes generate a spectrum of peptides that are qualitatively similar to proteasomes, but quantitatively superior via enhanced epitope liberation and increased relative abundance of antigenic peptides [106]. The peptides are then transported into the endoplasmic reticulum by transporters associated with antigen processing (TAP), where they are subjected to further trimming by aminopeptidases such as ERAP1 and ERAP II to ensure the correct length. The 8-11 amino acid peptides then compete for binding to the HLA molecule. Once the peptide is bound, chaperones ERp57 and tapasin complete the fully folded peptide-HLA structure. The stabilized peptide-HLA complex is then released from the loading complex, where it leaves the ER and is transported via the Golgi to the cell surface for recognition by CTL.

The class I molecule is expressed on the surface in association with β2 microglobulin (β2M), which is essential for class I surface expression. The most distinguishing feature among HLA class I alleles is sequence polymorphism clustered in and around the peptide-binding groove. Sequence polymorphisms alter their biochemical properties to dictate binding specificity, and thus different HLA class I alleles typically bind different peptides. However, this is not always the case, as seen with HIV Gag peptides such as QW9 that binds both HLA-B*57:01 and B*53:01. HLA lass I molecules have a closed binding groove that restricts the length of the peptide. The polymorphic HLA residues alter the surface of the peptide binding groove to form ‘pockets’, and the peptides associated with a particular HLA allele usually have conserved residues known as ‘anchors’ that interact with residues in the pockets of the HLA molecule. In contrast, other residues

are surface exposed and serve as TCR contact residues that heavily influence TCR recognition.

Because of HLA restriction in T cell immunity and the enormous number of class I alleles in the human population, there is great diversity among individuals in terms of pathogen-derived peptides presented for recognition by CTL [107]. Inter-individual HLA variation plays a critical role in the selection and specificity of epitopes from particular pathogens. Notably, several groups have shown that expression of certain HLA alleles is associated with HIV immune control and others with rapid disease progression. Yet, the mechanism for these associations is not entirely understood. Current studies have typically evaluated CTL responses restricted by HLA class I alleles that present different epitopes, which complicates the subsequent analysis, as protection may be conferred by the HLA and/or the epitope. To address the impact of HLA in a setting in which peptide variation is not a confounding factor, chapter 2 of this dissertation investigates CTL targeting of an identical Gag-QW9 epitope that is presented by a protective HLA-B*57:01 linked to better viral control and a non-protective HLA-B*53:01 allele linked to faster disease progression.

1.5 ATYPICAL CD8$^+$ T CELL RECOGNITION OF HIV-INFECTED CELLS

The lack of effective HIV control by HLA class I-restricted CD8$^+$ T cells in most infected persons raises the important question as to what determines effective CTL responses that are able to durably suppress viral replication and whether there are alternative ways to mobilize CD8$^+$ T cells to recognize and kill virus-infected cells.

In certain cases, T cells with atypical modes of MHC restriction have been reported. CD8$^+$ T cell responses restricted by MHC class II have been described in animal models [108, 109, 110, 111, 112, 113, 114]. In humans, reports have also described alloreactive CD8$^+$ T cell responses that cross-recognize both HLA class II and class I [115, 116], indicating that unconventional HLA and TCR

interactions may be an important feature of allo-recognition. Virus-specific $CD8^+$ T cells restricted by MHC class II as well as by the non-classical MHC-E were recently detected in the context of immunization with a recombinant fibroblast-topic rhesus Cytomegalovirus (RhCMV) vector in a macaque simian immunodeficiency virus (SIV) vaccine model in which approximately 50% of challenged monkeys are able to clear infection in the early days following challenge [117, 118, 119]. What is most remarkable about this vaccine is that it does not prevent infection, but clears infection without the establishment of a viral reservoir. These studies demonstrate that unconventional $CD8^+$ T cell responses can be elicited by engineered RhCMV vaccine vectors and suggest that these responses may contribute to the control and ultimate eradication of viral replication (reviewed in [120]). The extent to which HLA class II-restricted $CD8^+$ T cell responses play a role in natural human immunity is unclear. To address this question in a chronic human viral infection, Chapter 3 of this dissertation shows the identification and characterization of the antiviral properties of HIV-specific, HLA class II-restricted $CD8^+$ T cell responses in three HIV controllers.

An alternative mode of recognition of HIV-infected cells through engineering T cells to express chimeric antigen receptors (CARs) was first demonstrated *in vitro* two decades ago, by construction of human CD4 or HIV-1-specific Ig sequences linked to the signaling domain of the CD3ζ chain [121]. This approach relied on the fact that HIV envelope is expressed on the surface of infected cells [122], providing a marker to target and kill HIV infected cells. Subsequent clinical trials of this approach were not successful, but did show that these transduced cells could persist *in vivo* [123]. Moreover, the potential role of antibodies in clearance of infected cells has been shown for antibody-dependent cellular-mediated cytotoxicity (ADCC) by non-neutralizing antibodies targeting Env, a response determined to be a correlate of protection for HIV-1 infection acquisition in the RV144 (Thailand) vaccine trial [124]. Therefore, cytotoxic killing of infected cells that express Env on their surface is a mechanism known to help against infection.

Based on positive results in the cancer field [125, 126, 127, 128], there has been renewed interest in another method of $CD8^+$ T cell recognition of infected cells, namely the adoptive cell transfer of T cells expressing CARs targeting HIV. CARs are synthetic transmembrane proteins designed to have the specificity of an antibodies and the effector functions of TCRs. The specificity of T cells can be redirected to a desired target by engineering them to express CARs on their surface (CAR T cells). When the CAR is engaged by its cognate antigen, it sends downstream signaling events to make the cell proliferate, produce cytokines, and kill target cells in a similar way to when a TCR is engaged by peptide-HLA complexes and activates the cell [129]. The main advantage of the CAR approach is that since the specificity of the CAR is given by an antibody and not by a TCR, it is not dependent on HLA presentation, but rather can target an epitope that would be presented in all infected persons. Therefore, a possible therapeutic impact will not be limited to a subset of patients with certain HLA alleles or be affected by downregulation of the expression of HLA in HIV-infected cells. Another advantage of using CAR T cells is that, their design can be based on antibodies that have a much higher affinity to their cognate antigen than the typical affinity with which TCRs bind to their cognate peptide-HLA complex (reviewed [130]). An additional benefit of using a CAR is that the new constructs can include co-stimulatory and/or survival signals to prevent anergy and increase persistence respectively [131]. Consequently, Chapter 4 of this dissertation presents work on designing CARs that are specific for HIV Env to target HIV infected cells.

1.6 SUMMARY

In summary, this thesis is focused on mechanisms of recognition of HIV-infected cells, a topic of central importance to developing durable control of HIV and to emerging cure strategies. Understanding the structural basis of HLA class I in restricting effective and ineffective $CD8^+$ T cell responses extends previous studies by addressing mechanisms of T cell mediated control. Work on alternative mechanisms of recognition of HIV-infected cells by $CD8^+$ T cells that could

potentially be used in translational medical applications is also crucial This is addressed in part by studies of unconventional $CD8^+$ T cell responses that are restricted by HLA class II, and in part by the design and development of CAR T cells to target HIV-infected cells. Together these studies provide additional perspectives on immune control of HIV infection, and have implications for preventive vaccines, immunotherapy and cure strategies.

CHAPTER 2: Molecular mechanisms of differential T cell functional activity against the HIV-1 Gag p24 QW9 epitope presented by human leukocyte antigen B*5701 or B*5301 molecules.

2.1 SUMMARY

Long-term control of HIV-1 infection is associated with certain human leukocyte antigen (HLA) class I alleles, whereas disease progression is linked to other alleles. Protective alleles often present conserved epitopes, suggesting that specificity is an important mechanism for this protection, but there is also evidence that $CD8^+$ T cells, targeting peptides presented on protective HLA molecules, have responses with higher functionality. These studies, however, have compared responses restricted by different HLA alleles presenting different epitopes. To investigate potential peptide-independent effects of $CD8^+$ T cells targeting different HLA alleles, we examined recognition of the QASQEVKNW (QW9) epitope of Gag p24 that is presented by HLA molecules B*57:01 and B*53:01, which are linked to a better viral control or faster disease progression, respectively. Analyzing $CD8^+$ T cells from HIV-infected persons we found that responses recognizing QW9 differ functionally but not quantitatively in the context of disparate restricting HLA molecules. Using x-ray crystallography and molecular dynamics simulation, we structurally identified an unusual mode of distinctive presentation of the QW9 epitope by two HLA molecules. These data show that HLA alleles can have epitope-independent effects on functional T cell recognition, and possibly HIV control.

2.2 BACKGROUND

HIV-1 control is associated with certain human leukocyte antigen (HLA) alleles [68, 69, 70, 81], whereas rapid disease progression is linked to other alleles [70, 132, 133]. Even though the mechanism for these associations is not entirely understood, several studies have shown that protective alleles present highly conserved and constrained epitopes from the viral genome, where viruses cannot have mutations in them without greatly impairing their fitness [82, 83, 84, 85, 86].

Besides the specificity selection of the HLA molecules, there is also some evidence that there are other functional mechanisms by which HLA can contribute to viral control. HIV-specific cytotoxic

T lymphocytes (CTL) responses restricted by protective HLA alleles proliferate more [134], have better in-vitro killing against wildtype and variant epitopes [135], and have a greater ability to inhibit virus replication [136] than those restricted by non-protective alleles. Importantly, HLA-B*27:05 and B*57:01 associated with HIV control have also been found to be associated with increased CTL responses to disorders not related to HIV such as: clearance of chronic hepatitis C viral infection [137, 138], autoimmunity [139], CTL mediated adverse reactions to drugs [140], and resistance to regulatory T cell suppression [141]. These data support the hypothesis that certain HLA alleles are associated with a more functional CTL phenotype.

All these previous studies have compared CTL responses restricted by HLA alleles presenting different epitopes. To investigate potential peptide-independent effect of CTL responses targeting different HLA alleles, one would ideally compare HIV-specific CTL responses restricted by different alleles but presenting the same peptide. The QW9 epitope (QASQEVKNW) of HIV-1 Gag p24 can be presented by both HLA-B*57:01 and HLA-B*53:01 molecules, linked to better viral control [68, 69, 70], and faster disease progression [70, 133], respectively.

We hypothesized that CTL responses restricted by protective alleles have a better disease-controlling phenotype than CTLs restricted by non-protective alleles, even when targeting the same epitope. To address this question, we analyzed CTL responses from HIV controllers targeting the QW9 peptide that is promiscuously presented by a protective HLA B*5701 and a non-protective HLA B*53:01. Even though CTL responses were quantitatively indistinct, we found significant functional differences between CTLs targeting QW9 on B*57:01 and B*53:01 regarding their antiviral activity and cross recognition of epitope variants. Consistent with our functional data, we used x-ray crystallography and molecular dynamics simulation to study the structural basis for differences in epitope presentation and T cell receptor (TCR) recognition. We structurally identified an unusual mode of distinctive presentation of QW9 epitope by these two HLA

molecules. These data show that CTL responses specific for the same QW9 epitope differ significantly in the context of different HLA molecules (B*57:01 or B*53:01), implicating that the HLA allele, as a host genetic factor, could have an epitope-independent protective effect for HIV-1 control.

2.3 RESULTS

2.3.1 CD8$^+$ T cell responses recognizing QW9 differ functionally but not quantitatively in the context of disparate restricting HLA molecules.

The HIV-1 Gag p24 peptide QASQEVKNW (QW9) is known to be presented by HLA-B*5701, which is associated with enhanced control of HIV infection [68, 69, 70], as well as HLA-B*53:01, which has been associated with more rapid disease progression [70, 133]. To assess magnitude of responses and possible T cell cross-recognition of the QW9 presented by these two HLAs, we first synthesized HLA-B*57:01/QW9 and B*53:01/QW9 tetramers, and then tested them in five HLA-B*57:01 and five HIV-B*53:01 expressing HIV-infected persons (clinical characteristics in **Supplemental Table 2.1**). The tetramers only reacted with T cells from persons expressing the matched HLA molecule, with no evidence of cross recognition of T cells from persons expressing HLA-B*5701 by the HLA-B*5301 tetramer, or vice versa **(Figure 2.1A)**. There was no quantitative difference between HLA-B*57:01 and B*53:01 subjects in the percentage of CD8$^+$ T cells targeting QW9 tetramers **(Figure 2.1B)**. In addition, we generated QW9-specific CD8$^+$ T cell lines for each subject by *in-vitro* stimulation of peripheral blood mononuclear cells (PBMC) and tested for the ability to lyse autologous cells expressing the QW9 epitope. At saturating peptide concentrations, QW9-specific CD8$^+$ T cells from HLA-B*5701 donors had greater killing capacity than those targeting QW9-HLA-B*53:01 **(Figure 2.1C)** ($p=0.0397$). These results indicate that both peptide and HLA allele contribute to the specificity of QW9 recognition and that, despite similar quantitative measurements, the functional ability to kill cells expressing QW9 is greater in the context of HLA-B*5701 than HLA-B*5301.

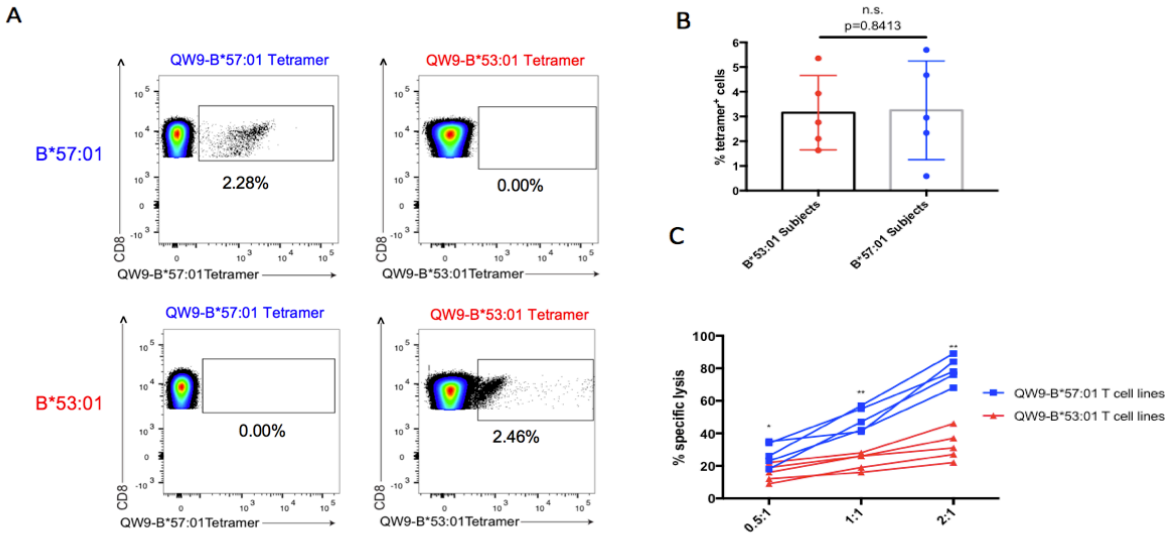

Figure 2.1. Quantitative and functional characteristics of QW9-specific CD8+ T cells. **(A)** Flow cytometry plots for representative examples of QW9-tetramer positive cells for either B*53:01 or B*57:01. Each sample was dual stained with B*53:01-QW9-APC and B*57:01-QW9-PE tetramers. Systems were gated on $CD3^+CD8^+CD19^-CD14^-CD56^-$ live lymphocyte singlet cells. **(B)** Percentage QW9-tetramer positive cells from total $CD8^+CD3^+CD19^-CD14^-CD56^-$ live lymphocyte singlet cells. Each dot represents a research subject. (Mann-Whitney test; Error bars represent SD). **(C)** Summary data assessing specific lysis of target cells by QW9-specific T cell lines in a standard 6 hr chromium release assay at effector cell/target cell ratios of 0.5:1, 1:1 and 2:1. Autologous EBV-transformed BCLs pulsed with either QW9 or no peptide were used as target cells. (The Mann-Whitney test was used to calculate the *p* value for each E:T ratio condition. * $p \leq 0.05$, ** $p \leq 0.01$. Error bars represent SD.)

*2.3.2 QW9 specific $CD8^+$ T cells that recognize B*57:01 are more cross-reactive against epitope variants than those that recognize B*53:01*

A major challenge for $CD8^+$ T cell control of HIV is the evolution of epitope escape mutations under immune selection pressure. We next determined the extent to which T cells targeting QW9 in the context of these two different HLA class I molecules were able to recognize mutations known to arise *in vivo* in QW9. The ability of $CD8^+$ T cell lines to lyse target cells presenting the QW9 variants QATQEVKNW (S3T) (p=0.0079) and QASQDVKNW (E5D) (p=0.0397) was higher for persons expressing B*57:01 than for those expressing B*53:01 **(Figure 2.2A).**

To further validate this cross-reactivity, we next constructed B*57:01 and B*53:01 HLA class I tetramers refolded with wildtype QW9 peptide (QW9-WT) or the QW9 variants S3T and E5D (QW9-S3T and QW9-E5D). For persons expressing B*57:01, similar percentages of cells were stained by tetramers complexed with QW9-WT and the QW9 variants (p=0.7849). In contrast, there was a significant decrease in the percentage of cells targeting the QW9 variants for B*53:01 (*p*=0.0487), consistent with less avid cross recognition by these effector cells **(Figure 2.2B)**.

Proliferation in response to recognition of targeted peptides has been shown to correlate with effective HIV control [73, 134]. We therefore examined functionality of HIV-specific T cells recognizing QW9-WT and QW9 variants by measuring proliferation by carboxyfluorescein diacetate succinimidyl ester (CFSE) dilution in response to peptide stimulation in persons expressing either B*57:01 or B*53:01. Consistent with the killing assays, we found that B*57:01-specific cells proliferated more than B*53:01-specific cells when stimulated with QW9-WT (*p*=0.0317) **(Figure 2.2C)**. Moreover, HLA-B*57:01 expressing subjects had QW9-specific responses that were significantly more cross-reactive to S3T (p=0.0079) and E5D (p=0.0397) than cells from B*53:01 subjects.

Together these studies show that, despite similar quantitative responses to QW9 in B*57:01 and B*53:01 expressing persons, cross reactivity for QW9 variants and functional properties, including proliferation and cell killing, were enhanced when QW9 was presented in the context of the protective HLA-B*5701 allele, compared to the progressive allele B*5301.

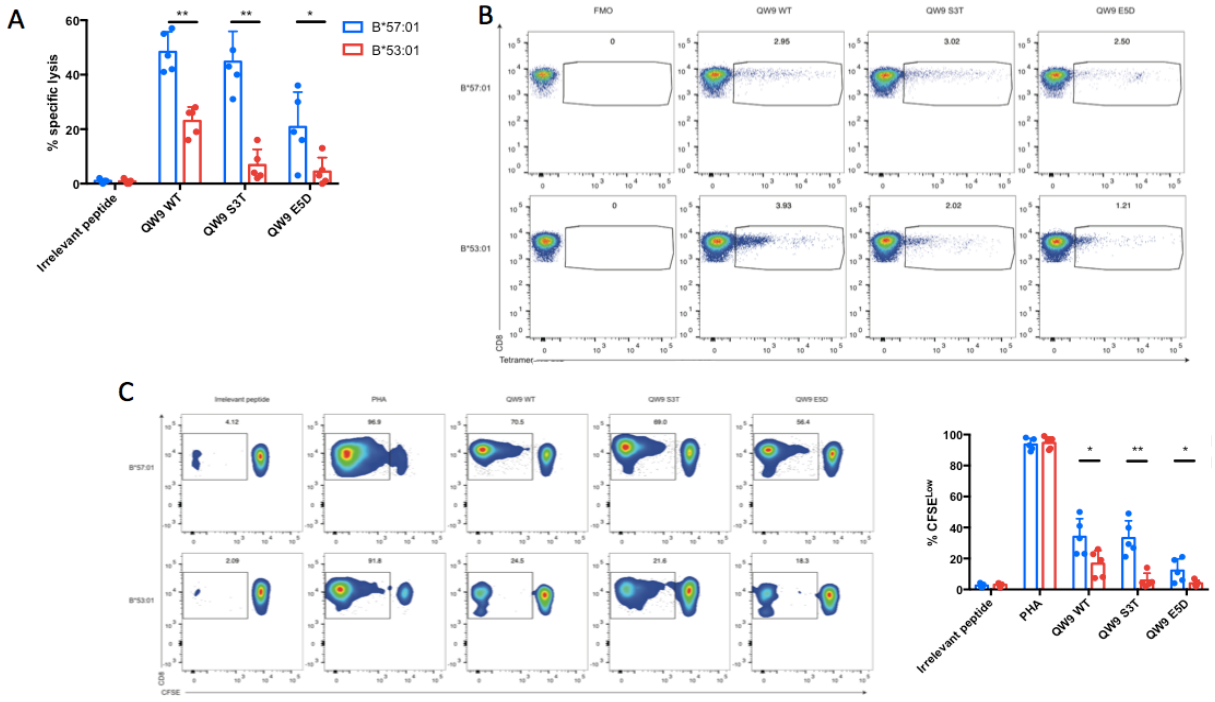

Figure 2.2. Cross-reactivity of QW9-specific CD8$^+$ T cells. (A) Summary data assessing specific lysis of target cells by QW9-specific T cell lines in a standard 6 hr chromium release assay at effector cell/target cell ratio of 1:1. Autologous EBV-transformed BCLs pulsed with WT, S3T, or E5D QW9 peptides were used as target cells. Each dot represents a T cell line grown from a particular research subject where blue dots indicate B*57:01 responses and red dots indicate B*53:01 responses. (Mann-Whitney test, ** p≤0.01. Error bars represent SD). **(B)** Flow cytometry plots for representative examples of QW9-tetramer positive cells for either B*53:01 or B*57:01. Each sample is dual stained with B*53:01-QW9-APC and B*57:01-QW9-PE tetramers. Systems were gated on CD3$^+$CD19$^-$CD14$^-$CD56$^-$ live lymphocyte singlet cells. **(C)** (Left) Representative flow cytometry plots showing cell expression of CFSE at day 7 after stimulation of bulk *ex-vivo* peripheral blood mononuclear cells (PBMCs) from B*53:01 and a B*57:01 subjects. Systems were gated on total CD8$^+$CD3$^+$CD19$^-$CD14$^-$CD56$^-$ live lymphocyte singlet cells. (Right) Quantification of cells that proliferated (CFSE^{Low} cells). Each dot represents a research subject; blue dots indicate B*57:01 responses and red dots indicate B*53:01 responses. (Mann-Whitney test, * p≤0.05 ** p≤0.01. Error bars represent SD).

*2.3.3 QW9-specific CD8$^+$ T cells that recognize B*57:01 have TCR beta clonotype repertoires different from those that recognize B*53:01*

We next performed sequencing of the T cell receptor (TCR) beta chain of QW9-B*57:01- and QW9-B*53:01-specific CD8$^+$ T cells. Tetramers refolded with the WT peptide were used to stain cells for sorting, and cells were then subjected to TCR sequencing. For each subject, we identified a single dominant clonotype, but no clonotypes were shared among research subjects **(Figure 3A)**. Fewer TCR beta clonotypes were identified for responses restricted by B*57:01 than to

B*53:01. To further define parameters that might differentiate HIV-specific $CD8^+$ T cells in these two HLA backgrounds, we examined the germline-like index for the TCRs, which has been shown previously to correlate with HIV control [79]. Here, we found that clonotypes from HLA-B*57:01-positive subjects were closer to the germline than those who express HLA-B*53:01 **(Figure 2.3B)** (p<0.001), suggesting that HLA-B*57:01-derived clonotypes might be associated with better control.

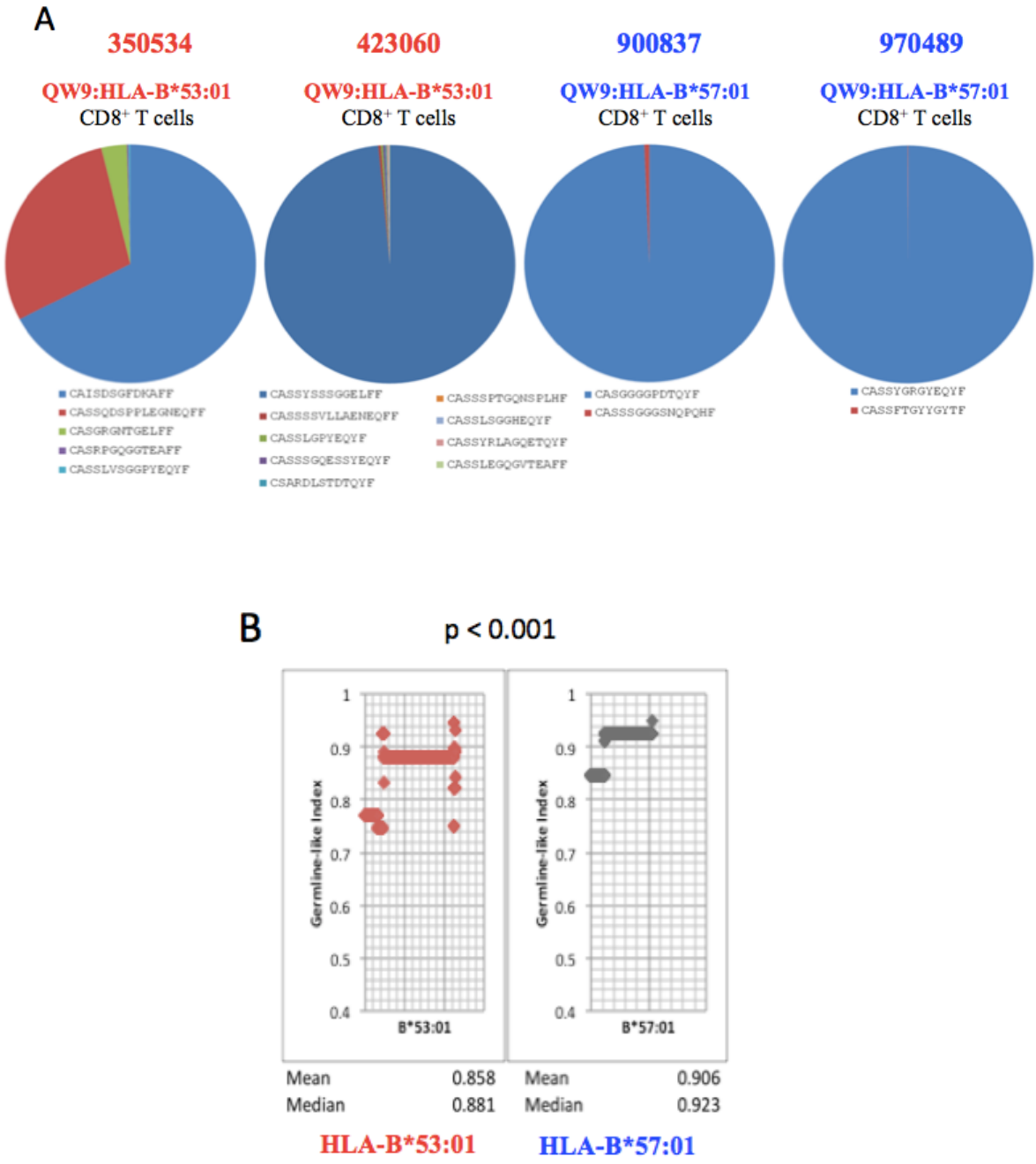

Figure 2.3 (A) TCR repertoire analysis showing clonotypic diversity of QW9-specific CD8$^+$ T cells from B*53:01$^+$ and B*57:01$^+$ subjects. **(B)** Calculation of the germline like index = (CDR3 length – nucleotide insertions) / CDR3 length. Each dot represents a clonotype identified. (Mann-Whitney test).

*2.3.4 Structural data for B*53:01- and B*57:01-QW9 complexes and discovery of K7 conformational distribution*

In order to further define the structural features of QW9 recognition, we established collaboration with Professor Jia-huai Wang and Dr. Xiaolong Li at the Dana Farber Cancer Institute. Multiple crystal structures of both B*57:01 and B*53:01 in complex with QW9 were obtained, revealing that QW9-K7 buries its side chain into the peptide binding groove of B*57:01 **(Figures 4A-C)**; in contrast, QW9-K7 can either be buried in the groove of B*53:01 or point out into solvent **(Figure 2.4D)**. Careful analysis of peptide-HLA interactions within the peptide-binding grooves of B*57:01 and B*53:01 indicates that position 97, which is an arginine in B*53:01 and a valine in B*5701, plays a critical role in determining the K7 configuration **(Figures 2.4E, F)**, as GWAS data corroborate [70].

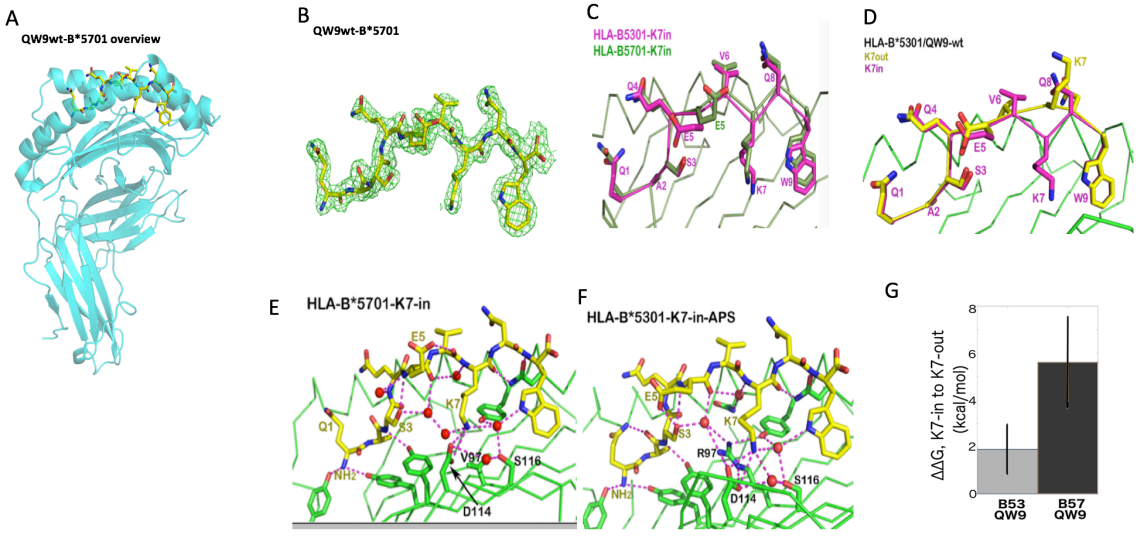

Figure 2.4 Crystal structure data for HLA-QW9 complexes and *Computation of free energy differences between K7 states*. (A) QW9wt/HLA-B*57:01 structure, **(B)** QW9wt stick model fitting into its electron density, **(C)** overlay of B*57:01(K7-in) and B*53:01(K7-in), **(D)** overlay of two different conformation QW9wts in B*53:01 binding groove, **(E)**. Hydrogen-binding network for B*57:01(K7-in), **(F)**. Hydrogen-binding network for B*53:01(K7-in), **(G)** FEP cycles for B*57:01 and B*53:01, Binding free energy changes for HIV-peptide QW9, moving from K7in to K7out configurations. Error bars are presented as 95% confidence intervals.

Free energy perturbation cycles can be leveraged to estimate binding free energy differences between K7-in and K7-out QW9 configurations. To address this, we established collaboration with Dr Ruhong Zhou and Dr. Jeffrey Weber at IBM to perform molecular dynamic simulations. **Figure. 4G** illustrates that B*53:01/QW9 incurs in an ~2 kcal/mol binding free energy penalty after moving from K7-in to K7-out; B*57:01/QW9 suffers a nearly 6 kcal/mol cost while undergoing the same transformation. These results imply that, in the context of both HLAs, K7 favors burial into the peptide binding groove. However, while B*57:01 favors QW9-K7-in conformations >99.9% of the time, QW9-K7-out configurations occur with approximately 10% probability in B*53:01-QW9 complexes. This variation in presented QW9 conformations likely complicates the immune response related to B*53:01-QW9 binding, as QW9-specific TCRs would need to contend with a combination of exposed and buried lysine side chains in order to be activated.

2.3.5 Molecular dynamics simulations of HLA-QW9-TCR complexes

After generating initial docked structures for ternary HLA-QW9-TCR complexes, extensive molecular dynamics (MD) simulations were applied to explore the details of MHC-peptide-TCR interactions. QW9-TCR interaction energies indicate that B*53:01-QW9-K7-out and B*57:01-QW9 both have strong epitope-restricted interactions with their respective TCRs (C3 and C8); by contrast, B*53:01-QW9-K7-in gives rise to very weak epitope-restricted interactions **(Figure 2.5)**. In general, these QW9-TCR interaction energies are dominated by their electrostatic components, in contradistinction to past results obtained for the HIV antigen KK10 [142]. More detailed analysis shows that the QW9 amino acid E5 dynamics play a role in differentiating interaction energy strengths: static E5-TCR interactions seem to stabilize the QW9-TCR complexes in B*53:01-QW9-K7-out-C3 and B*57:01-QW9-C8, whereas a dynamic E5 contributes little to the stability of B*53:01-QW9-K7in-C3. Interestingly, the specific QW9-TCR interactions that emerge from MD simulations vary in each case. For B*53:01-QW9-K7-in-C3, TCR interactions are spread throughout the peptide (with weak and transient interactions at E5); when K7 is out, however,

stable K7-TCR and E5-TCR contacts seem to pull the entire QW9 C-terminus toward the TCR. The interaction with the QW9 epitope for B*57:01-QW9-C8 is more N-terminus centric, but still exhibits strong and stable interactions via E5 and N8.

Regarding B*53:01, the K7-out epitope interacts much more strongly with C3 than does the K7-in epitope, suggesting that C3 was perhaps selected to recognize K7-out configurations. C3 activation derived from K7-in conformations, in that case, would be correspondingly weak. Since ~10% of B*53:01-QW9 conformations feature K7 in the out position **(Figure 2.4G)**, it is possible that only a fraction of B*53:01-QW9 complexes are immunologically active at any given time. In comparison to B*57:01, thus, the above calculations suggest that QW9 presentation by B*53:01 could be less immunologically efficient.

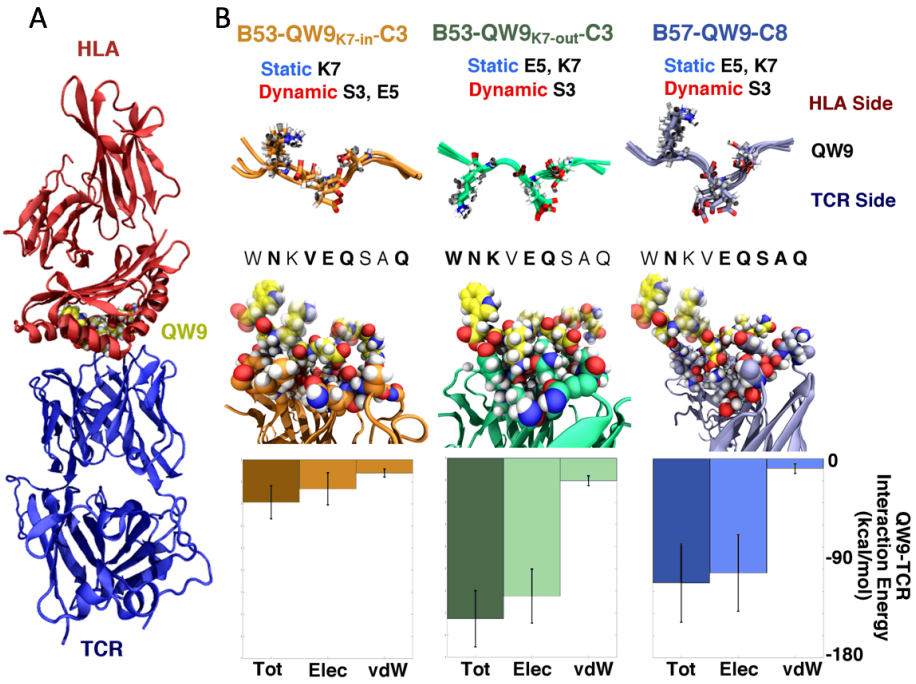

Figure. 2.5 (A) Example of docked HLA-QW9-TCR structure (in this case, derived from C3 and B*53:01/QW9-K7-in crystal structures). **(B)** Exposition of ternary complex interactions, as determined by molecular dynamics simulations. Residues involved in the QW9 TCR epitope (as determined by > 5 kcal/mol mean interaction energies) are indicated by bold text in sequence representations of QW9. Four representative structures for each complex are overlaid at top, with crucial residues S3, E5, and K7 rendered in stick representations.

*2.3.6 Unrestricted features and interactions of B*57:01 and B*53:01*

In addition to the potential immunological inefficiency of B*53:01/QW9 presentation, differences in unrestricted HLA-TCR interactions could also contribute to the protective nature of B*57:01. A sequence alignment between B*53:01 and B*57:01 shows high variation in the 1 helix of the HLAs. Corresponding surface representations of B*57:01-QW9 and B*53:01-QW9-K7-in are clearly distinct in this region of high variation (sequence shown in **Figure 2.6a**), with more expansive positive regions in B*57:01. The presenting surface of the HLA is less featured in these K7-in configurations, a factor that may make unrestricted HLA-TCR interactions more prominent.

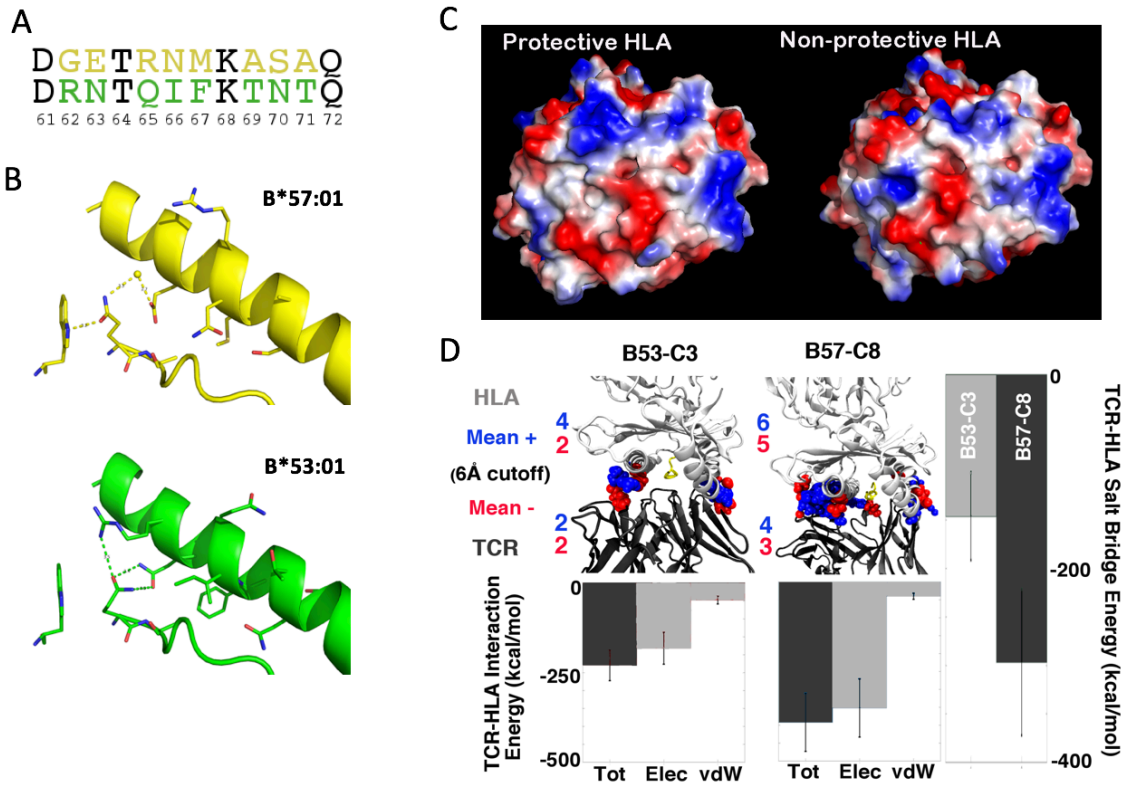

Figure 2.6. Sequence alignment and surface representations of HLA B*57:01 and B*53:01. **(A)** Alpha-1 helix sequence alignment, **(B)** cartoon models of B*57:01 and B*53:01, **(C)** surface representations of B*57:01 and B*53:01, **(D)** unrestricted HLA-TCR interactions between B*53:01 and its TCR, C3, and B*57:01 and its TCR, C8. Data corresponding to C3 are presented as weighted averages of K7-in and K7-out observations. Blue and red numbers indicate the average counts of basic and acidic residues (respectively) within 6Å of the HLA-TCR interface on either side. Salt bridge energies are computed as the electrostatic components of interaction energies among these charged interfacial residues.

Strikingly, MD simulations also reveal that interactions between B*57:01 and C8, exclusive of QW9, are nearly twice as strong as those between B*53:01 and C3 (B*53:01 data are presented as a 90%/10% weighted average of K7in/K7out data). The bulk of this energetic difference is derived from electrostatic interactions; in particular, the energy associated with HLA-TCR salt bridges is more than twice the magnitude in B*57:01/C8 of that in B*53:01/C3 **(Figure 2.6D)**. Analysis of dynamical trajectories indicates that, on average, B*57:01/C8 exhibits significantly more basic and acidic residues near the binding interface on both the HLA and TCR sides. The positions of charged residues on B*57:01 thus seem to cultivate the presence of complementary residues on the TCR paratope; these effects synergize yielding stabilizing interactions that are independent of QW9. Thus, part of the relative protection offered by B*57:01 may also be derived from factors that aren't restricted to a particular epitope.

2.3.7 Structural and Dynamical Underpinnings of QW9 epitope variants

Though direct TCR-HLA interactions might endow B*57:01 with more protective properties, our functional data indicate that mutations can still facilitate immune escape from both HLA alleles **(Figure 2.2A)**. However, these data also show that B*57:01 can better retain its function in the face of escape mutations within the QW9 epitope. In light of these observations, we determined B*57:01 and B*53:01 structures in complex with QW9-S3T and QW9-E5D. Based on a comparison between mutated QW9 and QW9-WT structures, these mutations either remove features from the TCR-facing interface of QW9, or largely keep that interface the same.

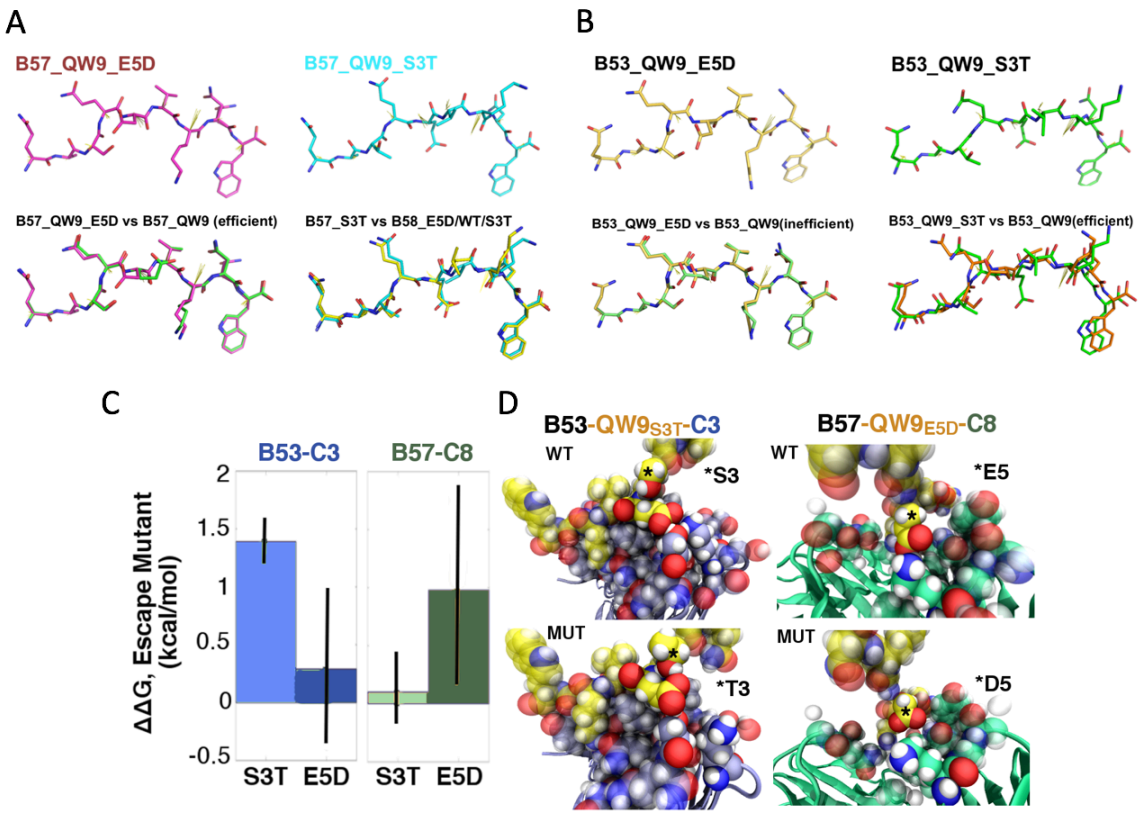

Figure 2.7. Crystal structure data related to epitope variants S3T and E5D. **(A)** QW9_E5D and S3T on B*57:01 and their overlaying to QW9wt effective conformation, **(B)** QW9_E5D and S3T on B*5301 and their overlaying to QW9wt ineffective conformation, **(C)** TCR-binding free energy changes for QW9 epitope variants S3T and E5D, **(D)** structural differences between mutant and wildtype complexes. Error bars are presented as 95% confidence intervals derived from 5 independent simulation runs.

Free energy perturbation calculations on S3T and E5D epitope variants yield binding free energy change values in good agreement with functional data. B*53:01 exhibits a loss of binding affinity in the face of both escape mutations, especially with respect to S3T. B*57:01, by contrast, loses only a small amount of binding affinity with S3T, but shows a significantly unfavorable free energy change with E5D. These results align well with the specific lysis data presented in **Figure 2.2a**. In the most dramatic cases for C3 and C8 (S3T and E5D, respectively) with respect to free energies, the escape mutation subtly impacts important interactions with the TCR. For C3-S3T, steric occlusion places the threonine hydroxyl hydrogen in direct contact with QW9-E5, weakening the E5 interaction with C3(A)-K68. In the case of C8-E5D, shortening of the side chain partially

breaks a salt bridge with C8(A)-K48. On average, the effects of the escape mutations on complex binding free energies seem to be more drastic for B*53:01 than for B*57:01, as the functional results corroborate. These data support the idea that B*57:01 can also mitigate the effects of QW9 mutations more completely than B*53:01, highlighting another factor that could make B*57:01 more protective than B*53:01.

2.4 MATERIALS AND MEHTODS

Samples and research subjects

All samples were obtained from cryopreserved PBMC from HIV-1-infected individuals according to protocols approved by the Institutional Review Board of the Massachusetts General Hospital. Characteristics of the research subjects are shown in **Supplemental Table S2.1.**

Elite Controllers were defined as having plasma HIV-1 RNA below the level of detection for the ultrasensitive assay (< 75 RNA copies/mL by cDNA or < 50 copies/mL by ultrasensitive PCR) without antiretroviral therapy and Viremic Controllers as having HIV-1 RNA < 2000 RNA copies/mL without antiretroviral therapy. $CD4^+$ T cell counts and viral loads were determined as described [143].

High resolution HLA genotyping was performed by Dr. Mary Carrington at the National Cancer Institute using sequence-specific PCR in accordance with standard procedures. Briefly, HLA class I–encoding genes were amplified by PCR with primers spanning exons 2 and 3, and HLA class II DRB1–encoding genes were identified by PCR amplification and sequencing of exon 2. ASSIGN 3.5 software developed by Conexio Genomics was used to interpret the sequencing results.

Tetramer Staining

HLA-B*57:01 and HLA-B*53:01 tetramers refolded with QW9-WT (QASQEVKNW) were obtained

from Dr. Søren Buus (University of Copenhagen). Tetramers with variants QW9-S3T (QATQEVKNW), QW9-E5D (QASQDVKNW) were obtained from the National Institutes of Health Tetramer Core. Tetramer were validated to rule out non-specific binding with HLA-matched HIV negative samples **(Supplemental Figure 2.1).** Cryopreserved PBMCs from research subjects were incubated with the corresponding QW9 tetramers for 25 minutes at 37^{o}C and 5% CO_2. The cells were then stained for viability and surface markers (CD3, CD4, CD8, CD14, CD19, CD56), fixed, and analyzed by flow cytometer (LSR Fortessa BD biosciences).

Proliferation Assay

The PBMCs from the patients were stained with CFSE by incubating the cells with CFSE solution for 7 minutes at 37^{o}C and 5% CO_2 and then washed twice. The cells were plated at 250,000 cells per well in a 96-well round bottom plate with 0.5µg/mL of the corresponding peptides for seven days. The peptides used were QW9-WT (QASQEVKNW), QW9-S3T (QATQEVKNW), QW9-E5D (QASQDVKNW), and QW9-A7K (QASQEVANW). The negative control well had no peptide and positive control well had PHA at 5µg/mL. On day 7, the cells were stained according to the tetramer staining protocol and analyzed by flow cytometer (LSR Fortessa BD Biosciences).

Generation of autologous targets cells for killing assays

Autologous Epstein-Barr virus-transformed B cell lines were used as targets in the chromium release assays. Ten million frozen PBMC were thawed and resuspended in 1mL of RMPI, 1.5mL of fetal bovine serum (FBS), and 1.5mL of unconcentrated supernatant of Epstein-Barr virus. Cyclosporine A (sigma) was added in a 1 µg/ml concentration. Cells were cultured for 6 to 8 weeks at 37°C and 5% CO2.

Generation of QW9-specific T cell effector cells for killing assays

QW9-specific T cell lines (TCL) were generated from each research subject as following: 10% of the total PBMC cells were incubated with QW9 (QASQEVKNW) peptide at a concentration of 5µg/mL for 1 hour at 37°C and 5% CO_2, washed three times to remove unbound peptides, and then transferred to the remaining 90% PBMCs. The cells were added to 96-well round bottom plate with 50U/mL of interleukin-2 (IL-2) in 200µL per well. The plate was incubated at 37°C and 5% CO_2 for seven days and the TCL were tested by tetramer staining on day 7. Fluorescence activated cell sorting (FACSAria II BD) was used to sort QW9 tetramer$^+$CD8$^+$CD3$^+$ cells to use as effectors in chromium release assay.

Chromium release assay

Targets cells were incubated with respective QW9-WT and QW9 variant peptides at a concentration of 10µg/mL and incubated with ^{51}Cr at a concentration of 250µCi/mL for one hour in a 37°C and 5% CO2 incubator. ^{51}Cr-Labelled cells were washed 3 times in RPMI media with 10% FBS and resuspended at a concentration of 1 million cells/ml. Target cells were plated in a flat bottom 96-well plate. To ensure an equal number of QW9-specific cells, tetramer positive cells were sorted to be used in the killing assay and were added at the appropriate effector-target ratios. Spontaneous and maximum releases were determined by incubating the labeled target cells with medium alone or 5% Triton X-100, respectively. The supernatant was collected after 6 hours of incubation at 37°C in 5% CO2. We used a Perkin Elmer TopCount NXT Microplate Scintillation & Luminescence Counter to measure radioactivity present in the supernatant. Quantification of specific killing was calculated by specific killing =100 x (sample release – spontaneous release) / (maximum release - spontaneous release).

Sequencing of T cell receptors

Fluorescence activated cell sorting (FACSAria II BD) was used to sort QW9 tetramer^{+}CD8^{+}CD3^{+} cells into RLT buffer with 1% beta mercaptoethanol. RNA was purified with RNeasy Micro Kit – QIAGEN and converted to cDNA with 5'RACE cDNA amplification kit from Clontech/Takara. Gene-specific amplification was done using nested PCR and primers to TRBC region. Amplicons were cloned into a topo TA vector for sequencing and One Shot® TOP10 Chemically Competent E. coli (Thermo Fisher) were transformed. Bacterial colonies were picked at 24hrs. DNA was extracted with Miniprep Kit (Qiagen) and sent for Sanger sequencing at the MGH DNA core. IMGT v-quest tool was used for identification of TCR gene segments and CDR3 regions. Germline like index (GLI) was calculated as GLI = (CDR3 length – nucleotide insertions) / CDR3 length.

Statistics for functional assays

For statistical analysis, we used the Prism 7 program from GraphPad Software Inc. Paired t-test or non-parametric Mann-Whitney tests were used to compare groups as noted on the figure legend of each experiment. *p*-values ≤0.05 were considered statistically significant. Error bars represent standard deviation.

Cloning

The full DNA sequence of the HLA-B*53:01 and B*57:01 heavy chains are from EMBL-EBI IPD-IMGT/HLA, and amino acid codons of the HLA-B*53:01 and B*57:01 ecto-domains were optimized for the bacterial E.coli BL21(DE3) expression system. The synthesized gene with a stop codon was inserted into the cloning site of the pUC57 vector, between NdeI and XhoI. Then the HLA-B*53:01 and B*57:01 /pUC57 plasmids were transferred into E.coli Top10 competent cells for amplification and then extracted by using Qiagen kit. Instead of PCR, the HLA-B*53:01 and B*57:01 gene fragments were cut off from the HLA-B*53:01 and B*57:01 /pUC57 plasmids by NdeI and XhoI restriction enzymes and separated by agarose gel electrophoresis. Eventually,

the HLA-B*53:01 and B*57:01 DNA fragments were integrated into the expression vector pET22b(+) at the same cloning site.

Expression and purification of inclusion bodies

Recombinant HLA-B*53:01 and B*57:01 inclusion bodies were produced in E.coli BL21(DE3) cells harboring the HLA-B*53:01 and B*57:01 /pET22b(+) expression plasmids. When the E.coli cell density OD600 reached 0.6-0.8, inclusion body expression were induced with a final concentration of 1 mM IPTG for 4 hours at 37°C [144]. Cells pellets were harvested and then suspended in the extraction buffer (50 mM Tris-HCl, 100 mM NaCl, 10 mM $MgCl_2$, 1% Triton-X100, pH 8.2) mixed with fresh lysoenzyme, DNase-I and PMSF. After sonification, inclusion bodies were collected at 8000 rpm. To sufficiently lyse cells and make inclusion bodies purer, we resuspended the inclusion bodies and repeated the lysis step. Then the inclusion bodies were washed 3 times with wash buffer (50 mM Tris, 20 mM EDTA, pH 8.0) to further remove Mg^{2+}, detergent and soluble proteins including the enzymes added. The light chain, β2m construct, was from the Barbara Uchańska-Zieger's lab (Institut für Immungenetik, Charité-Universitätsmedizin Berlin, Freie Universität Berlin, Berlin, Germany). Expression and purification methods for β2m were the same as for heavy chain. The purified inclusion bodies were dissolved in 8 M urea and stored at -20 °C.

Refolding and purification of HLA

Specific peptide is essential for HLA refolding. The peptide QW9 and its variants in this study were synthesized by United BioSystems Inc., and were dissolved in DMSO before refolding. To refold those proteins, HLA-B*53:01 & B*57:01 (56 mg), β2m (28 mg) and peptide (10 mg) were diluted in 100 mM Tris-HCl pH 8.0, 0.4 M arginine, 0.5 mM oxidized glutathione, 1.5 mM reduced glutathione, 2 mM EDTA, 4 M urea and in 0.2 mM PMSF in a volume of 500 ml over 24 hours at 4°C. The refolding solution was then dialyzed for 4 hours against 0.1 M urea, 10 mM Tris-HCl pH

8.0, and overnight against 10 mM Tris-HCl pH 8.0 at 4 °C using a 6-8 kDa molecular mass cut-off dialysis membrane (Spectrum). After dialysis, concentrated sample was loaded onto a superdex75 (GE Health) gel filtration column for separation and the correctly refolded HLA-B*53:01 and B*57:01 protein fraction appeared from 57 ml in 10 mM Tris-HCl pH 8.0, 100 mM NaCl. In addition, the Mono-Q ion exchange column was used in the final step purification.

Crystallization

HLA-B*53:01 and B*57:01 proteins loaded with QW9 or its variants were concentrated to 7-10 mg/ml in 10 mM Tris-HCl buffer, pH 8.0. Hampton kits were selected as initial screen conditions, and crystals were obtained at room temperature by using the sitting drop vapor diffusion method from 0.1 M sodium citrate tribasic dihydrate pH 5.6, 20% v/v 2-propanol, 20% w/v polyethylene glycol (PEG) 4,000. We optimized the conditions and found that crystals from 15-20% w/v PEG 4000, 20% w/v 2-propanol, 0.1 M MES, pH 6.5 are the best. A drop contained 0.1μL protein solution mixed with 0.1μL reservoir solution could form crystals within 3 days. The robots NT8 and Rack Imager made by Formulatrix were employed in both crystallization condition screening and optimization.

Data collection, processing and refinement of crystal structures

Diffraction data were collected from cryo-cooled crystals to a resolution range from 2.1 to 2.9 Å at the APS, Argonne National Laboratories, 19ID beam-line and the ADSC Quantum 315 X-ray diffraction detector. The cryo-protectant solution we used was the crystallization buffer plus 10-20% PEG 400. Diffraction data were processed with the program HKL2000 [145] and CCP4i, and molecular replacement was carried out using Phaser in the PHENIX Program Suite. The search model for all of the structures is 1A1M from the Protein Data Bank. Structure refinement was also performed in PHENIX with XYZ coordinates, real-space, rigid body, individual B-factor,

occupancies and CNS refinement. The resulting models were manually inspected and modified with the program COOT.

Molecular dynamics simulations

Each HLA-peptide-TCR complex was solvated in a 77.5 A° 3 128.0 A° 3 76.5 A° water box, where the system was first neutralized with counter ions, and then further ionized in a 150 mM NaCl in order to mimic *in-vivo* physiological environment. The solvated system was minimized by 20,000 steps, then followed by ~1ns equilibration (with a 0.5-fs timestep) in 1 atm and 310 K. In each system, five snapshots at the second half of the equilibration were randomly picked as starting structures for up to 50 ns long molecular dynamics simulations and independent 60 + ns free energy perturbation (FEP) calculations for each system, with an aggregate of 1.7 microseconds MD simulation time for all clonotypes and their variants. The particle-mesh Ewald (PME) method was used for the long-range electrostatic interactions, while the van der Waals interactions were handled with usual smooth cutoff with a cutoff distance of 12 A°. All molecular dynamics simulations were performed with a specially optimized NAMD2 molecular modeling package for Blue Gene, with a 1.5-fs timestep in NPT ensemble at 1 atm and 310 K. Molecular dynamics simulations have been widely used in modeling biological systems to complement experiments, which can provide atomic details that are often inaccessible in experiments due to resolution limits even with the current most sophisticated experimental techniques. The CHARMM22 force field and TIP3P water model are used for proteins and solvents, respectively.

Free energy perturbation protocol

The binding affinity changes, due to antigenic variations, between the TCR and HLA-QW9 complex were estimated by the free energy perturbation (FEP) method. We calculate the free energy changes for the same mutation(s) in both the bound state (HLA-peptide-TCR 3-way

binding complex) and the free state (HLA-QW9 binary complex). For each mutation, at least five independent runs starting from different initial configurations (taken from the molecular dynamic simulations) were performed for better sampling. The simulation time for each run is 6.0 ns, thus, at least 60 ns (6.0-ns X 5-runs X 2-states) simulation time was generated for each mutation. Larger window sizes and longer simulation durations have also been tested in our previous studies, and we found that the current protocol gives us a reasonable convergence in the final binding affinities.

2.5 ACKNOWLEDGEMENTS AND AUTHOR CONTRIBUTIONS

We thank all research subjects and study participants, as well as, M.C. Carrington for HLA typing and we appreciate the tetramers provided by Dr. Søren Buus (University of Copenhagen) and the National Institutes of Health Tetramer Core. Pedro A. Lamothe is supported by a HHMI International Student Research Fellowship, CONACYT, and Fundacion Mexico en Harvard.

Pedro A. Lamothe, Huabiao Chen, Bruce D. Walker, Xiaolong Li, Jia-huai Wang, Jeffrey Weber, and Ruhong Zhou contributed to the experimental design and data analysis. Pedro A. Lamothe, Priya Jani, and Chioma Nwonu performed the functional experiments. Xiaolong Li, performed the structural experiments. Jeffrey Weber performed the molecular dynamics simulation and free energy perturbation experiments. Srinika Ranashinge provided intellectual input, editorial comments, and reagents. Bruce D. Walker. provided clinical samples. Bruce D. Walker, Jia-huai Wang, and Ruhong Zhou provided oversight of the project; Pedro A. Lamothe, Bruce D. Walker, Xiaolong Li, Jia-huai Wang, Jeffrey Weber, and Ruhong Zhou wrote the manuscript. Huabiao Chen started the project and conceived the idea of the dual presentation of the QW9 peptide. The manuscript of this project is currently in preparation and should be ready to submit for publication soon.

CHAPTER 3: Antiviral CD8+ T cells restricted by human leukocyte antigen class II exist during natural HIV infection and exhibit clonal expansion.

Antiviral CD8$^+$ T cells restricted by human leukocyte antigen class II exist during natural HIV infection and exhibit clonal expansion

Srinika Ranasinghe*[,1,13], Pedro A. Lamothe*[,1,2,3], Damien Z. Soghoian[1], Samuel W. Kazer[1,4,5], Michael B. Cole[6], Alex K. Shalek[1,4,5], Nir Yosef[6], R. Brad Jones[1,7], Faith Donaghey[1], Chioma Nwonu[1], Priya Jani[1], Gina M. Clayton[3,8], Frances Crawford[3,8], Janice White[8], Alana Montoya[8], Karen Power[1], Todd M. Allen[1], Hendrik Streeck[9,10], Daniel E. Kaufmann[1,11], Louis J. Picker[12], John W. Kappler[3,8] and Bruce D. Walker[1,2,3,4,5]

***Co-first Authors: These authors contributed equally to this work**

[1]Ragon Institute of MGH, MIT and Harvard, Cambridge, MA, 01239, USA

[2]Harvard T.H. Chan School of Public Health, Harvard University, Boston, MA, 02115, USA

[3]Howard Hughes Medical Institute, Chevy Chase, MD, 20815, USA

[4]Institute for Medical Engineering & Science, Massachusetts Institute of Technology, Cambridge, MA, 01239, USA

[5]Broad Institute, Cambridge, MA, 01239, USA

[6]Department of Physics, University of California, Berkeley, CA, 94720, USA

[7]George Washington University, Washington DC, 20052, USA

[8]Department of Biomedical Research, National Jewish Health, Denver, CO, 80206, USA

[9]Institute for HIV Research, University Hospital, University Duisburg-Essen, Essen, 45147 Germany

[10]U.S. Military HIV Research Program, Henry M. Jackson Foundation, Rockville, MD, 20910, USA

[11]Centre de Recherche du Centre hospitalier de l'Université de Montréal, Montreal, Quebec, H2X 3J4, Canada,

[12]Vaccine and Gene Therapy Institute and Oregon National Primate Research Center, Oregon Health & Science University, Beaverton, OR, USA

[13]Lead Contact

Correspondence: sranasinghe@mgh.harvard.edu or bwalker@mgh.harvard.edu

3.1 SUMMARY

$CD8^+$ T cell recognition of virus-infected cells is characteristically restricted by major histocompatibility complex (MHC) class I, although rare examples of MHC class II-restriction have been reported in *Cd4*-deficient mice and a macaque SIV vaccine trial using a recombinant cytomegalovirus vector. Here, we demonstrate the presence of human leukocyte antigen (HLA) class II-restricted $CD8^+$ T cell responses with antiviral properties in a small subset of HIV-infected individuals. In these individuals, T cell receptor β (TCRβ) analysis revealed that class II-restricted $CD8^+$ T cells underwent clonal expansion and mediated killing of HIV-infected cells. In one case, these cells comprised 12% of circulating $CD8^+$ T cells, and TCRα analysis revealed two distinct co-expressed TCRα chains, with only one contributing to binding of the class II HLA-peptide complex. These data indicate that class II-restricted $CD8^+$ T cell responses can exist in a chronic human viral infection, and may contribute to immune control.

3.2 BACKGROUND

Antigen-specific $CD8^+$ T cells are a major defense against invading viruses, killing infected cells harboring non-self proteins. The first step in this process involves T cell receptor (TCR) recognition of virus-derived peptides presented on the surface of infected cells by molecules of the major histocompatibility complex (MHC), or human leukocyte antigen (HLA) in humans. The dominant paradigm of T cell recognition dictates that $CD8^+$ T cells recognize viral peptides of 8-11 amino acids in length bound to MHC class I molecules, whereas $CD4^+$ T cells recognize peptides of 12 or more amino acids restricted by MHC class II [58]. During thymic selection, double positive T cells undergo a maturation process where they are selected as either $CD8^+$ T cells or $CD4^+$ T cells depending on TCR binding to peptide complexed with MHC class I or class II, respectively. However, in certain cases T cells with atypical modes of MHC restriction have been reported. $CD8^+$ T cell responses restricted by MHC class II have been described in approximately a dozen published reports over the past two decades. These responses have been observed in *Cd4*-deficient mice, where the complete absence of $CD4^+$ T cells led to the unexpected expansion of $CD8^+$ T cells restricted by class II [108, 109, 110, 111, 112, 113], and in mouse models of transplantation [114]. In humans, reports have also described alloreactive $CD8^+$ T cell responses that cross-recognize HLA class I and II [115, 116], indicating that unconventional HLA and TCR interactions may be an important feature of allorecognition.

Remarkably, virus-specific $CD8^+$ T cells restricted by MHC class II were recently found to be the immunodominant responses detected in the context of immunization with a recombinant rhesus Cytomegalovirus (RhCMV) vector in a macaque simian immunodeficiency virus (SIV) vaccine model [117], which also induced non-classical MHC-

E restricted $CD8^+$ T cell responses [118]. In this setting, the induction of $CD8^+$ T cells with unconventional MHC restriction was predominantly under the genetic control of the strain 68-1 RhCMV vector and the epitopes targeted by these responses did not overlap with traditional MHC class I-restricted responses. These studies demonstrate that unconventional $CD8^+$ T cell responses can be elicited by engineered RhCMV vaccine vectors and suggest these responses may contribute to the control of viral replication [120].

The extent to which HLA class II-restricted $CD8^+$ T cell responses play a role in natural human immunity is unclear. To address this in a chronic human viral infection, we screened a large cohort of HIV-1 infected persons, including HIV controllers who spontaneously control virus in the absence of antiretroviral therapy. In these HIV controllers, we and others have shown that class I-restricted $CD8^+$ T cell responses, particularly HLA-B restricted responses targeting epitopes within the highly conserved Gag protein, are associated with enhanced control of viral replication [66, 67, 68, 69, 70, 71, 72]. We now provide data showing induction of class II HLA-DR-restricted $CD8^+$ T cell responses in three of 101 HIV controllers tested. These class II-restricted $CD8^+$ T cells exhibited potent antiviral functions and were characterized by a single dominant TCRβ clonotype. In one individual, the HLA-DR-restricted $CD8^+$ T cells were immunodominant, comprising 12% of circulating $CD8^+$ T cells. These data reveal the rare presence of atypical $CD8^+$ T cells restricted by HLA-DR in a human viral infection and indicate T cells that violate immunologic paradigms may shape human antiviral responses.

3.3 RESULTS

3.3.1 CD8$^+$ T cell responses restricted by HLA-DRB1 exist in natural HIV infection

Virus-specific CD8$^+$ T cells typically recognize infected cells through presentation of processed viral peptides on HLA class I molecules, but class II-restricted responses have been detected in some experimental systems and in the context of CMV vector immunization in a macaque SIV vaccine model [117]. In order to determine whether such responses exist in a chronic human viral infection, we screened 129 people with untreated HIV-1 infection, all of whom expressed common class II DRB1 alleles (**Supplemental Table S3.1**). These included 101 untreated HIV controllers who maintained viral loads of less than 2000 RNA copies/ml plasma, as well as 28 individuals with untreated chronic HIV infection exhibiting high viral loads.

Purified CD8$^+$ T cells isolated from the peripheral blood mononuclear cells (PBMC) of each subject were co-cultured with mouse lymphoblastoid cell lines (LCL) stably expressing a single recombinant human DRB1 molecule [146, 147] matched to the donor, which had been pulsed with individual overlapping peptides spanning the HIV Gag protein. In initial screening, we identified an HIV controller, subject 474723, in whom a single Gag peptide presented by class II HLA DRB1*11:01 resulted in a robust interferon gamma (IFN-γ) Elispot response mediated by CD8$^+$ T cells **(Figure 3.1A)**. This targeted peptide, Gag41 (YVDRFYKTLRAEQASQEV, aa 164-181) is also known to be presented by DRB1*11:01 for CD4$^+$ T cell recognition in HIV-infected persons [147]. N and C terminal truncations indicated that presentation of the FYKTLRAEQA peptide contained within the larger peptide likely represented the core residues sufficient to elicit a response **(Figure 3.1B),** with phenylalanine or tyrosine likely to be the P1 anchor residue. Of the truncated

peptides tested, the most robust response was to the 16 amino acid peptide DRFYKTLRAEQASQEV, which is expected to extend out of the open class II binding groove. Class II restriction of the Gag41-specific $CD8^+$ T cell response was verified using an anti-HLA-DR blocking antibody that inhibited IFN-γ production in a dose dependent manner **(Figure 3.1C)**.

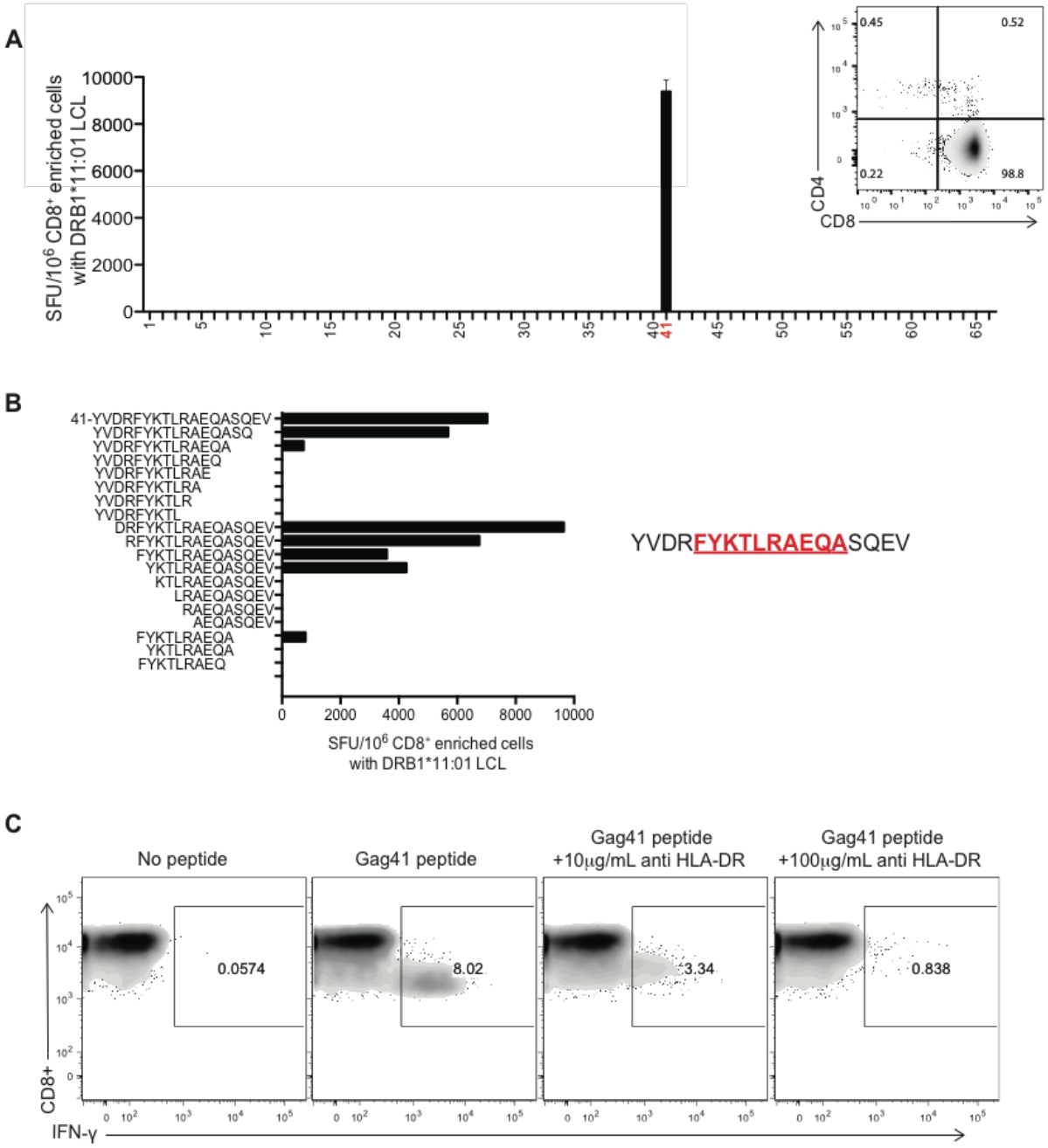

Figure 3.1 Elucidation of a HLA class II DRB1-restricted CD8$^+$ T cell response in HIV controller 474723 (**A**) Representative IFN-γ HLA-DR Elispot using magnetically-enriched CD8$^+$ T cells (FACS plot insert) co-cultured with an LCL stably transfected with DRB1*11:01 (matching the HLA type of subject) pulsed with 66 overlapping peptides (OLPs) spanning the HIV Gag protein. (**B**) Representative IFN-γ HLA-DR Elispot performed with N- and C-terminal peptide truncations presented on DRB1*11:01 LCL. Epitope FA10 within Gag41 is highlighted in red (**C**) Representative flow cytometric intracellular cytokine secretion (ICS) assay with anti-HLA-DR antibody performed on whole PBMC co-cultured with DRB1*11:01 LCL.

To further confirm that this response was indeed mediated by class II-restricted $CD8^+$ T cells, and to more precisely define the magnitude of the response, we constructed class II tetramers with a truncated version of the Gag41 peptide (DRFYKTLRAEQASQEV) that elicited the strongest Elispot response. Greater than 12% of circulating $CD8^+$ T cells were DR11-Gag41 tetramer positive directly *ex vivo* **(Figure 3.2A),** which was further confirmed by dual staining with both allophycocyanin (APC) and phycoerythrin (PE) conjugated versions of the tetramer **(Figure 3.2B)**.

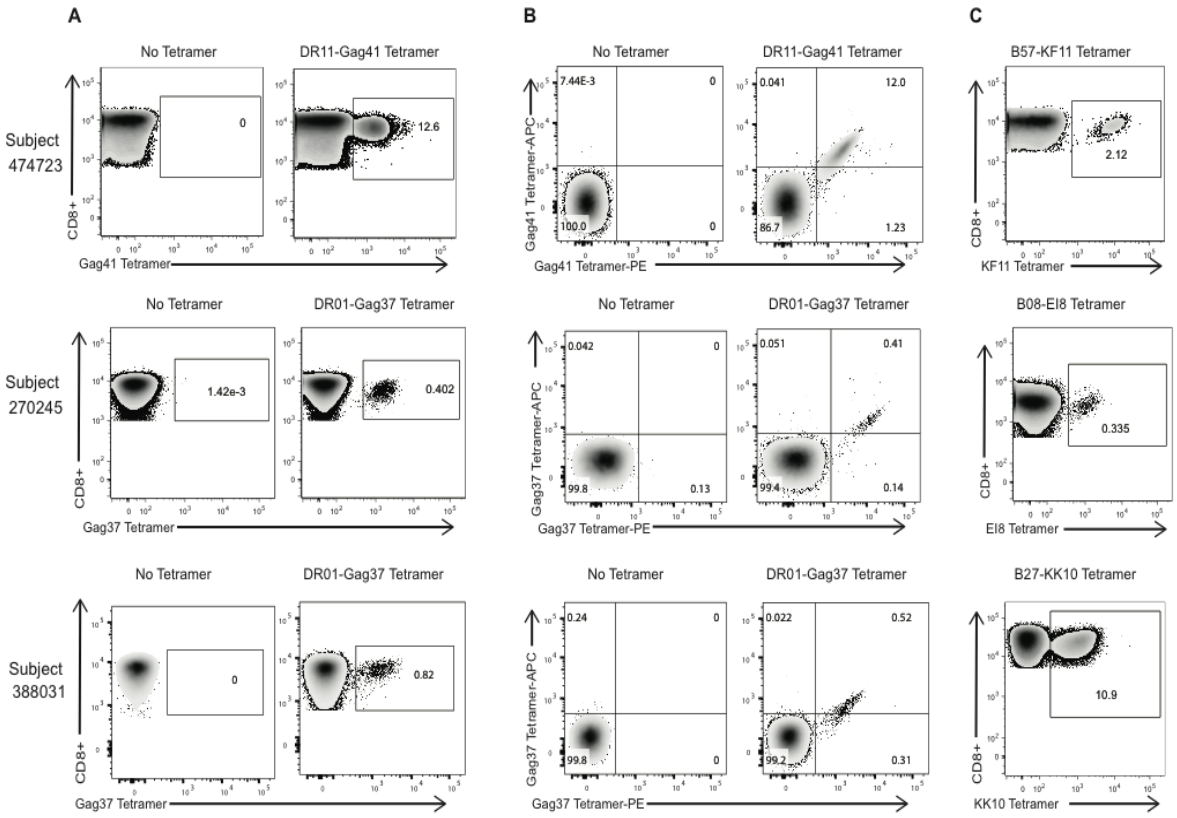

Figure 3.2 Detection of HLA class II DRB1-restricted $CD8^+$ T cell responses in three HIV Controllers by class II tetramers (**A**) Representative FACS plots of HLA class II tetramer staining using fresh PBMCs. Bulk $CD8^+$ T cells are shown in the absence and presence of DR11-Gag41 tetramer for subject 474723, and DR01-Gag37 tetramer for subjects 270245 and 388031. (**B**) Representative FACS plot of dual PE and APC conjugated class II tetramer staining (**C**) Representative FACS plots of class I tetramer staining. All populations shown are gated on $CD3^+CD8^+CD4^-CD19^-CD14^-CD56^-$ live lymphocyte singlets.

Assessment of subjects by IFN-γ Elispot revealed that this was the only person in whom a class II restricted $CD8^+$ T cell response could be detected to the Gag41 epitope, and this was further confirmed by staining PBMC of 76 persons expressing HLA DRB1*11:01 (including the 39 initially screened by IFN-γ Elispot) with DR11-Gag41 tetramers (**Supplemental Table S3.1**). However, extended IFN-γ Elispot screening and subsequent construction of class II tetramers revealed two additional subjects, 270245 and 388031, in whom class II-restricted $CD8^+$ T cell responses were detectable, both targeting a peptide designated Gag37 (LNKIVRMYSPTSILD, aa 136-151) restricted by HLA-DRB1*01:01. Although these responses were present at much lower frequencies than the DR11-Gag41 restricted response**,** dual APC and PE tetramer staining of the $CD8^+$ T cell populations using a DR01-Gag37 tetramer confirmed these were indeed class II-restricted **(Figure 3.2B**). All class II tetramers showed minimal non-specific staining when tested on HLA-matched HIV-negative and HIV-positive subjects **(Supplemental Figure S3.1)**. **Supplemental Table S3.2** shows HLA genotyping and clinical characteristics of these 3 subjects with class II restricted $CD8^+$ T cell responses.

We next compared the magnitude and specificity of the class II-restricted $CD8^+$ T cells with the most immunodominant class I-restricted Gag-specific $CD8^+$ T cells in each of the three subjects, using HLA tetramers **(Figure 3.2C)** and Elispot assays **(Supplemental Figure S3.2)**. In terms of magnitude, for subject 474723 the DR11-Gag41 restricted response was immunodominant over all class I-restricted Gag-specific responses tested, at 12% frequency compared to a class I B57-$KF11^+$ tetramer population of 2% frequency *ex vivo*. In terms of specificity, there was minimal overlap between HLA class I and class

II epitopes to which responses were detected **(Supplemental Figure S3.3A).** However, in the other two subjects, the unconventional responses were subdominant. The DR01-Gag37 epitope was adjacent to epitope B*08-EI8 in subject 270245, and partially overlapped with immunodominant epitope B*27-KK10 in subject 388031, yet each population was distinct by class I and II tetramer staining **(Supplemental Figures S3.3B-C**).

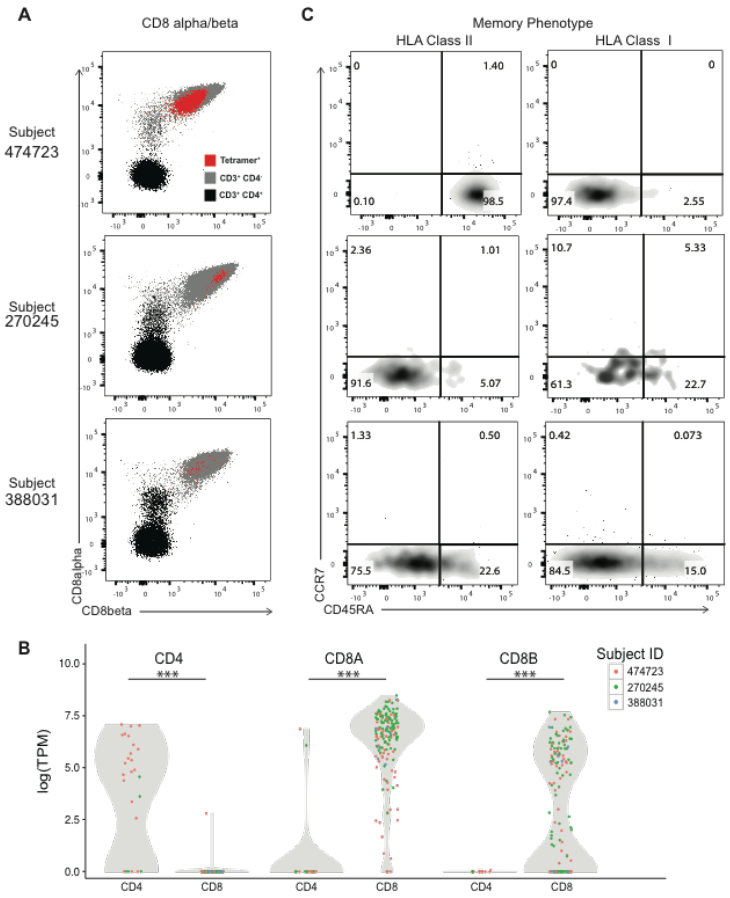

Figure 3.3 HLA class II-restricted CD8αβ T cells in three HIV Controllers exhibit heterogeneous memory phenotypes (**A**) Representative FACS plots denoting surface expression of CD8α and CD8β. Tetramer positive expression is shown in red. Bulk $CD3^+$ $CD4^-$ T cells are shown in grey. $CD3^+$ $CD4^+$ T cells are shown in black. (**B**) Violin plots denoting the distribution of single-cell expression levels of CD8α (CD8A), CD8β (CD8B), and CD4 RNA transcripts in unstimulated class II tetramer sorted $CD8^+$ and $CD4^+$ T cells estimated from single-cell RNA-Seq. (TPM: transcripts per kilobase million). Statistical significance was determined using Mann-Whitney-Wilcoxon test (*** denotes p<0.001). (**C**) Representative FACS plots show memory phenotype of tetramer positive HLA class I and class II-restricted $CD8^+$ T cells. All populations shown are gated on $Tetramer^+$ $CD3^+$ $CD8^+$ $CD4^-$ $CD19^-$ $CD14^-$ $CD56^-$ live lymphocyte singlets.

We next investigated the phenotypic characteristics of the patient-derived class II tetramer positive $CD8^+$ T cell populations using flow cytometry (**Figure 3.3A**) and single-cell RNA sequencing (scRNA-seq) (**Figure 3.3B**). We found that both CD8α and CD8β were expressed at the protein and transcript levels. The class II-restricted $CD8\alpha\beta^+$ T cells did not co-express CD4 protein or mRNA. Next, we assessed the memory phenotype of these responses. All three subjects exhibited antigen-experienced effector memory phenotypes, although the degree of differentiation was different for each subject. In 474723, the immunodominant DR11-Gag41 positive $CD8^+$ T cells manifested an unusual differentiation for HIV-specific $CD8^+$ T cells: all tetramer positive cells exhibited a highly differentiated effector memory (Temra) phenotype ($CCR7^-$, $CD45RA^+$) (**Figure 3.3C).** In contrast, the DR01-Gag37 positive $CD8^+$ T cells, which were subdominant *in vivo* in both individuals, predominantly exhibited an effector memory (Tem) phenotype ($CCR7^-$, $CD45RA^-$). PD-1 expression was found to be consistent with their memory phenotype **(Supplemental Figure S3.4)**.

Collectively, these data indicate that virus-specific $CD8\alpha\beta^+$ T cell responses restricted by HLA-DRB1 exist in the setting of natural HIV infection, and although this is a rare event, such responses can represent an immunodominant HIV-specific $CD8^+$ T cell response.

3.3.2 HLA class II DRB1-restricted $CD8^+$ T cells lyse autologous HIV infected targets ex vivo

Little is known about the function of $CD8^+$ T cells restricted by HLA class II, and particularly whether these cells have antiviral properties. Therefore, we examined the expression of granzyme B in class II-restricted $CD8^+$ T cells by intracellular staining and flow cytometry. The majority of class II tetramer$^+$ $CD8^+$ T cells from each subject was

granzymeB^{high} when compared to bulk CD8^{+} T cells (**Figure 3.4A**). Additionally, transcriptional profiling conducted by scRNA-Seq on tetramer sorted single cells confirmed that class II-restricted CD8^{+} T cells from all three subjects expressed perforin, granzyme B, granzyme H, MIP-1β, and RANTES (**Figure 3.4B**).

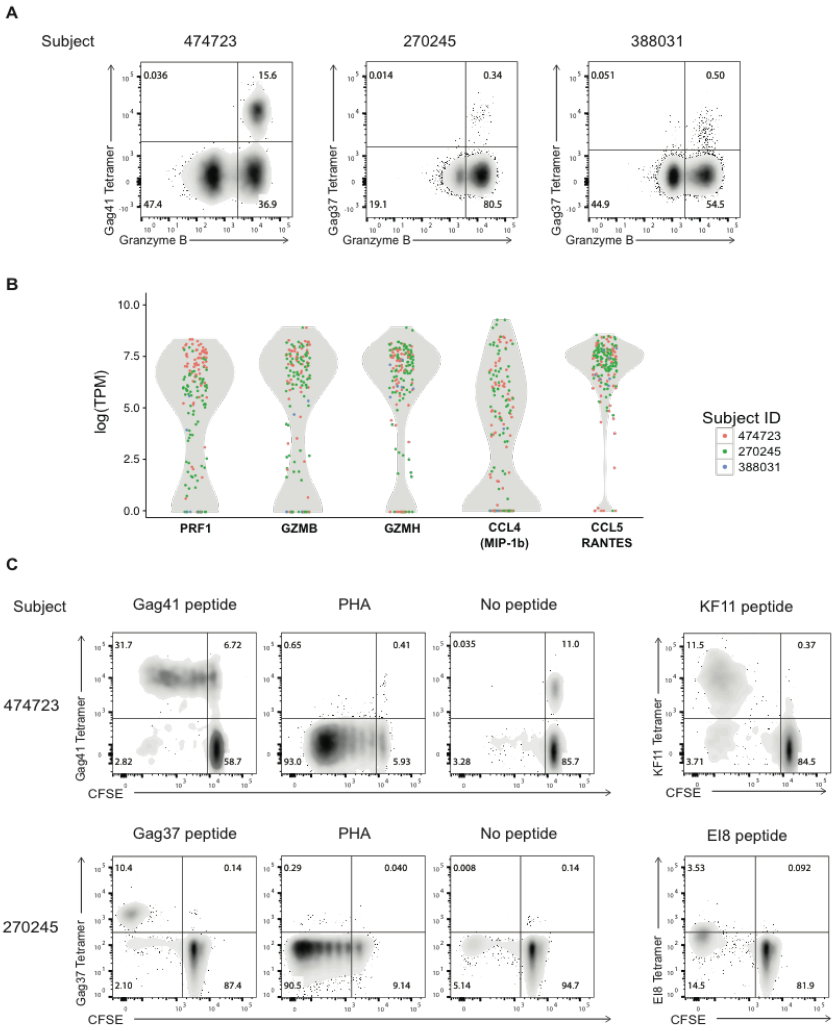

Figure 3.4 HLA class II-restricted CD8^{+} T cells exhibit cytolytic properties and proliferative capacity
(**A**) Representative FACS plots gated on unstimulated CD8^{+} T cells expressing intracellular granzyme B and tetramer in three HIV controllers. Tetramer populations are gated on Tetramer^{+}CD3^{+}CD8^{+}CD4^{-}CD19^{-} CD14^{-}CD56^{-} live lymphocyte singlets. (**B**) Violin plots denoting the distribution of single-cell levels of Perforin, Granzyme B, Granzyme H, MIP-1b and RANTES RNA transcripts in unstimulated class II tetramer-sorted CD8^{+} T cells from three HIV controllers by scRNA-Seq. (**C**) Representative FACS plots gated on CD8^{+} T cells expressing CFSE and tetramer at day 7 following stimulation of bulk PBMC from HIV controller 474723 and 270245. (TPM: Transcripts per kilobase million, PHA: phytohaemagglutinin)

As previous studies have shown proliferation in response to epitope recognition to be associated with antiviral function [73, 134], we next compared the proliferative capacity of class II-restricted $CD8^+$ T cells with the most immunodominant class I-restricted Gag-specific $CD8^+$ T cell response in subjects 474723 and 270245, for whom sufficient samples were available. The class II tetramer positive cells demonstrated specific proliferation upon stimulation with cognate peptide (**Figure 3.4C**). Of note, class I tetramer positive cells from subject 270245 showed populations that were carboxyfluorescein diacetate succinimidyl ester ($CFSE^+$) positive yet tetramer-negative, possibly due to TCR down-regulation or non-specific proliferation induced by activation. These data demonstrate that DR11-Gag41 positive $CD8^+$ Temra cells and DR01-Gag37 positive $CD8^+$ Tem cells have substantial proliferative capacity.

We next generated class II-restricted $CD8^+$ T cell clones from subjects 474723 and 270245. These clones demonstrated specific, potent killing of autologous Epstein–Barr virus (EBV)-transformed B cells (BCL) pulsed with the cognate class II peptide. Additionally, the class II restricted clones showed substantial cytolytic activity against autologous $CD4^+$ T cells super-infected with HIV-1 NL4.3 as well as against $CD14^+$ monocyte-derived macrophages super-infected with Vesicular stomatitis virus *G*-protein (VSV-G) pseudotyped HIV-1 NL4.3 expressing GFP **(Figure 3.5A)**.

Thereafter, we tested the ability of class II-restricted $CD8^+$ T cells to kill directly *ex vivo* and compared their antiviral efficacy with the class I-restricted $CD8^+$ T cell population (**Figure 3.5B**). BCLs, used as target cells for this assessment, displayed equivalent

surface expression of HLA-ABC and HLA-DR **(Supplemental Figure S3.5)**. The DR11-Gag41$^+$ and B57-KF11$^+$ populations from subject 474723, as well as the DR01-Gag37$^+$ and the B*08-EI8$^+$ populations from subject 270245, were tetramer-sorted from fresh blood, and then co-cultured with autologous BCL in a chromium release assay. The class II-restricted CD8$^+$ T cells from both subjects demonstrated direct *ex-vivo* specific killing of peptide-pulsed BCL akin to that of the immunodominant class I-restricted CD8$^+$ T cell responses, indicative that these populations exhibit a similar killing efficiency (**Figure 3.5B**). Longer incubation of Gag41-loaded target cells with either tetramer-sorted CD8$^+$ T cells or bulk CD8$^+$ T cells from subject 474723 in a modified *in Vitro* Technique for Assessing Lysis (VITAL) assay, resulted in greater than 98% elimination of target cells over a 36-hour incubation. The percentage of lysed target cells was similar to that achieved with bulk CD8$^+$ T cells co-cultured with KF11-loaded target cells, whereas target cells loaded with a control peptide were not eliminated **(Supplemental Figure S3.6)**.

We subsequently evaluated the ability of *ex vivo*-isolated class II-restricted CD8$^+$ T cells to recognize and kill HIV-infected cells displaying naturally processed HIV antigen resulting from productive infection. Due to limited sample availability from subject 474723 we focused on autologous monocyte-derived macrophage targets that express naturally high levels of surface HLA-DR. The monocyte-derived macrophages were super-infected with a VSV-G pseudotyped HIV-1 NL4.3 prior to co-culture with freshly isolated tetramer sorted DR11-Gag41$^+$ CD8$^+$ T cells. We observed that effectors lysed HIV-infected macrophages directly *ex vivo*, with 19% mean specific lysis compared to 4% mean specific lysis in the control (p=0.049) **(Figure 3.5C)**. Infection of viable macrophages,

measured by GFP$^+$ expression or p24$^+$ staining, was >92% **(Supplemental Figure S3.5)**. These data demonstrate that HIV-infected macrophages effectively process and present naturally-derived HIV peptide on the cell surface for recognition by class II-restricted CD8$^+$ T cells.

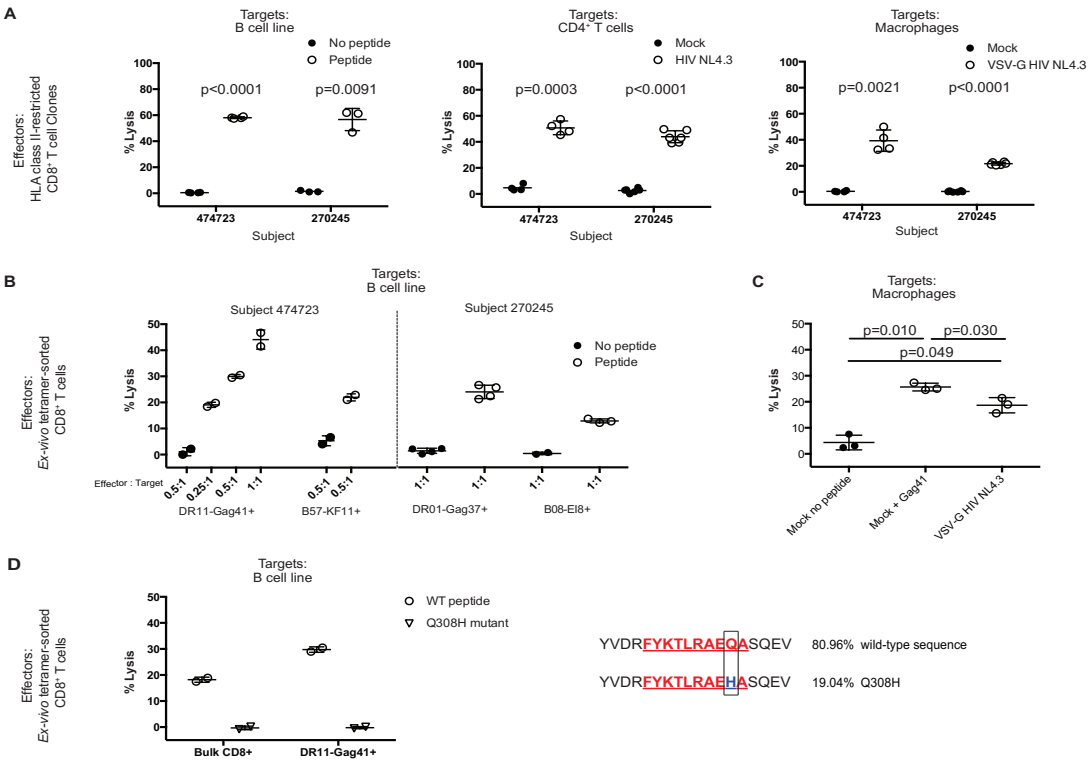

Figure 3.5 HLA class II-restricted CD8$^+$ T cells lyse autologous HIV infected targets *ex vivo* and exert putative immune selection pressure *in vivo* (**A**) Summary data assessing specific lysis of target cells by class II-restricted CD8$^+$ T cell clones from subject 474723 and 270245 in a standard 6 hr chromium release assay. Autologous targets included EBV-transformed BCL pulsed with peptide or no peptide, CD4$^+$ T cells infected with the HIV strain NL4.3, and monocyte-derived macrophages infected with VSV-G psuedotyped HIV NL4.3 encoding GFP, all at an effector to target cell ratio (E:T) of 1:1. Statistical significance was determined using a paired T-test (**B**) Summary data assessing specific lysis of target cells by *ex-vivo* tetramer$^+$ sorted HLA class I- and class II-restricted CD8$^+$ T cells in a standard 6 hr chromium release assay at multiple E:T ratios. *Ex-vivo* effector cells were derived from fresh blood and tetramer sorted within 12hrs of phlebotomy. As target cells, autologous EBV-transformed BCL from subjects 474723 and 270245 were pulsed with cognate peptide or no peptide. Statistical significance was determined using a paired T-test. (**C**) Summary data assessing specific lysis of autologous monocyte-derived macrophages pulsed with the cognate peptide Gag41 or infected with VSV-G psuedotyped HIV NL4.3 encoding GFP by *ex vivo* DR11-Gag41 tetramer$^+$ sorted CD8$^+$ T cells from subject 474723 in a standard 6 hr chromium release assay at an E:T ratio of 1:1. (**D**) Deep sequencing of autologous virus in subject 474723. Mutation Q308H within the Gag41 epitope is boxed. Specific lysis of EBV-transformed BCL pulsed with wild type Gag41 peptide or the Q308H mutant peptide was tested in a standard 6 hr chromium release assay with *ex-vivo* tetramer-sorted DR11-Gag41 tetramer$^+$ sorted CD8$^+$ T cells or bulk CD8$^+$ T cells at a 1:1 E:T ratio. All data points for each graph A-D represent biological replicates in a single experiment.

As a further measure of potential $CD8^+$ T cell mediated antiviral function, we examined the sequence of the HLA-DR-restricted epitope for evidence of immune selection pressure. Over 80% of sequences in subject 474723 showed homology to the Gag41 peptide sequence. However, almost 20% of sequences exhibited a Q308H mutation within the Gag41 epitope (**Figure 3.5D**). While the DR11-$Gag41^+$ effectors and the bulk $CD8^+$ T cells effectively lysed BCL pulsed with wild-type peptide, they showed no detectable lysis of the Q308H peptide, consistent with this being a putative escape mutation. There was no detectable $CD8^+$ T cell response to B57-QW9 in this subject and prior sequencing of B57 controllers has not detected any Q308H mutants [68], indicating that Gag41-specific T cells likely drive Q308H escape. These data suggest that the DR11-Gag41-restricted T cells may be capable of exerting immune selection pressure.

Taken together, our data assessing the cytolytic marker expression, epitope-specific proliferative capacity, target cell lysis, and immune selection pressure indicate that class II-restricted $CD8^+$ T cells demonstrate potent antiviral properties.

3.3.3 HLA class II-restricted $CD8^+$ T cells are constituted by one dominant TCRβ clonotype

To further define these HLA class II-restricted $CD8^+$ T cell responses, we computationally reconstructed TCR using scRNA-seq data from single tetramer-sorted class II restricted $CD8^+$ T cells from each of the three subjects. In each, we found that the class II-restricted $CD8^+$ T cell response was characterized by expansion of a single TCRβ clonotype (**Figure 3.6**).

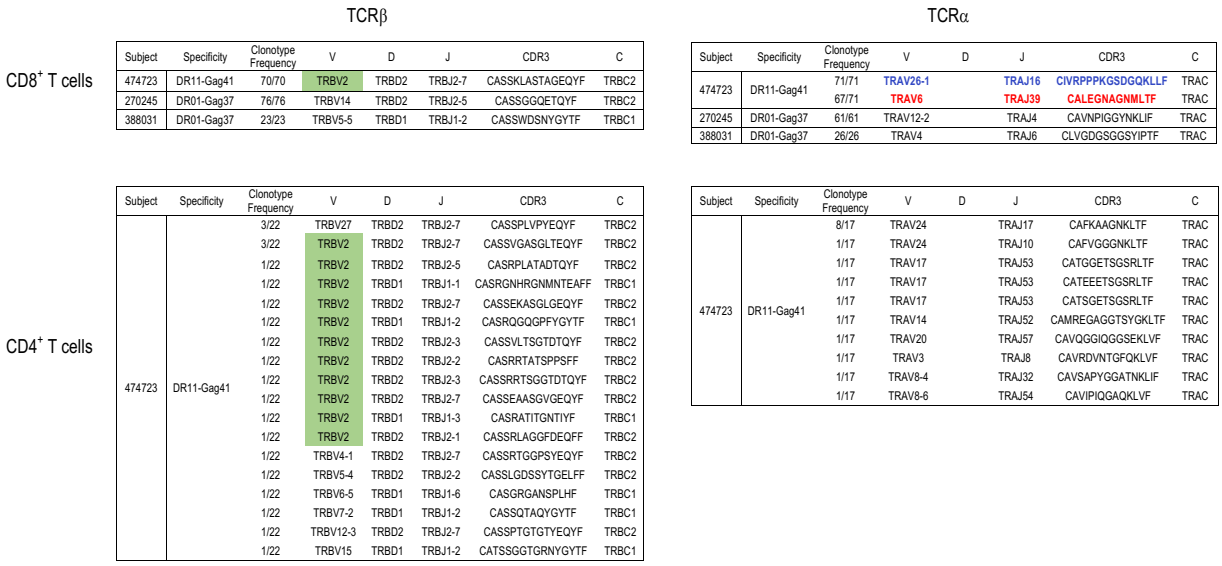

Subject	Specificity	Clonotype Frequency	V	D	J	CDR3	C
474723	DR11-Gag41	70/70	TRBV2	TRBD2	TRBJ2-7	CASSKLASTAGEQYF	TRBC2
270245	DR01-Gag37	76/76	TRBV14	TRBD2	TRBJ2-5	CASSGGQETQYF	TRBC2
388031	DR01-Gag37	23/23	TRBV5-5	TRBD1	TRBJ1-2	CASSWDSNYGYTF	TRBC1

Subject	Specificity	Clonotype Frequency	V	D	J	CDR3	C
474723	DR11-Gag41	71/71	TRAV26-1		TRAJ16	CIVRPPPKGSDGQKLLF	TRAC
		67/71	TRAV6		TRAJ39	CALEGNAGNMLTF	TRAC
270245	DR01-Gag37	61/61	TRAV12-2		TRAJ4	CAVNPIGGYNKLIF	TRAC
388031	DR01-Gag37	26/26	TRAV4		TRAJ6	CLVGDGSGGSYIPTF	TRAC

Subject	Specificity	Clonotype Frequency	V	D	J	CDR3	C
474723	DR11-Gag41	3/22	TRBV27	TRBD2	TRBJ2-7	CASSPLVPYEQYF	TRBC2
		3/22	TRBV2	TRBD2	TRBJ2-7	CASSVGASGLTEQYF	TRBC2
		1/22	TRBV2	TRBD2	TRBJ2-5	CASRPLATADTQYF	TRBC2
		1/22	TRBV2	TRBD1	TRBJ1-1	CASRGNHRGNMNTEAFF	TRBC1
		1/22	TRBV2	TRBD2	TRBJ2-7	CASSEKASGLGEQYF	TRBC2
		1/22	TRBV2	TRBD1	TRBJ1-2	CASRQGQGPFYGYTF	TRBC1
		1/22	TRBV2	TRBD2	TRBJ2-3	CASSVLTSGTDTQYF	TRBC2
		1/22	TRBV2	TRBD2	TRBJ2-2	CASRRTATSPPSFF	TRBC2
		1/22	TRBV2	TRBD2	TRBJ2-3	CASSRRTSGGTDTQYF	TRBC2
		1/22	TRBV2	TRBD2	TRBJ2-7	CASSEAASGVGEQYF	TRBC2
		1/22	TRBV2	TRBD1	TRBJ1-3	CASRATITGNTIYF	TRBC1
		1/22	TRBV2	TRBD2	TRBJ2-1	CASSRLAGGFDEQFF	TRBC2
		1/22	TRBV4-1	TRBD2	TRBJ2-7	CASSRTGGPSYEQYF	TRBC2
		1/22	TRBV5-4	TRBD2	TRBJ2-2	CASSLGDSSYTGELFF	TRBC2
		1/22	TRBV6-5	TRBD1	TRBJ1-6	CASGRGANSPLHF	TRBC1
		1/22	TRBV7-2	TRBD1	TRBJ1-2	CASSQTAQYGYTF	TRBC1
		1/22	TRBV12-3	TRBD2	TRBJ2-7	CASSPTGTGTYEQYF	TRBC2
		1/22	TRBV15	TRBD1	TRBJ1-2	CATSSGGTGRNYGYTF	TRBC1

Subject	Specificity	Clonotype Frequency	V	D	J	CDR3	C
474723	DR11-Gag41	8/17	TRAV24		TRAJ17	CAFKAAGNKLTF	TRAC
		1/17	TRAV24		TRAJ10	CAFVGGGNKLTF	TRAC
		1/17	TRAV17		TRAJ53	CATGGETSGSRLTF	TRAC
		1/17	TRAV17		TRAJ53	CATEEETSGSRLTF	TRAC
		1/17	TRAV17		TRAJ53	CATSGETSGSRLTF	TRAC
		1/17	TRAV14		TRAJ52	CAMREGAGGTSYGKLTF	TRAC
		1/17	TRAV20		TRAJ57	CAVQGGIQGGSEKLVF	TRAC
		1/17	TRAV3		TRAJ8	CAVRDVNTGFQKLVF	TRAC
		1/17	TRAV8-4		TRAJ32	CAVSAPYGGATNKLIF	TRAC
		1/17	TRAV8-6		TRAJ54	CAVIPIQGAQKLVF	TRAC

Figure 3.6 TCR repertoires of HLA Class II-restricted CD8$^+$ T cells are comprised by monoclonal responses. *Ex-vivo* class II-restricted CD8$^+$ and CD4$^+$ T cells were tetramer-sorted to be used for scRNA-Seq and subsequent TCR reconstruction. TCR β and α clonotypes are shown for each identified subject, with relevant sequences highlighted in color. Relative α and β clonotype frequency was calculated as following: number of cells with a particular clonotype / total number of cells from which any TCR Vβ or Vα gene was reconstructed, respectively. (CDR3: complementarity-determining region 3)

As the HLA class II-restricted CD8$^+$ T cell responses identified here are also immunodominant epitopes normally seen by conventional class II restricted CD4$^+$ T cell responses [147, 148], we next analyzed whether both CD4$^+$ and CD8$^+$ T cells could bind the class II tetramers. The same class II tetramers that recognized CD8$^+$ T cells also stained *ex-vivo* CD4$^+$ T cells, albeit very weakly in two of the three subjects (**Figure 3.7A**). These tetramer positive CD4$^+$ T cells were within the expected range for an epitope-specific response [149], yet the frequency of the class II-restricted CD8$^+$ T cell population intra-patient was dramatically larger. Together, these data reveal an immunological phenomenon in which conventional HLA class II-restricted CD4$^+$ and unconventional class II-restricted CD8$^+$ T cells can bind the same peptide-HLA complex.

We next examined whether $CD8^+$ and $CD4^+$ T cells targeting the same peptide-HLA had similar TCR rearrangements. Due to sample availability and tetramer-positive $CD4^+$ cell number constraints, we were limited to analysis of subject 474723. As we had already identified the TCRβ V gene for the DR11-Gag41$^+$ restricted $CD8^+$ T cells, we used the class II tetramers and a TRBV2-specific fluorescent antibody to analyze both $CD8^+$ and $CD4^+$ populations (**Figure 3.7B**). Consistent with the sequencing results, we found that the class II restricted $CD8^+$ population was comprised of 99.9% TRBV2-positive cells, and that 73.9% of the tetramer positive $CD4^+$ response was also TRBV2 positive.

We also computationally reconstructed TCRs using scRNA-seq data from single DR11-Gag41 tetramer-sorted $CD4^+$ T cells. We identified 22 TCR β sequences for the DR11-Gag41 restricted $CD4^+$ T cells. In contrast to the DR11-Gag41 restricted $CD8^+$, where there was only one dominant clonotype, we observed a more diverse response comprised of 16 different clonotypes for the $CD4^+$ T cells. Many clonotypes (13/22) used the same TRBV2 gene but had different rearrangements, highlighted in green in **Figure 3.6**. Thus in subject 474723, we found that TRBV2 is preferentially selected by both $CD8^+$ and $CD4^+$ T-cell responses that target this class II HLA-peptide complex.

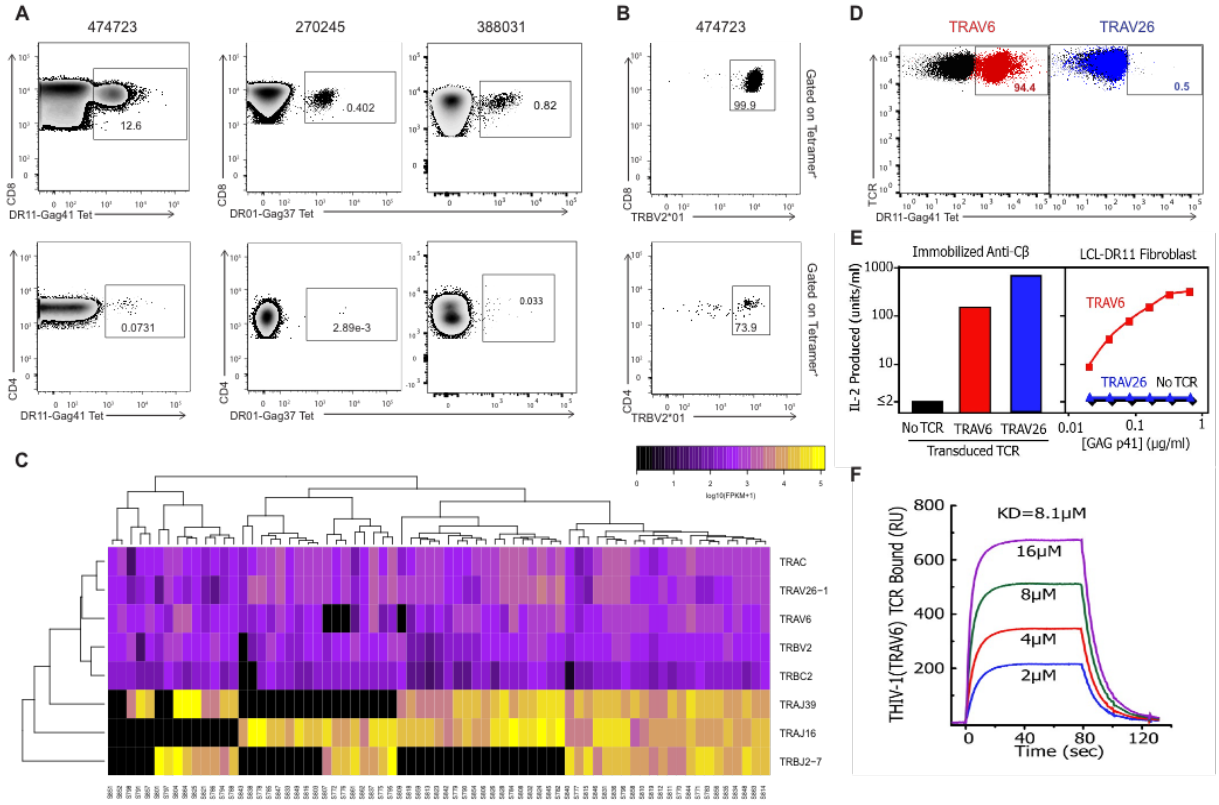

Figure 3.7 DR11-Gag41-restricted CD8$^+$ T cells are constituted by one dominant TCRβ clonotype yet co-express two different TCRα chains (**A**) Representative FACS plots of CD8$^+$ T cell responses (top) and CD4$^+$ T-cell responses (bottom) for each of three subjects stained with the same class II tetramers. PBMC from subject 474723 were stained with DR11-Gag41 tetramer, and from subjects 270245 and 388031 with DR01-Gag37. All populations shown are gated on CD3$^+$CD19$^-$CD14$^-$CD56$^-$ live lymphocyte singlets. (**B**) Representative FACS plot gated on CD8$^+$ and CD4$^+$ T cells from subject 474723 stained with a fluorescently-conjugated TCR TRVB2*01-specific antibody and DR11-Gag41 tetramer. Populations shown are gated on DR11-Gag41 Tetramer$^+$CD3$^+$CD19$^-$CD14$^-$CD56$^-$ live lymphocyte singlets. (**C**) Heatmap showing expression of α and β TCR V, J and C segments (rows) from individual cells (columns) from subject 474723. Ex-vivo DR11-Gag41-specific CD8$^+$ T cells were tetramer-sorted as single cells for scRNA-Seq and subsequent TCR reconstruction. (**D**) Representative FACS plot of TRAV6 and TRBV2 expressing hybridomas (left) and TRAV26 and TRBV2 expressing hybridoma (right) stained with a fluorescent HLA-DR11-Gag41 tetramer (red or blue) or no tetramer (black). (**E**) Left panel: T cell hybridomas expressing no TCR (black) or transduced with either the TRAV6/TRBV2 TCR (red) or the TRAV26/TRBV2 TCR (blue) were stimulated non-antigen specifically overnight with a plate bound anti-Cβ Mab to confirmed the signaling ability of the TCRs. Supernatants were assayed for secreted IL-2. Right panel: The same T cells were cultured overnight with an HLA-DR11 bearing LCL and various concentrations of the Gag-41 peptide. Supernatants were assayed for secreted IL-2 by ELISA. (**F**) Biotinylated HLA DR11-Gag41 (~2000 RU) was captured in a flow cell of a BIAcore streptavidin biosensor chip. Various concentrations of soluble TRAV6 and TRBV2 were injected for 80 seconds, and the affinity was calculated with BIAEvaluation 4.1 software after correction for the fluid phase RU signal. (FPKM: fragments per kilobase million)

From characterization of the TCR β gene usages of both DR11-Gag41 $CD4^+$ and $CD8^+$ T cells using computational reconstruction from the scRNA-seq data, we obtained TCR β sequences from 71 and 17 single cells of the $CD8^+$ and $CD4^+$ populations, respectively. We found that the $CD8^+$ T cell repertoire had only one TCR β clonotype comprised of gene segments TRBV2, TRBJ2-7, TRBC2 but two distinct TCRα clonotypes. One was comprised of gene segments TRAV6, TRAJ39, TRAC and the second was comprised of TRAV26-1, TRAJ16, TRAC. However, the $CD4^+$ repertoire had 10 different TCR β clonotypes (**Figure 3.6**). Because this analysis was performed from sorted DR11-Gag41$^+$ T cells at a single cell per well for downstream RNA-Seq and TCR reconstruction, we could identify that the two different TCR α chains TRAV6-TRAJ39 and TRAV26-TRAJ16 were co-expressed within the same $CD8^+$ T cell, consistent with incomplete allelic exclusion of TCR α during thymic selection (**Figure 3.7C**).

Both TRAV26 and TRAV6 sequences in the class II restricted $CD8^+$ T cells were productively rearranged. Therefore, to test for functionality, we cloned the TCR constructs and generated two TCR hybridomas that either expressed TRAV6 and TRBV2, or TRAV26 and TRBV2. Both TRAV26 and TRAV6 were able to refold properly to pair with the β, TRBV2, and be expressed on the surface of cells. However, we found that only TRAV6 (shown in red), but not TRAV26 (shown in blue), bound to the DR11-Gag41 complex when paired with TRBV2 (**Figure 3.7D**). To evaluate the functionality of the hybridomas, we measured interleukin 2 (IL-2) secretion following stimulation with the Gag41 peptide. We found that TRAV6 and TRBV2, but not TRAV26 and TRVB2, was able to produce IL-2 in a dose-dependent manner in response to peptide (**Figure 7E**).

Both assays showed that only the TRBV2 and TRAV6 pair was functional, confirming that TRAV6 was necessary for TCR recognition of DR11-Gag41 complex. Next, we produced soluble TCR of TRAV6 and TRBV2 to assess the binding kinetics to DR11-Gag41 using surface plasmon resonance. The interaction of TRAV6 and TRBV2 with DR11-Gag41 showed an overall dissociation affinity constant (KD) of 8.1μM, which is typical for MHCII-peptide-specific TCRs [150] (**Figure 3.7F**). Collectively, these data indicate that these class II-restricted $CD8^+$ cells express two different TCR α genes, only one of which targets HIV epitopes, possibly due to inefficient allelic exclusion during thymic T-cell development, a phenomenon that is known to occur for the TCR α in ~20% of conventional T cells [151].

Collectively, our data from sequencing the TCR β revealed that class II-restricted $CD8^+$ T cells are monoclonal in all three subjects. Additionally, in subject 474723, a specific TRBV is preferentially selected and shared by $CD8^+$ and $CD4^+$ T cells targeting the same DR11-Gag41 complex. Finally, we showed that DR11-Gag41-specific $CD8^+$ express two distinct TCR α chains, with only one contributing to the binding of this class II HLA-peptide complex.

3.4 MATERIALS AND METHODS

Subjects

A total of 129 HIV-infected individuals were recruited from Massachusetts General Hospital after providing informed consent. 101 individuals were defined as 'HIV Controllers': HIV infected individuals who spontaneously control HIV infection in the absence of antiretroviral therapy for greater than 1 year. Additionally, 28 treatment-naive

HIV progressors with viral loads of greater than 2,000 HIV RNA copies/ml were utilized (see also Table S3.1 and S3.2, and Supplemental Methods).

HLA-DR $CD8^+$ Elispot

Screening for class II-restricted HIV-specific $CD8^+$ T cell responses and epitope fine mapping was conducted by enzyme-linked immunospot (Elispot) assay, using $CD8^+$ T cells enriched by CD8 MACS MicroBeads selection (Miltenyi). Antigen presenting cells expressing the HLA-DRB1 of the subject consisted of mouse lymphoblastoid cell line (LCL) fibroblasts stably transfected with a plasmid encoding a single recombinant human HLA-DRB1 variant spanning common Caucasian alleles: DRB1*01:01, *03:01, *04:01, *07:01, *11:01, *13:01 and *15:01. LCL were split across 70 wells of a V-bottom 96-well plate and pulsed with 10 µg/mL peptide. We used 66 individual overlapping peptides (OLPs) spanning HIV Gag protein (clade B 2001 consensus-sequence) tested in singlet and had 4 negative control wells without peptide. Plates were incubated at 37 °C and 5% CO_2 for 90 minutes, and washed 6X to remove any unbound peptide. We then cultured 20,000 LCL with 100,000 $CD8^+$ T cells per well on a pre-coated interferon gamma (IFN-γ) plate. As a positive control, phytohemagglutinin (Sigma) was added at 1.8 µg/mL. The plates were incubated overnight at 37 °C and 5% CO_2 and processed as previously described [147]. We used the AID Elispot reader (Autoimmun Diagnostika GmbH, Strasbourg, Germany) to determine the number of spot-forming cells per 100,000 $CD8^+$ T cells. A HLA-DR restriction was considered positive only if ≥3 times the mean background and also ≥3 times the standard deviation of negative control wells. A caveat is that each OLP was only tested once and some responses may be below the threshold

for a 'positive' result. To rectify this, any responses deemed above or close to the 'positive' threshold were independently re-tested in quadruplicate.

HLA class I and II tetramers

Class II tetramers, custom-manufactured by MBL International (Worburn, MA.) included DRB11:01-Gag41 (DRB1*1101-DRFYKTLRAEQASQEV) and DRB1*0101-Gag37 (DRB1*01:01-LNKIVRMYSPTSILD) conjugated to either PE or APC. Class I tetramers were made in collaboration with Soren Buus, Denmark as described [152]. The class I tetramers included B57-KF11 (KAFSPEVIPMF), B08-EI8 (EIYKRWII), and B27-KK10 (KRWIILGLNK) in either PE or APC. Tetramers were incubated with whole PBMC (25 min at 37 ºC, 5% CO_2) and then stained for viability and surface markers prior to fixation. Tetramer staining of hybridomas was conducted with the same protocol. Intracellular staining was used for Granzyme B and IFN-γ using the Cytofix/Cytoperm kit (BD PharMingen) according to the manufacturer's instructions. All fixed samples were analyzed on a LSRII flow cytometer (BD Biosciences) with FlowJo software (Treestar, Ashland, OR).

Functional characterization of class II restricted $CD8^+$ T cells

To determine HIV-specific cytokine secretion in response to peptide-HLA-DR stimulus, whole PBMC were incubated with 2 µg/ml of peptide pulsed onto LCL or left unstimulated in the presence of anti-HLA-DR (azide-free clone L243, Biolegend) to efficiently block HLA class II recognition. BFA and monensin were added to prevent cytokine secretion. IFN-γ secretion in response to peptide stimulus was measured from $CD8^+$ T cells. To

confirm the restriction of the $CD8^+$ T cells, class I and class II tetramers were utilized. To determine proliferative capacity, PBMC were stained with carboxyfluorescein diacetate succinimidyl ester (CFSE; Molecular Probes, Life Technologies) for 7 min at 37°C, then washed. Appropriate class I and class II peptides were added at 0.1 µg/mL to CFSE labeled whole PBMC for 7 days in RPMI 1640 medium in the absence of IL-2 at 37 ºC, 5% CO2. PHA was used as a positive control and the absence of peptide stimulation was used as a negative control. After 7 days, cells were labeled with appropriate tetramer in APC together with antibodies to CD3, CD4, CD8, CD25 and analyzed on a LSRII flow cytometer (BD Biosciences).

Chromium release assay

Chromium release assays were conducted with autologous targets (EBV-transformed B cell lines, $CD4^+$ T cells, and monocyte-derived macrophages), as described in supplemental information. Activated autologous $CD4^+$ T cell were infected with HIV NL4-3 by spinoculation at 800g for 1 hr at 37 °C and cultured for 48 hours at 37 °C and 5% CO2. Autologous monocyte-derived macrophages were plated at 30,000 per well and VSV-G-pseudotyped SIV mac251 VLPs were added 3 hrs prior to HIV challenge to abrogate host restriction factors and subsequently increase HIV infectivity. Macrophages were then infected with VSV-G-pseudotyped HIV NL4.3 expressing GFP by spinoculation at 800g for 1 hr at 37 ºC and cultured for 48 hrs at 37 °C and 5% CO2. The CXCR4-utilizing HIV-1 laboratory strain NL4-3 and its VSV-G pseudotyped version were obtained from the AIDS Research and Reference Reagent Program, Division of AIDS, NIAID, NIH (Bethesda, Maryland, USA).

48 hrs after HIV infection, $CD4^+$ T cells or macrophage target cells were labeled with chromium for 1 hr at 37°C, and then washed 3 times. Tetramer-sorted $CD8^+$ T cells isolated from PBMC or $CD8^+$ T cell clones were then added at the indicated effector-target ratios, and a standard 4-6 hr chromium release assay was performed as previously described [79].

Single-Cell RNA-seq

Whole transcriptome amplification of single cells in 96 well plates was performed with a modified SMART-Seq2 protocol, as described previously [153]. Samples were sequenced on an Illumina NextSeq 500 instrument using either 30bp paired-end reads or 150bp single-end reads. RNA-seq reads were first trimmed using Trimmomatic [154] and then aligned to the RefSeq hg38 transcriptome and genome using RSEM and TopHat. Considering only single-cell libraries in which we could reconstruct a productive TCR alignment, we excluded from further analysis genes and libraries with poor performance or coverage, leaving 205 cells and 3274 genes. Out of the 205 cells with reconstructed TCR sequences, 30 were $CD4^+$ and 175 were $CD8^+$ by Flow Cytometry gating. The TPM expression of CD4, CD8A, and CD8B transcripts between the $CD4^+$ and $CD8^+$ cells was compared using Mann-Whitney-Wilcoxon test.

TCR α and β chain sequencing

In order to reconstruct CDR3 sequences from single-cell RNA-sequencing data we developed TrapeS ("TCR Reconstruction Algorithm for Paired-End Single cells"), a software package for reconstruction of TCR sequences using short (~25bp) single cell paired-end RNA-sequencing based on TopHat genomic alignments (supplemental information). TrapeS is available upon request.

TCR-expressing T cell hybridomas.

As previously described [155], an MSCV-derived retrovirus encoding GFP and the common TRBV2 V-domain fused to mouse Cα and either the TRAV6 or TRAV26 domain fused mouse Cβ was prepared. The virus was used to transduced a TCR^{-} variant of the mouse T cell hybridoma that had been previously transduced to express human CD8α chain. T cells expressing high levels of TCR and CD8 were single cell cloned by FACS. 10^5 transduced T cell hybridomas were placed in 250ul culture wells that had been either previously coated with an anti-mouse Cβ Mab (H57-597) or contained 10^5 HLA-DR11 bearing LCL cells and various concentrations of the Gag41 peptide. After overnight culture at 37° C the culture supernatants were assayed for IL-2 using the IL2-dependent cell line, HT2.

Statistical analysis

Paired T-tests and Mann-Whitney-Wilcoxon test were used to compare different conditions, when each condition was tested in triplicate or greater. All p-values are two-sided and $p< 0.05$ was considered significant. Statistical analysis and graphing were performed using GraphPad Prism 5.0 or R.

3.5 ACKNOWLEDGEMENTS AND AUTHOR CONTRIBUTIONS

We thank all study participants, as well as A. Sette and J. Sidney for the LCL, M.C. Carrington for HLA typing, and M. Nakayama for 5KC mouse hybridomas. This study was funded by the Bill & Melinda Gates Foundation Collaboration for AIDS Vaccine Discovery (CAVD) grant APP1108533 to L.J.P, B.D.W, and S.R. S.R is also supported by a CFAR

Developmental Award (NIH/NIAID 5P30AI060354). P.A.L is supported by a HHMI International Student Research Fellowship. D.E.K is supported by a Research Scholar Career Award of the Quebec Health Research Fund. T.M.A and K. P. are supported by NIAID grant AI104715. S.W.K is supported by a NSF Graduate Research Fellowship. A.K.S. is supported by the Ragon Institute, the Searle Scholars Program, the Beckman Young Investigator Program, the NIH New Innovator Award (DP2 OD020839), and NIH U24 AI11862-01 from NIAID.

S.R., P.A.L., and B.D.W. contributed to the experimental design and data analysis; S.R., P.A.L., D.Z.S., R.B.J., F.D., C.N., P.J. performed the experiments; S.W.K. and A.K.S. conducted single cell RNA Seq; M.B.C. and N.Y. computationally reconstructed TCR; G.M.C., F.C., J.W., A.M., and J.W.K. constructed TCR hybridomas and performed SPR; K.P. and T.M.A conducted viral sequencing; H.S., D.E.K., and L.J.P. provided intellectual input and editorial comments; B.D.W. provided clinical samples and oversight of the project; S.R., P.A.L., and B.D.W. wrote the manuscript, and all authors contributed to revisions.

CHAPTER 4: Chimeric antigen receptors based on broadly neutralizing antibodies effectively recognize multiple strains of HIV and do not confer susceptibility to infection.

4.1 SUMMARY

Chimeric antigen receptors (CARs) have the specificity of antibodies and the effector function of T cell receptors (TCR). The specificity of T cells can be redirected to a desired target by expressing CARs on their surface (CAR T cells). There have been remarkable clinical results using CAR-based adoptive cell therapy for B cell leukemia, providing proof-of-principle that it is safe and effective to use CAR T cells in humans. Previous attempts to use CAR T cells against HIV showed *in-vitro* antiviral function but failed to control viral replication or to reduce the viral reservoir in humans. It is considered that one reason for these failures is the use of a CD4-molecule-based CAR, which enhances infectability of the CAR-bearing cells. Basing CAR construct design on anti-HIV broadly neutralizing antibodies (bNAbs), we generated CAR T cells capable of binding to multiple strains of HIV Env and showing HIV-specific activation. In a controlled setting of a knock-down and rescue experiment using a CD4-null Jurkat cell line, we proved that, unlike CD4-molecule-based CARs, bNAb-based CARs do not induce infectability in CAR T cells. These findings were further validated with an infection challenge in CAR-transduced primary $CD8^+$ T cells. Furthermore, we demonstrated that bNAbs are sensitive enough to detect HIV-infected cells supporting the rationale for their use in designing CARs and reinforcing the concept that Env expression on infected cells is a suitable target for CAR T cells. We conclude that using bNAbs as the basis for the design of anti-HIV CARs is a promising approach allowing for HIV-specific recognition of multiple strains without increasing susceptibility to infection. This approach, having an HLA-independent mode of recognition, makes a potential therapeutic application more broadly useful.

4.2 BACKGROUND

Chimeric antigen receptors (CARs) are synthetic transmembrane proteins designed to have the specificity of an antibody and the effector function of T cell receptor (TCR). The specificity of T cells can be redirected to a desired target by engineering them to express CARs on their surface

(CAR T cells). When the CAR is engaged by its cognate antigen, it sends downstream signaling events that make the cell proliferate, produce cytokines, and kill target cells analogous to TCR engagement [129].

CARs usually consist of an extracellular single chain variable fragment (scFv) of an antibody constituted by the variable domains of the heavy and light immunoglobulin (VH and VL) chains connected to each other by a linker sequence [156] (**Figure 4.1**). Alternatively, in some cases the extracellular domain could be constituted by a receptor or a ligand of interest [157]. CARs also have a flexible hinge and a transmembrane region. The first-generation CARs had only the intracellular domain of CD3ζ of the TCR complex or high-affinity receptor FcγRI. However, next generation constructs have included co-stimulatory and survival signals [129, 158], as complete activation of T cells requires not only TCR, but other co-stimulatory signals as well.

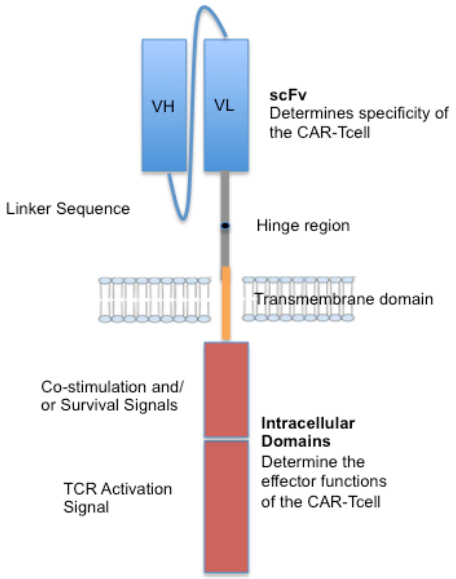

Figure 4.1 Schematic representation of a chimeric antigen receptor.

In the cancer field, there have been recent impressive clinical results with CARs targeting CD19 in B cell leukemia. Treatment of these malignancies using autologous T cells lentivirus-transduced with CARs and adoptively transferred into humans were successful in patients whose cancers

were refractory to all other available therapeutic options [126, 127, 128]. These initial results not only are a major advance in the cancer field, but also provide proof-of-principle that it is safe and effective to use therapeutic CAR T cells in humans. This means that the distance from bench to bedside might be reduced when CARs are used to target other diseases such as HIV infection.

There have been previous attempts to use CAR T cells against HIV (reviewed by [159]), with some of the original studies in the HIV setting having been done in the Walker laboratory [121, 157]. Unlike TCRs that bind viral peptides processed and presented on HLA molecules, CARs have an alternative mode of recognition, that is not HLA-dependent but directly target viral Env protein antigens expressed on the surface of infected cells. Although HIV-infected cells express Env on their surface membrane only during certain parts of the virus replication cycle [122], there is ample scientific evidence to support the idea of targeting Env on the surface of HIV-infected cells as a viable approach to attempt control of viral replication [160, 161, 162, 163]. CARs act very similar to antibodies with Fc-mediated effector function; they bridge the gap between the recognition of the antibody portion and the effector function of the cytotoxic immune cell.

Since Env binds to CD4, initial anti-HIV CAR designs used the CD4 molecule itself instead of an antibody to target HIV infected cells (reviewed by [159]). Some of these constructs went all the way to clinical trials but were not effective at containing viremia in patients receiving antiretroviral therapy [164]. It is not entirely clear why these CAR treatments did not work but there are some important considerations regarding their design. They were first generation CARs, which did not include survival or co-stimulatory signals. There is now a much better understanding of the TCR signaling pathway and the requirements for complete activation of a T cell. Consequently, more recent clinical trials using CARs for cancer immunotherapy have included a survival and/or co-stimulation signal [126, 127, 128]. Additionally, better *in-vitro* assays and *in-vivo* models for testing effector mechanisms of CAR-T cells against HIV infection and latency are now also available

(reviewed by [165]). Thus, the disappointment of earlier trials in the HIV setting is not necessarily because there was a failure of the concept but could be due to technological challenges that might now be addressed with next generation CAR T cells.

Newer versions of anti-HIV CARs included co-stimulatory signals but still used the CD4 molecule as a receptor [166]. Recent data from two different groups [167, 168] showed that the problem with using CD4 molecule as the basis for CAR design is that the $CD8^+$ T cells expressing CD4-molecule-based CARs become susceptible to infection by HIV. One approach being pursued is to use a two-step process to knock down the co-receptor CCR5 needed by the virus to enter the cell [167]. However, this approach might alter the T cell trafficking or function. Broadly neutralizing antibodies (bNAbs) have also been previously used as the basis for the design of CARs that include appropriate costimulatory/survival signaling domains [125, 169, 170]. These studies have shown effective anti-HIV properties but have not formally addressed whether bNAb-based CARs confer susceptibility to infection. It is worth mentioning that the neutralization properties of the bNAb are not of interest for CAR design, only their ability to cross-recognize multiple HIV strains.

The overall goal of this study was to determine the feasibility of generating CAR T cells to control HIV replication in vitro, with the long-term goal of taking promising compounds forward to provide an alternative to augmenting class I restricted $CD8^+$ T cells as a means of enhanced viral control. In this study, which is still underway at the time of this writing, we designed CAR constructs based on anti-HIV bNAbs, cloned them into lentivirus vectors and expressed them in primary human T cells and T cell lines. We engineered cell lines and primary $CD8^+$ T cells to efficiently express CAR synthetic constructs that bind to HIV Env and maintain the cross-reactivity to multiple viral strains. Our findings showed that bNAb are sensitive enough to detect HIV-infected cells, supporting their use in designing CARs and reinforcing that Env is a suitable target for CAR T cells. We also showed HIV-specific activation of CAR T cells. Finally, in a controlled setting of

knock-down and rescue experiments, using a CD4-null Jurkat cell line, we proved that, unlike CD4-receptor-based CARs, bNAb-based CARs do not induce infectability in CAR T cells. These findings were further validated with an infection challenge in CAR-transduced primary $CD8^+$ T cells. Together these studies represent progress toward the use of alternative methods beyond class I restricted CD8 T cells to control HIV infection.

4.3 RESULTS

4.3.1 Broadly neutralizing antibodies have sufficient sensitivity to detect HIV infected cells

Anti-HIV CARs have a distinct mode of recognition of HIV-infected cells compared to conventional class I restricted $CD8^+$ T cells. They target viral protein Env on the surface of infected cells instead of linear viral peptides loaded onto HLA molecules. A lower sensitivity of this method of recognition might be a concern. To assess whether bNAbs used in our constructs are able to bind to Env on the surface of HIV-infected cells we used soluble bNAbs and a secondary anti-human IgG antibody to stain primary $CD4^+$ T cells 36-hours post infection with HIV IIIB. We used an intracellular Gag $p24^+$ stain to detect infected cells and correlated it with staining of Env on the surface. We observed that both PG9 and VRC01 can detect infected cells. However, the percentage of cells detected by VRC01 is higher than PG9 (**Figure 4.2A**). Additionally, we could detect specific binding of VRC01 CAR to Env on Gag $p24^+$ cells in a dose-dependent manner (**Figure 4.2B**)

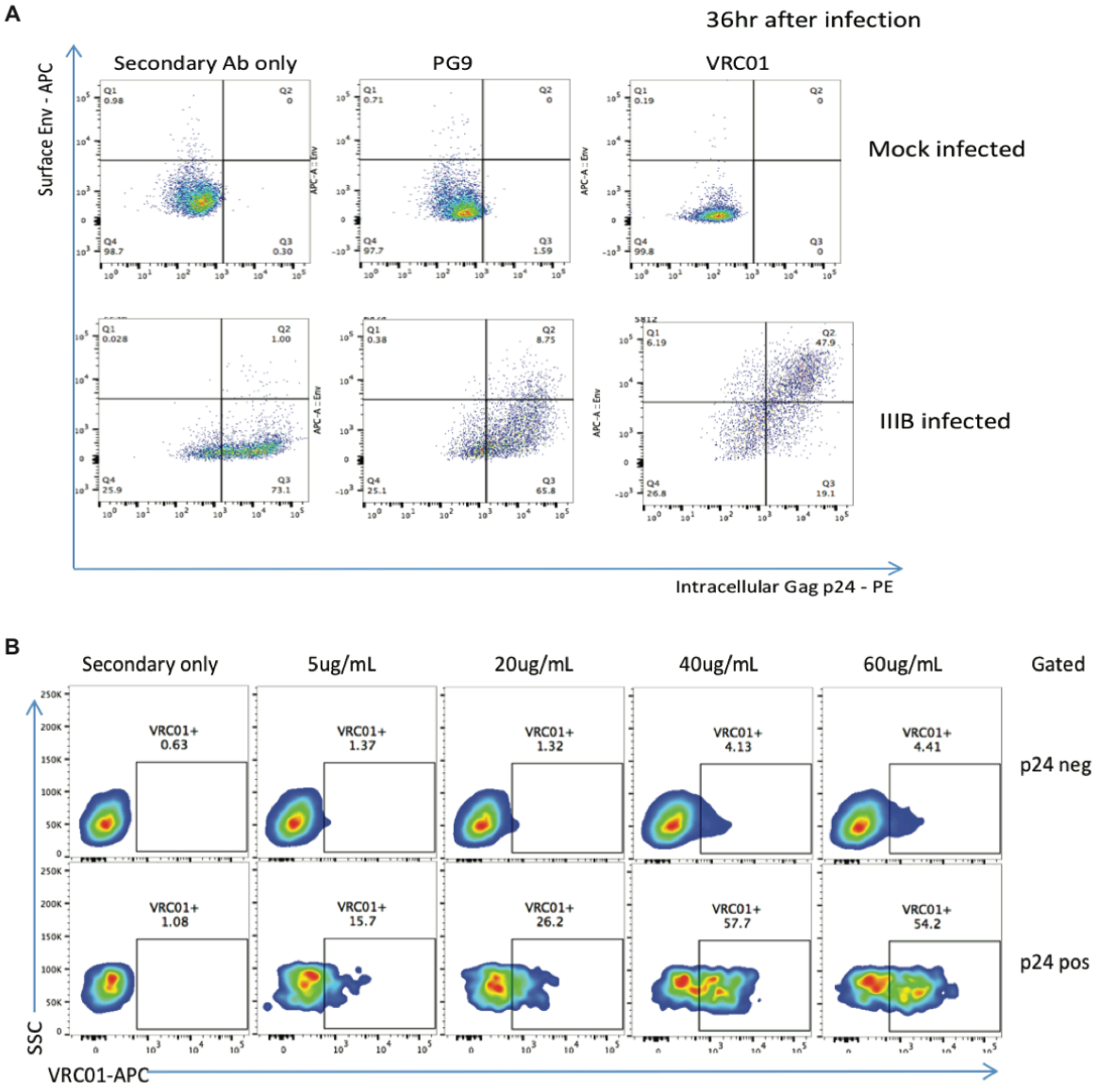

Figure 4.2 Soluble broadly neutralizing antibodies bind to Env on surface of HIV-infected CD4$^+$ T cells. After 3 days of activation with CD3/CD28 dynabeads, we infected primary CD4$^+$ T cells with IIIB HIV and incubate for 36 hours. **(A)** Flow cytometry staining of surface HIV Env using broadly neutralizing antibodies PG9 and VRC01 along with intracellular staining of Gag p24. **(B)** Titration of antibody concentrations shows a dose-dependent increase of staining of infected CD4$^+$ T cells.

4.3.2 CAR-transduced cells express constructs that can bind to multiple strains of HIV Env

We used the following HIV bNAbs in these studies: VRC01, VRC03, PG9, PGV04, and PGT121 **(Figure 4.3A)**. Most of our constructs were in an scFv conformation using a $(G_4S)_3$ linker between the VH and VL domains and contained an N-terminal Flag tag. Because scFv conformations of bNAbs have been shown to lose breath and affinity in comparison to their native conformations [171], we also made VRC01 and PG9 CARs using their full-length IgG **(Figure 4.3B)**. For the transmembrane domain, we used CD28. For the intracellular signaling domain we used CD28, CD137, and CD3 ζ. (**Figure 4.3B**)

A

Extracellular Specificity Domains	Epitope targeted
VRC01, VRC03, PGV04	CD4 binding region
PG9 antibody	V1/V2 loops
PGT121 antibody	V3 loop glycan dependent
PGDM1400 antibody	Trimer apex
CD4 molecule	CD4 binding region

B

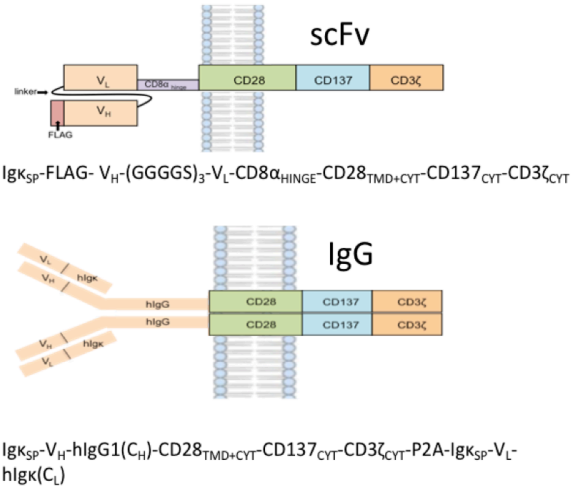

$Igκ_{SP}$-FLAG- V_H-$(GGGGS)_3$-V_L-$CD8α_{HINGE}$-$CD28_{TMD+CYT}$-$CD137_{CYT}$-$CD3ζ_{CYT}$

$Igκ_{SP}$-V_H-$hIgG1(C_H)$-$CD28_{TMD+CYT}$-$CD137_{CYT}$-$CD3ζ_{CYT}$-P2A-$Igκ_{SP}$-V_L-$hIgκ(C_L)$

Figure 4.3 Chimeric antigen receptor constructs based on broadly neutralizing antibodies. (A) List of antibodies used for CAR designs and their respective targeted site. **(B)** Schematic representation of the design of our CAR in two different conformations: scFv and full-length IgG.

We cloned these constructs into a lentiviral vector under the spleen focus-forming virus (SFFV) promoter and produced lentivirus pseudotyped with vesicular stomatitis virus-G (VSV-G) for the transduction procedure (**Figure 4.4**).

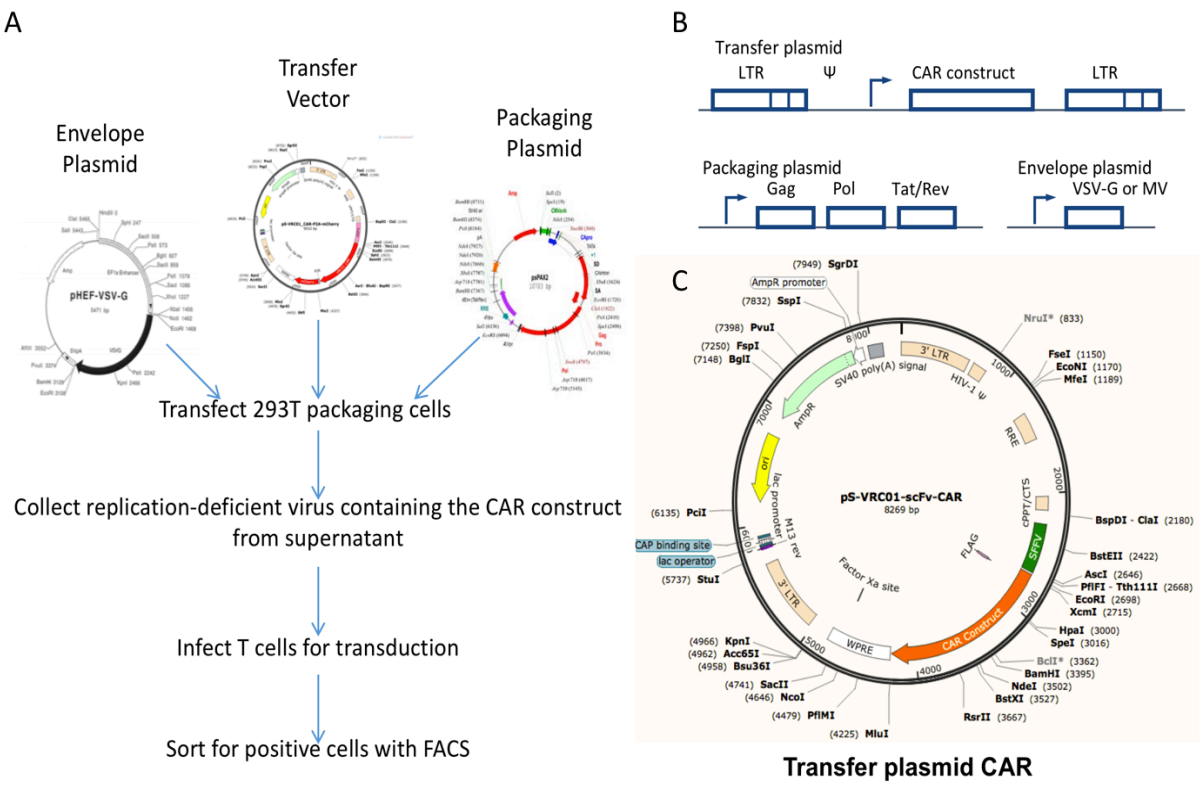

Figure 4.4 Lentivirus production process overview. Trans-complementation method to produce pseudotyped replication deficient lentivirus (See methods section for detailed description).

We lentivirus-transduced 721.221 cell lines with our constructs. We used an anti-Flag or an anti-human IgG antibodies to detect expression of constructs in the scFv and full-length IgG conformations, respectively. Using a fluorescently-conjugated gp140 (truncated portion of the Env) from HIV-YU2 strain, we found that the fluorescence intensity of binding correlated linearly with the surface expression using a dual stain in the same experiment (**Figure 4.5A**). We also showed that the CAR in a scFv/membrane-bound conformation still maintained the cross-reactivity of the original antibody (**Figure 4.5B**). Furthermore, we showed that primary $CD8^+$ T cells were efficiently transduced with CAR constructs and remain viable after transduction **(Figure 4.5C).**

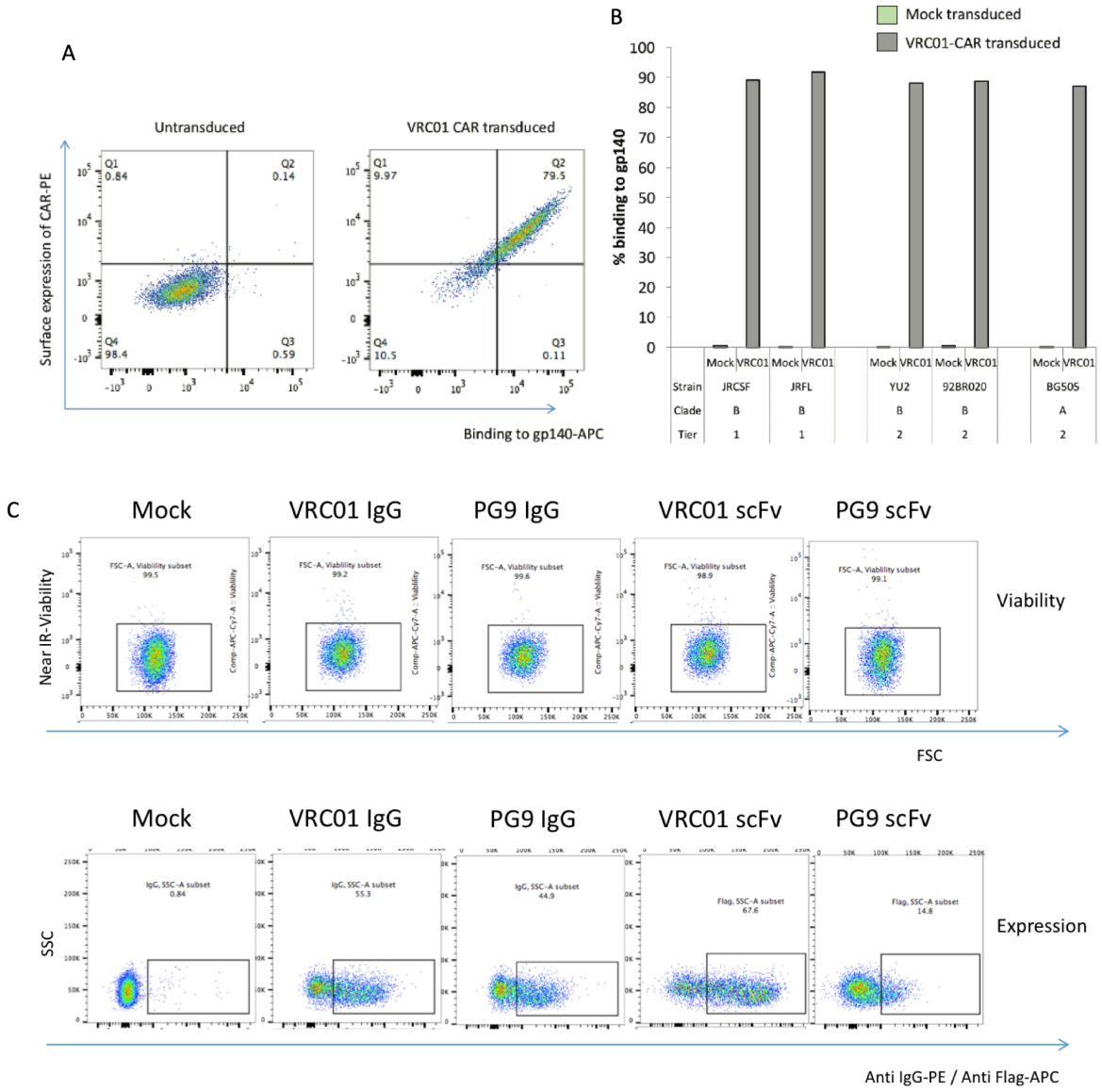

Figure 4.5 Expression of CAR constructs on the surface of CAR-transduced cells and binding to HIV Env. (A) Flow cytometry surface stain of CAR-transduced cell line with an anti-Flag antibody to show surface expression of the CAR constructs and fluorescently-conjugated soluble gp140 to test for HIV-specific binding. (**B)** Quantification of percentage of CAR-transduced cells binding to different strains of HIV assessed by flow cytometry surface staining. **(C)** Flow cytometry viability and surface staining of primary $CD8^+$ T cells transduced with bNAb-based CAR constructs in a whole IgG and scFv conformations.

4.3.3 HIV-specific activation of CAR-transduced cells

Cells expressing CAR construct should upregulate activation markers upon engagement of the receptors by HIV Env. To test for signaling of the CAR constructs, we measured the upregulation of the T cell activation marker CD69 after 4 hours of stimulation with plate-bound crosslinking anti-flag antibody. The cross-linking experiments were done in Jurkat cells expressing the CAR construct. We observed a shift in the expression of CD69 in the CAR transduced constructs cross-linked with Flag but not in the untransduced control (**Figure 4.6A**). The level of upregulation with flag crosslinking was comparable to that achieved by the positive control crosslinking CD3 (**Figure 4.6A**).

Because Jurkat cells have CD4 on their surface, this molecule will compete with the CARs to bind to HIV Env and thus we could not test for HIV-specific activation using these cells. To solve this issue, we generated a Jurkat Cas9 cell line. We sorted on the CD4 high population and then transduced with sgCD4 to knockout the gene by CRISPR/Cas9. From transduced cells, we sorted CD4 negative to subclone and verify knockout by flow cytometry **(Figure 4.6B)** and sequencing. Next, we transduced our CAR constructs into this CD4-null cell line and performed an Env-specific crosslinking experiment. Measuring CD69 upregulation after 4 hours of culture in a plate coated with YU2 gp140 by flow cytometry, we found that VRC01-CAR transduced cells become activated upon encountering HIV antigen **(Figure 4.6C).** These results showed HIV specificity of CAR constructs and activation of cells upon receptor engagement.

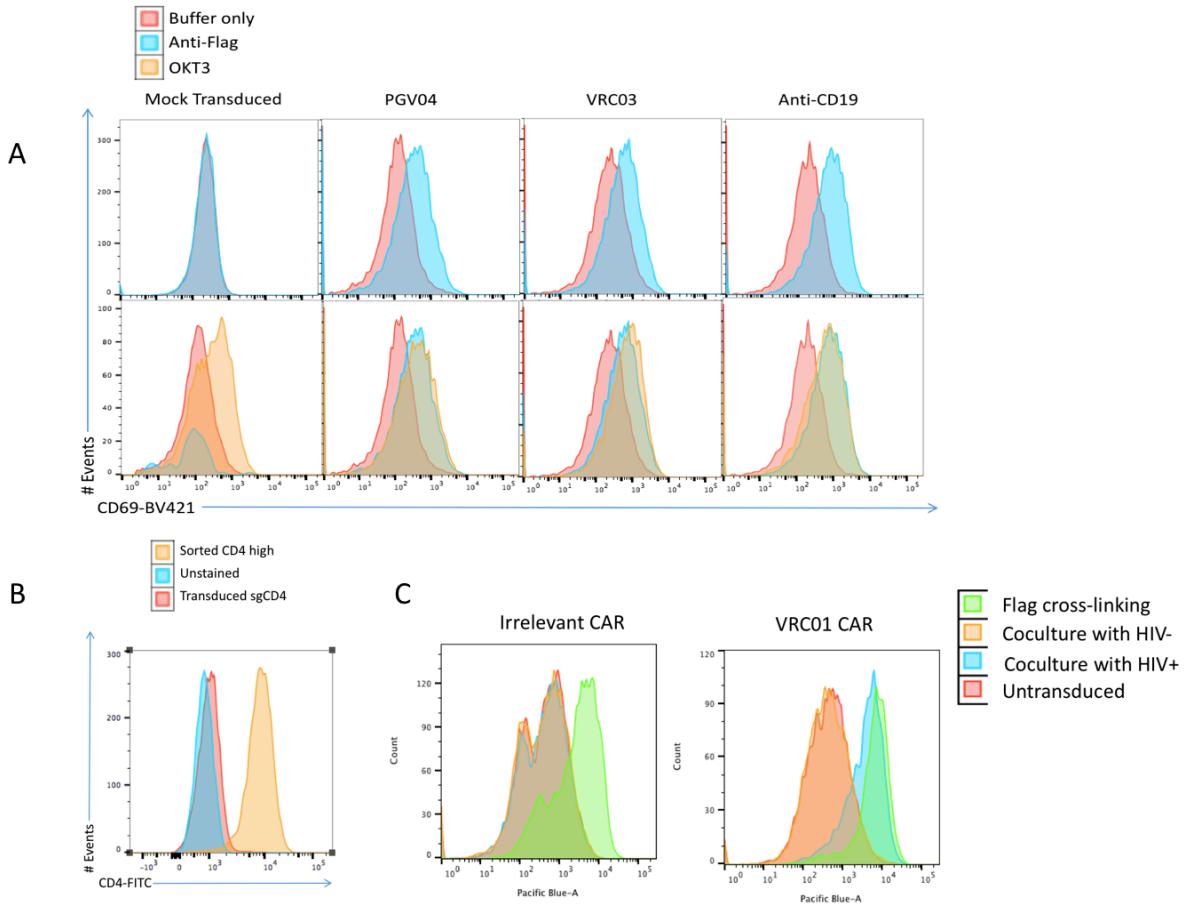

Figure 4.6 CAR-transduced cells upregulate CD69 when receptor is cross-linked. (A) Flow cytometry surface staining for CD69 expression on CAR-transduced Jurkat cells incubated for 4 hours with plate-bound anti-flag antibodies to cross-link receptors and activate cells. **(B)** Generation of CD4-null Jurkat cell line using CRISPR/Cas9. Shown is flow cytometry surface staining using an anti-CD4 antibody. **(C)** HIV-specific activation of CAR-transduced cells. Flow cytometry surface staining for CD69 expression on CAR-transduced, CD4-null Jukat cells incubated for 4 hours HIV positive and HIV negative $CD4^+$ T cells.

4.3.4 CARs based on bNAb do not confer susceptibility to infection by HIV

For our CAR constructs we used antibodies that do not trigger a conformational change in the Env trimer [172]. Since conformational change of the Env is required for viral fusion with the host membrane [173], this fact might help to prevent infection of the CAR-expressing cells. To determine whether our CAR constructs render cell expressing them susceptible to infection, we used two different approaches: a very well controlled setting with our CD4-null Jurkat cell line **(Figure 4.7A)** and a validation experiment with primary $CD8^+$ T cells **(Figure 4.7B)**.

We used flow cytometric analysis of intracellular Gag p24 staining to assess infection of cells after incubation with HIV IIIB for 36 hours. We observed that wildtype Jurkat cells are 38% infected but the same amount of virus does not produce infection in the CD4-null Jurkat cell line. Moreover, when this CD4-nul Jurkat cell line is transduced with CD4-molecule-based CAR construct the infection reappears in 15.7% of cells. However, none of the bNAb-based CARs rendered cells susceptible to infection when transduced into the CD4-null Jurkat cell line. Hence, we conclude that unlike cells expressing CARs based on CD4 molecule, cells transduced with our constructs based on bNAb do not become infected when challenged with HIV.

Next, we challenged CAR-transduced primary $CD8^+$ T cells for *in-vitro* HIV infection with the CXCR4-tropic IIIB virus. We observed that $CD4^+$ T cells as well as $CD8^+$ T cells transduced with the control CD4-CAR showed infection by intracellular Gag p24 stain. However, untransduced and VRC01 CAR-transduced $CD8^+$ T cells did not become infected (**Figure 4.7B**). By staining for CXCR4, we showed that the lack of infection was not due to low levels of coreceptor expression (**Figure 4.7C**). These data show that CAR designs based on bNAb do not confer susceptibility to infection to the cells bearing them.

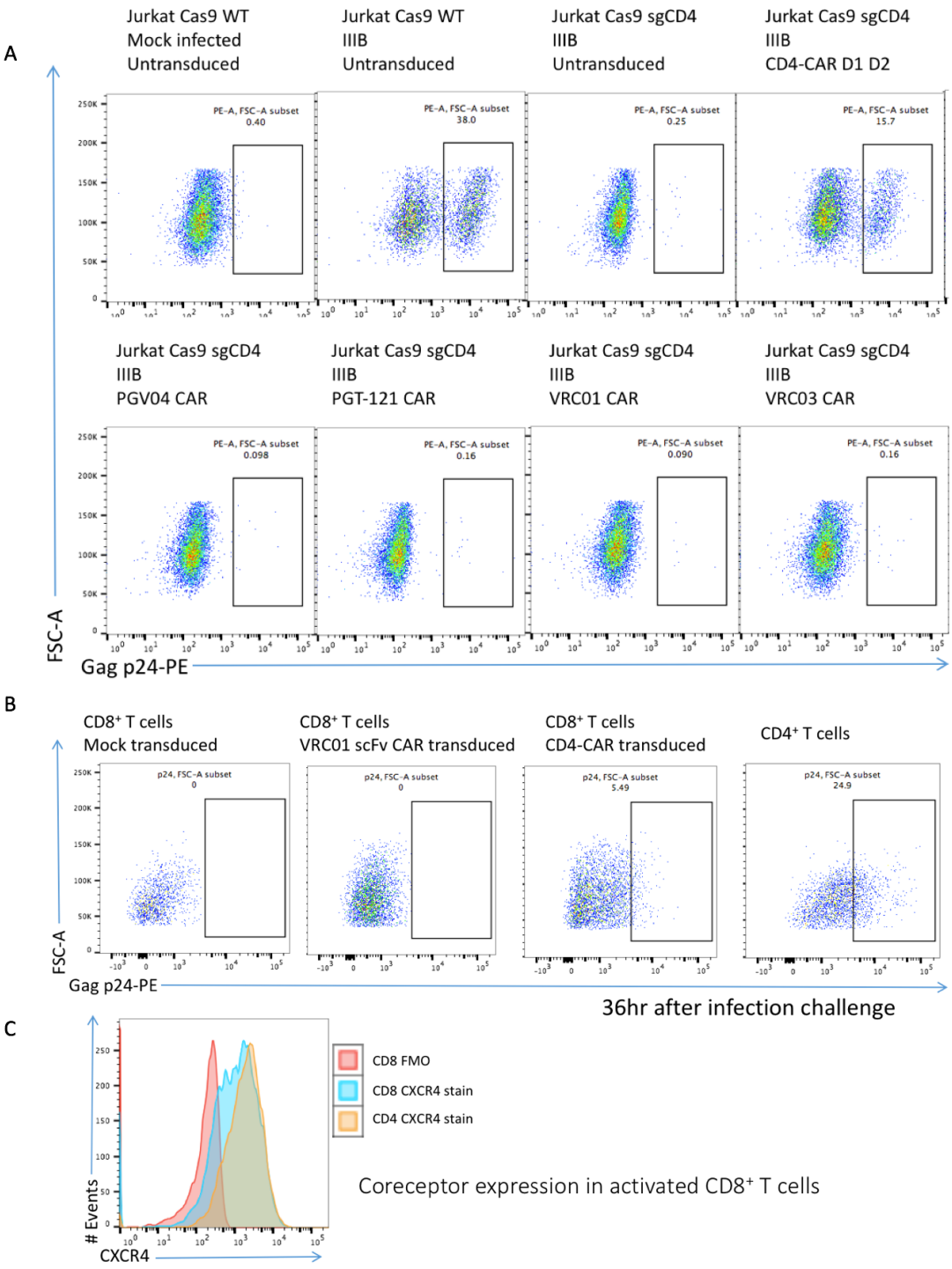

Figure 4.7 CD4-molecules based CARs but not bNAb-based CARs confer susceptibility to HIV infection. (A) Flow cytometry intracellular Gag p24 staining to assess infection of cells expressing CD4-molecule based CARs and bNAb-based CARs. Infection was performed with HIV IIIB in CD4-null Jurkat cell line. As a positive control, a CD4 expressing WT cell line was used. The negative controls are the following: No virus (mock infection), CD4-null cell line incubated with virus. **(B)** CAR-transduced CD8+ T cells are resistant to in-vitro infectious challenge with HIV IIIB. Experiments were performed with activated primary CD8+ T cells with a CD4 based CAR, VRC01-based CAR, and activated primary CD4+ T cells. **(C)** Flow cytometry surface staining of the CXCR4 coreceptor in activated primary $CD4^+$ and $CD8^+$ T cells.

4.4 MATERIALS AND METHODS

Human Samples and Viruses

Fresh buffy coat samples from healthy donors were used in this study in accordance to protocols approved by Partners Human Research Committee and Institutional Review Board of Massachusetts General Hospital. HIV-1 NL4-3 and HIV-1 IIIB were obtained from the Virology Core of the Ragon Institute of MGH, MIT, and Harvard, and are titered on stimulated human PBMCs by $TCID_{50}$ assay.

Data acquisition and analysis

Flow cytometry data was acquired on BD LSR Fortessa and analyzed using FlowJo2 software version (Tree Star) and statistical analyses were performed using GraphPad Prism 7 (GraphPad Software).

Cloning bNAb-based CAR constructs into lentiviral vectors

DNA and amino acid sequences of the bNAbs were obtained from the bNAber (bNAb Electronic Resource). scFv or full-length IgG CAR gene blocks were designed using SnapGene software and codon optimized for human expression. Constructs were synthesized by Integrated DNA Technologies or by GeneArt (Life Technologies). Synthesized gene blocks were designed to included 15 base pair overlaps with the Clontech pLVX-EF1alpha-IRES-ZsGreen1 lentiviral vector to allow for In-Fusion cloning into the EcoRI and MluI restriction sites, downstream of the EF1-a or SFFV promoter and upstream of the woodchuck hepatitis virus post-transcriptional response element. FLAG sequence was included between the (GM-CSF or Igk) signal peptide and VH portion of the sequence to allow for monitoring of expression. Confirmatory Sanger sequencing was obtained from MGH DNA core facility or EtonBio.

Lentivirus production

The outline of the entire process of transduction is illustrated in **Figure 4.4**. The first step is to transfect a packaging cell line with our plasmids to produce replication-incompetent lentivirus. The packaging cells designated for production of lentiviruses are human embryonic kidney 293T cell line/17 (ATCC). These cells express SV40 large T-antigen that stimulates replication of the viral genome and suppresses p53. We used characteristic lentivirus system where we co-transfected 293T cells with a transfer plasmid along with a packaging and envelope plasmids **(figure 4.4a). Figure 4.4b** shows a schematic representation of the plasmids used. Packaging plasmid (HIV-1 gag-pol packaging vector (psPAX2), obtained from NIH AIDS Reagent Program) contains structural and enzymatic components necessary for virion maturation, upregulation of transcriptional activity and nuclear export of genomic RNA [174]. The other plasmid includes the envelope components to direct tropism. In this case, we pseudotyped our vector using the coating fusogenic envelope G glycoprotein of vesicular stomatitis virus (VSV-G) (pHEF-VSVG, obtained from NIH AIDS Reagent Program). This allows for non-specific fusion with plasma membrane to be able to infect multiple different cell types [174]. 293T cells produce virons with a genome that only contains the DNA from the transfer plasmid but not from the other two because the transfer plasmid is the only one that includes the retroviral packaging signal Ψ (**Figure 4.4b**). The transfer plasmids (**Figure 4.4c**) used have the sequence of our bNAb-based CARs. HEK293T/17 cells (ATCC) were transfected with these three plasmids that, together, have all required proteins to build infectious virions with our CAR construct sequence. Lentivirus-containing supernatants were collected 72 hours post-transfection and were concentrated using PEG-It (Systems Bioscience) to generate stocks that were 100X concentrated and stored at -80°C until used.

HIV in-vitro infection

Primary $CD4^+$ T cells, $CD8^+$ CAR T cells, or Jurkat CAR T cells were used accordingly. Primary $CD4^+$ T cells from HIV-negative donors were obtained using EasySep direct isolation (STEMCELL

Technologies), activated with Human T cell activator CD3/CD28-coated dynabeads (Thermofisher) at a bead:cell ratio of 1:1, and cultured in supplemented RPMI with IL-2 (50 U/mL) for three days before infection. IIIB HIV previously concentrated with PEG-it (Systems Bioscience) was obtained from the Ragon Institute virology core and used to infect 10^5 cells. Cells were suspended in 30μL of RPMI containing 100 U/mL of IL- 2 in a 96-well flat-bottom plate and 10ul (10^5 $TCID_{50}$) of replication-competent virus was added. Cells were spinoculated with virus in 1X polybrene and expanded after 4 hours of incubation at 37°C/5% CO_2. The level of infection was determined by flow cytometry (LSR Fortessa BD) at 36 to 72 hours after infection accordingly. Cells were fixed and permeabilized with the FIX & PERM ® Cell Fixation and Cell Permeabilization Kit (Life Technologies) to stain with anti-HIV-1 p24 (clone: KC57, BD Biosciences) and a surface stain with anti-human CD4-APC conjugated antibody (Biolegend).

Using bNAbs to stain Env on the surface of HIV-infected cells

Appropriate bNAb was added to 10^5 cell at 50 μg/mL (VRC01) or 10 μg/mL (PGT121) and incubated for half hour at room temperature (VRC01) or 4°C (PGT121 to reduce background). Following a wash, secondary antibody (we used AF647 goat anti-hu IgG (H+L) from Invitrogen cat# A21445) was added at 500 ng/mL. A second wash was preceded by a 15-minute incubation at room temperature. p24 intracellular stain was done as described above. Flow cytometry (LSR Fortessa BD) and FlowJo software were used for analysis after 36 to 48 hours of incubation at 37°C/5% CO_2.

Lentivirus transduction of cell lines and primary T cells

Primary $CD8^+$ T cells, Jurkat cells, or 721.221 cells were used accordingly. Cell lines stably expressing genes of interest were generated via lentiviral transduction. Primary $CD8^+$ T cells from HIV-negative donor were obtained using EasySep direct isolation (STEMCELL Technologies),

activated with Human T cell activator CD3/CD28-coated dynabeads (Thermofisher) at a bead:cell ratio of 1:1, and cultured in supplemented RPMI with IL-2 (50 U/mL) for 24 hours before lentivirus transduction. Virus, cells, and 96-well flat-bottom plate on ice were kept on ice during the procedure. Cells were added to the plate (cell lines: 10^6 cells/well, for activated primary $CD8^+$ T cells: $3x10^4$cells/well). To set up a titration curve, 10, 20, 40, 80 μL of lentivirus were added to a total volume of 100μL with culture media (RPMI with 10% fetal bovine serum (FBS) in 1X polybrene). Cells were next incubated at 37°C/5% CO_2 for 72 hours before expanding to an appropriate volume to maintain $5x10^5$ cell/mL

Testing transduction efficiency and HIV binding of CARs.

Cells were stained for viability (Live-dead blue Invitrogen) and APC-labelled anti-flag antibody (Biolegend) (scFv constructs) or goat anti- human IgG(Fc) F(ab')2 PE-conjugated antibody (Life Technologies) (full-length IgG constructs) were used for detection of CAR expression 72 hours after transduction. 6X-His-tagged mosaic protein from Dan Barouch's laboratory from (Beth Israel Deaconess Medical Center) was added to CAR T cells at a concentration of 25μg/mL for 30 min before staining with a FITC anti-6X-His antibody for 15 min. Cells were fixed with 4% paraformaldehyde in PBS before flow cytometric analysis. Expression of CARs and Env was analyzed for specific binding to CAR T cells using flow cytometry (LSR Fortessa BD) and FlowJo2 software.

Generating CD4-null Jurkat cell line

Cas9-jurkats were obtained from Dr. Wilfredo Garcia-Beltran (Ragon Institute). After subcloning, clones highly expressing CD4 were selected by FACS Aria (BD) using CD4 surface stain (clone: RPA-T4, BioLegend). These clones were transduced with a CD4 sgRNA-containing lentiviral vector. CD4 sgRNA was obtained from Ryan Park (Ragon Institute). Bulk population was

assessed for depletion in CD4 expression by flow cytometry before subcloning. Sub clones with lowest expression of CD4 were expanded and transduced with CAR lentiviruses. Confirmatory CRISPR sequencing was obtained from MGH DNA core facility.

Activation assessment by CD69 up-regulation

Non-tissue culture treated flat-bottom 48-well plates were coated with purified anti-FLAG (clone M2), anti-CD4 (clone RPA-T4), YU2 Env protein, or anti-CD3 (clone OKT3: Biolegend) at a concentration of 10 ng/ml in sodium bicarbonate buffer. 10^5 cells were added to each well and incubated overnight at 37°C/5% CO_2 in RPMI with 10% FBS and 50U/ml of IL-2. After the incubation, cells were stained for CD69 with BV421-conjugated antibody expression (clone: FN50, BioLegend). The expression of CD69 relative to negative and positive controls was assessed by flow cytometry (LSR Fortessa BD)

Activation assessment of $CD8^+$ CAR T cells when co-culture with HIV-infected $CD4^+$ T cells

10^5 CAR T cells were cultured either alone, with uninfected autologous $CD4^+$ T cells (1:1 ratio), IIIB infected CD4s (1:1 ratio), or stimulated with PMA/ionomycin (Cell Stimulation Cocktail used at 0.25X; eBioscience) in a 96-well round bottom plate in RPMI with 10% FBS and 50U/mL of IL-2. Brefeldin A (5 µg/mL) and monensin (Biolegend) were added to cultures and 3 µL of anti-CD107a-PE-Cy7 antibody (BioLegend) was added after a 30-minute incubation at 37°C/5% CO_2. After an overnight incubation, cells were first stained with LIVE/DEAD® Fixable Blue Dead Cell Staining Kit (Life Technologies) following manufacturer's instructions and then stained with anti-CD8, anti-CD4, and anti-FLAG for 15 min at 4°C. Cells were then fixed with BD Cytofix/Cytoperm solution (BD Biosciences) and permeabilized with BD Perm/Wash solution (BD Biosciences) following manufacturer's instructions, after which intracellular cytokine staining was carried out using the following antibodies: anti-IFN-γ-Alexa Fluor 647 (clone: 4S.B3, BioLegend), and anti-

TNF-α-BV650 (clone: Mab11, BioLegend). After washing, flow cytometric analysis was performed on a BD LSR Fortessa.

4.5 ACKNOWLEDGEMENTS AND AUTHOR CONTRIBUTIONS

We thank Dr. Zelda Euler, Dr. Galit Alter, Professor Shiv Pillai and Dr. Jason Park for input in CAR design. We appreciate the antibodies and tetramer reagents provided by Dr. Alex Balazs, Dr. Anne-Sophie Dugast, Dr. Galit Alter, Dr. Dan Barouch, and Dr. Saheli Sadanand. Pedro A. Lamothe is supported by a HHMI International Student Research Fellowship, CONACYT, and Fundacion Mexico en Harvard.

Pedro A. Lamothe conceived the idea of this project. Pedro A. Lamothe, Bruce D. Walker, Priya Jani, Wilfredo Garcia-Beltran, contributed to the experimental design and data analysis. Priya Jani, Pedro A. Lamothe, and Felipe Bedoya performed the functional experiments. Pedro A. Lamothe, Priya Jani, and Wilfredo Garcia-Beltran designed the CAR constructs. Geetha Mylvaganam, Marcela Maus, and Felipe Bedoya provided intellectual input. Ryan Park and Dylan Koundakjian made virus and the Cas9 Jurkat cell line, tested the sgCD4 guide, and provided intellectual input. Keira Clayton provided antibody reagents, Env purified protein and intellectual input. Bruce D. Walker provided oversight of the project.

CHAPTER 5: DISCUSSION

5.1 PROTECTIVE HLA ALLELES CAN HAVE EPITOPE-INDEPENDENT EFFECTS ON HIV CONTROL

5.1.1 Specificity versus function

Certain human leukocyte antigen (HLA) alleles have been associated with HIV immune control and others with rapid disease progression (reviewed by [32]). The mechanism for these associations is not entirely understood. Having a protective HLA allele is neither necessary nor sufficient to mediate effective long-term viral control [70, 81, 175]. Several studies have shown that protective alleles shape the specificities of T cell responses by presenting highly conserved and constrained epitopes from the viral genome, where viruses cannot have mutations without greatly impairing their fitness [82, 83, 84, 85, 86]. However, there is some evidence that there could be alternative mechanisms by which the HLA allele can contribute to viral control. HIV-specific cytotoxic T cell (CTL) responses targeting protective alleles are generally more functional and exhibit better recognition against escape mutants [134, 135, 136, 176]. Moreover, protective alleles are also linked to more effective CTL responses not related to HIV, such as clearance of chronic hepatitis C [137]. If specificity were the only responsible mechanism, it would be difficult to think that protective alleles could also present the most conserved epitopes of pathogens with a completely different genome.

Arguably, previous studies have lacked a crucial control because they have compared CTL responses to disparate HLA alleles presenting different epitopes. To formally determine whether there is an epitope-independent effect of a protective HLA allele, we compared HIV-1-specific CTL responses targeting the same peptide in the context of both protective and non-protective HLA alleles. We hypothesized that CTLs restricted by protective alleles have a better disease-controlling phenotype than those restricted by non-protective alleles, even when recognizing the same peptide. To address this question in this setting where peptide variation is not a confounding factor, we analyzed CTL responses targeting the QASQEVKNW (QW9) peptide from Gag p24

that is promiscuously presented by the molecules of the protective HLA B*57:01 allele and the non-protective HLA B*53:01 allele.

Previous studies have shown that the magnitude of HIV-specific CTL responses does not correlate well with long-term viral replication suppression [79, 88, 89]. Unsurprisingly, when assessed by ex-vivo tetramer staining, we found no quantitative difference in the percentage of $CD8^+$ T cells targeting QW9 on B*57:01 versus B*53:01. We also found that tetramer staining was highly specific, we found that QW9-specific CTLs could only be identified by peptide-HLA tetramers in HLA matched subjects and that the tetramer positive cells could not be dually stained by both QW9 tetramers. This confirms that TCR not only recognizes antigenic peptide, but also directly interacts with the specific HLA molecule that presents it.

However, there was a significant difference in the ability of QW9-specific CTLs to lyse infected cells, proliferate in the context of cognate peptide, and recognize epitope variants QW9-S3T and E5D that are known to arise *in vivo*. For each of these parameters, responses restricted by HLA-B*57:01 were superior. Our findings suggest that HLA molecule B*57:01 has an immunological advantage besides the presentation of peptides from conserved parts of the viral genome.

5.1.2 Cross recognitions of epitope variants

Our data also show that TCR sequences encoding the CDR3 loop from B*57:01-restricted QW9-specific CTLs were significantly more “germline-like’ to those from B*53:01-restricted responses. Unlike antibodies, TCRs do not undergo somatic hypermutation to achieve affinity maturation and a previous study from our group showed that this TCR CDR3s that more closely resemble the germline are associated with better viral control [79]. This advantage may be related to a greater ability to recognize mutational variants of an epitope. CTL-mediated control in rapidly mutating viral infections results from specific TCR-peptide-HLA interactions that trigger antiviral efficacy as

well as non-specific interactions that provide a degree of tolerance to the sequence variation of the viral peptide (reviewed by [177]). Consistently, B*57:01-restricted QW9-specific CTLs were more cytotoxic and cross-reactive to the epitope variants. These findings reinforce computational predictions done previously of TCR recognition, which show that HLA-B*57 binds fewer self-peptides during thymic development than alleles associated with progression, and that HLA-B*57 restricted CTL are more cross reactive [176].

5.1.3 The structural determinants of QW9 functional findings

Importantly, our studies also provide insights regarding structure-function relationships in the relative ability of TCRs to recognize naturally occurring variants within the targeted epitope in the context of protective and non-protective HLA presentation. The genes coding for the heavy chain of HLA molecules are highly polymorphic, which determines differential peptide-presentation and TCR-recognition. The sequence variation between the HIV-1 "protective" allele HLA-B*57:01 and the progressive allele HLA-B*53:01 consists of only eight residues **(Figure 2.6A)**, which cluster on the α1-helical region of the heavy chain. HLA residues determine which peptides are presented. While some distinct HLA-alleles can present the identical peptide, the polymorphism may cause disparate HLA molecules to have different peptide binding affinities and kinetics, which will also affect TCR recognition [178]. Here, through crystallographic analysis of the peptide-HLA complexes, we show that the same peptide is presented in quite distinct configurations by the two alleles examined. In the context of B*53:01, K7 of QW9 exists in two different conformations. The K7-out epitope, in which K7 is solvent-exposed, interacts much more strongly with the C3 TCR than does the K7-in epitope, in which K7 is buried deep within the peptide binding groove, suggesting that C3 was perhaps selected to recognize K7-out configurations. C3 activation derived from K7-in conformations, in that case, would be correspondingly weak. Since only ~10% of B*53:01-QW9 conformations feature K7 in the out position **(Figure 2.4G)**, it is possible that only a small fraction of B*53:01-QW9 complexes can be targeted by C3 at any given time. In

comparison to B*57:01, thus, the above calculations suggest that QW9 presentation by B*53:01 could be less immunologically efficient. The presenting surface of the HLA is less featured in these K7-in configurations, a factor that may make peptide-independent HLA-TCR interactions more prominent. We may have provided a structural rationale as to why the naturally occurring E5D and S3T mutations would not be expected to significantly alter presentation and recognition of epitope QW9 presented by HLA-B*57:01 [179].

5.1.4 Limitations

There are several limitations in our study that we wish to acknowledge. The numbers of subjects studied and the TCRs examined were limited, and thus broad extrapolation of these results will require additional studies. Co-crystallization of the TCR-peptide-HLA complex is a very challenging, and even after multiple attempts to produce a co-crystal, we were not able to achieve this. A trimolecular crystal would have given additional insights as how the TCR-QW9-HLA interactions differ in the context of protective and non-protective alleles. Although we show data supporting the idea that at least part of the relative protection offered by B*57:01 may be derived from factors that depend on the actual conformation of the peptide within the binding groove, we did not show why these cells are more functional. Further experiments to address this would include measurements of binding affinity and kinetics of the TCR to QW9 presented on different HLA molecules, analysis of co-stimulatory/exhaustion surface markers and identification of memory phenotype of these responses, confocal microscopy to observe the immunological synapse formation, and assessment of activation of TCR signaling pathways.

5.1.5 Use of molecular dynamics simulation to address some of the limitations

Because we were unsuccessful at obtaining crystal structures of TCR-QW9-HLA complexes, we used molecular dynamics simulation to asses these interactions. The TCR-peptide-HLA ternary complex cannot be easily extrapolated from the free peptide-HLA structure, since TCR-peptide

recognition is mainly determined by the highly flexible and variable CDR loops. Using TCRs specific for the same peptide but different presenting HLA molecules, we showed that B*53:01-QW9-K7-out and B*57:01-QW9 both have strong epitope-restricted interactions with their respective TCRs (C3 and C8); However, B*53:01-QW9-K7-in exhibits very weak epitope-restricted interactions. These structural analyses were further validated by calculating the binding affinity changes due to point mutations in the viral peptide with the rigorous FEP method. The robust agreements between *in-silico* and *ex-vivo* mutagenesis studies indicate that our current structural models and analyses are consistent and reasonable. In particular, our FEP calculations successfully predicted cross reactivity, which were confirmed by our experimental assays.

Our structural studies also demonstrated that TCR binding to QW9-B*57:01 displayed more epitope independent TCR-HLA molecular interactions than the TCRs targeting QW9-B*53:01, allowing for more flexibility to peptide residue changes. Though direct TCR-HLA interactions might endow B*57:01 with protective properties, our functional data indicate that mutations can still facilitate immune escape from both HLA alleles. Our results using TCRs from HIV controllers show the impact of the interplay of both specific hydrophobic interactions and non-specific hydrogen bonds in the TCR-viral peptide interaction. We conclude that, by applying rigorous binding affinity prediction tools with *in-vitro* mutagenesis studies, we not only capture structural and energetic details of residue substitutions, but also reveal an underlying molecular mechanism for differences among TCR recognition of QW9 in the context of protective and non-protective HLA molecules.

5.2 $CD8^+$ T CELL RESPONSES WITH ANTIVIRAL ACTIVITY CAN BE RESTRICTED BY HLA CLASS II

5.2.1 The identification of HLA class II-restricted CD8$^+$ T cell responses in HIV infection violates the paradigms of TCR antigen recognition.

CD8$^+$ T cells play a critical role in control of viremia, typically through the recognition and killing of infected cells presenting pathogen-derived peptides on HLA class I molecules. Yet, whether CD8$^+$ T cells restricted by HLA class II exist in natural human viral infections and exert antiviral functions is unclear. Here, we report the existence of CD8$^+$ T cells that recognized HIV Gag peptides presented on HLA class II. Although these were rare events—found in 3% of the HIV controller population in this study—in one individual the class II-restricted CD8$^+$ T cells were the most immunodominant CD8$^+$ response detected, encompassing 12% of circulating CD8$^+$ T cells. These cells exhibited high proliferative capacity, potent lysis of target cells and may have imposed selection pressure for the generation of viral escape mutants, comparable to the well-characterized antiviral efficacy of class I-restricted CD8$^+$ T cells. These data illustrate that paradigm-violating HLA class II-restricted CD8$^+$ T cells can be elicited in a chronic human viral infection. Moreover, our findings reveal an unexpected flexibility in CD8$^+$ T cell recognition, and demonstrate that the paradigm of CD8$^+$ T cell restriction by HLA class I molecules is not absolute in human anti-viral immune responses.

5.2.2 Atypical TCR usage of HLA class II-restricted CD8$^+$ T cell responses.

Our analysis also revealed that class II-restricted CD8$^+$ T cells demonstrated atypical patterns of TCR usage that challenge the current paradigm of T cell recognition. Firstly, in all three subjects, the class II restricted CD8$^+$ T cell response was characterized by expansion of a single TCR β clonotype, rather than the typically oligoclonal TCR repertoires observed for epitope-specific class I-restricted CD8$^+$ T cells [74, 79, 180]. Secondly, we observed a phenomenon in which class II-restricted CD8$^+$ T cells targeted the same HLA-peptide complex as conventional CD4$^+$ T cells. Our data indicated that, in one subject, this was associated with preferential selection of TRBV2 usage in all CD8$^+$ T cells and most CD4$^+$ T cells targeting the DR11-Gag41 complex. Although

other studies have demonstrated TCR β 'public clonotypes' among virus-specific $CD8^+$ [93] or $CD4^+$ [181] T cells in unrelated individuals, here TCR sharing occurred between antigen-specific $CD8^+$ and $CD4^+$ T cells within an individual. Lastly, analysis of the TCR α chain revealed expression of two α chains. However, only TRAV6 in combination with TRBV2 was able to bind DR11-Gag41. We hypothesize that the second α chain (TRAV26) in combination with TRBV2 may have interacted with a class I molecule occupied by a self-peptide or foreign-peptide at sufficient affinity, leading to its positive selection resulting in differentiation into a $CD8^+$ single positive T cell in the thymus with subsequent migration into the periphery. Subsequent HIV infection may have then fortuitously selected this peripheral $CD8^+$ T cell clone in the context of the DR11-Gag41 peptide (via its TRAV6 TCR specificity), resulting in an expanded population of memory cells with potent antiviral function. Taken together, our data imply that these unconventional $CD8^+$ T cells exhibit distinctive TCR characteristics, and suggest a mechanistic explanation as to how class II-restricted $CD8^+$ T cells can be selected; this phenomenon may also in part explain the rarity of these responses.

5.2.3 Implications of the discovery of antiviral $CD8^+$ T cells restricted by HLA-DR in natural HIV infection.

Our data revealed that Gag-specific $CD8^+$ T cells restricted by HLA-DR had a cytotoxic T lymphocyte-like phenotype and effectively killed autologous HIV-infected cells. HLA-DR-restricted $CD8^+$ T cells may confer multiple advantages in the context of HIV infection. Unconventional restriction may allow $CD8^+$ T cells to exert antiviral effector functions on infected macrophages and activated $CD4^+$ T cells that typically express high levels of HLA-DR. Cytotoxic $CD8^+$ T cells restricted by HLA-DR may also have an advantage in settings where HIV Nef-mediated class I down-regulation may impair recognition [182]. Furthermore, targeting of the Gag-37 and -41 peptides may allow HLA-DR-restricted $CD8^+$ T cells to target a virus that has already escaped

within epitopes restricted by conventional $CD8^+$ T cells. Yet, it is difficult to assess the contribution of these unconventional $CD8^+$ T cells to immune control. Subjects 474723 and 388031 express class I alleles B*5703 and B*2705 respectively, which are strongly associated with HIV-1 control [32]. Subject 270245 lacks these 'protective' class I alleles, and exhibits a DR01-Gag37 restricted $CD8^+$ T cell response with demonstrable antiviral efficacy *ex vivo*. This raises the possibility that DR01-Gag37-restricted $CD8^+$ T cell antiviral functions, in addition to $CD8^+$ T cell responses restricted by 'non-protective' class I alleles, may contribute to immune control in this individual. Further studies aimed at inducing unconventional $CD8^+$ T cell responses in healthy humans would be required to determine their *in vivo* antiviral efficacy and delineate their overall contribution to control of viral replication.

The potential relevance of class II-restricted CD8 T cell responses is underscored by results from an SIV vaccine trial. In monkeys immunized with strain 68-1 RhCMV vector and challenged with pathogenic SIV, two-thirds of the $CD8^+$ T cell responses recognized a wide breadth of SIV Gag epitopes bound to class II molecules [117]. Induction of class II-restricted $CD8^+$ T cells, which occurs in every immunized animal, is a consequence of the absence of two viral genes (*Rh157.5* and *Rh157.6*) in the strain 68-1 vector, as repair of these 2 genes reverts $CD8^+$ T cell responses back to class I restriction [117]. The *Rh157.5* and *Rh157.4* gene products are part of a RhCMV receptor for non-fibroblasts and their absence changes the cellular tropism of the vector, making it more fibroblast-tropic, which in turn is thought to change the priming environment to favor generation of class II restricted $CD8^+$ T cells. As the modified vector does not change the $CD8^+$ naïve T cell repertoire, the implication of these findings is that atypical priming conditions efficiently prime pre-existing $CD8^+$ T cells with cross-reactive TCR. Class II-restricted $CD8^+$ T cell responses were also recently seen in 4 of 12 unvaccinated SIV-infected monkeys with controlled viremia (one such response per 'SIV controller monkey'; 4 MHC-II-restricted responses out of a total of 180 epitope-specific responses evaluated) [118]. These data support our findings that memory Gag-specific

$CD8^+$ T cell responses restricted by class II can be elicited in natural viral infection, and as such must exist in the naive T cell repertoire of at least some humans and macaques. Thus it may be possible to induce and expand these responses in healthy uninfected subjects. However, we currently do not know if class II-restricted $CD8^+$ T cells responses actually contribute to viral control *in vivo* in either the CMV vector-induced or natural SIV/HIV infection models.

5.2.4 Limitations

Although we showed that class II-restricted $CD8^+$ T cells can exist in natural HIV infection, we note a number of limitations. We only detected a single Gag-specific $CD8^+$ T cell response restricted to HLA-DRB1 in each of three HIV controller individuals and in none of the HIV chronic progressors. The low number of responses detected may be due to the method of screening; a modified IFN-gamma Elispot using LCL stably expressing a single recombinant HLA-DR molecule. Arguably, the reliance on IFN-gamma detection may thwart detection of unconventional $CD8^+$ T cell responses if they do not secrete this cytokine. To circumvent this limitation, we also screened HIV-infected individuals with class II tetramers, but $CD8^+$ T cell responses were only found in the aforementioned three individuals, confirming that the modified Elispot is unlikely to have missed low-level responses. As the macaque studies only evaluated SIV Gag-specific $CD8^+$ T cell responses restricted by *Mamu-DRB*, we focused this study on HIV Gag-specific $CD8^+$ T cell responses restricted by common HLA-DRB1 alleles. We did not test for class II-restricted $CD8^+$ T cell responses to other HIV proteins, or to class II DRB4, DRB5, DP or DQ. Another constraint in our study was limited sample availability and low numbers of tetramer positive cells, thus in some parts of this study, we primarily focused on the characterization of subject 474723. This subject demonstrated potent killing of target cells *ex vivo*, showed putative evidence of viral escape *in vivo* and exhibited unique TCR features. However, given the rarity of these unconventional $CD8^+$ T cell responses, it is not clear whether we can make generalizations between class I- and class II-restricted $CD8^+$ T cells. Indeed, further work will be required to determine whether these

unconventional responses represent a distinct subset of HIV responsive cells, or represent class I-restricted $CD8^+$ T cells that simply happen to bear TCR that cross-react with Gag peptide presented by class II. Finally, whether these results can be extrapolated to unconventional T cells in other pathogenic infections or vaccine settings will require additional study.

5.3 USING ENGINEERED T CELLS EXPRESSING CHIMERIC ANTIGEN RECEPTORS AS AN ALTERNATIVE STRATEGY TO TARGET HIV-INFECTED CELLS.

5.3.1 CARs based on bNAb are effective at targeting HIV and do not confer susceptibility to infection.

The CAR T cell approach to target HIV-infected cells has been re-examined by several laboratories in the last few years, utilizing the lessons learned from impressive results achieved with cancer immunotherapy [126, 127, 128]and from previously unsuccessful attempts to target HIV (reviewed by [159]). Instead of using antibodies, most early attempts to target HIV with CARs utilized the CD4 molecule, which is the natural ligand for Env. These first-generation CARs, from the Walker laboratory and others, contained only CD3ζ as the intracellular domain [121, 157] and were successful in targeting HIV *in vitro* but failed to provide long-term control *in vivo* [164]. Newer generations included co-stimulatory signals but still used the CD4 molecule as a receptor [166]. Recently, two different groups showed that using the CD4 molecule as the basis for a CAR on $CD8^+$ T cells makes them susceptible to HIV infection, and developed strategies to minimize this unwanted effect by knocking-down CCR5 [167, 168]. In the past few years, two publications showed that using bNAb as the basis for the design of anti-HIV CARs is effective *in vitro* [169, 170]. However, to our knowledge, it has never been formally shown that bNAb-based CARs do not confer susceptibility to infection of the transduced cells. This is an important concern given that many bNAbs target the CD4-binding site of the Env and can mimic the structure of the CD4 molecule (reviewed by Kwong and Mascola, 2012).

In this study, we have genetically engineered cell lines and primary $CD8^+$ T cells to efficiently express CAR constructs that bind to HIV Env and maintain cross-reactivity to multiple viral strains seen with the natural conformation of the bNAbs. We also showed in a very controlled assay using a CD4-null Jurkat cell line, that previous constructs using CD4-receptor-based CARs but not bNAb-based CARs confer susceptibility to infection. We further validated our findings in primary $CD8^+$ T cells showing that our constructs do not make the cells infectable, even in the presence of appropriate necessary co-receptors CXCR4 and CCR5. Although additional studies are needed to define the antiviral function of these constructs, these preliminary data show promise for further development of this approach as a means of immunotherapy for HIV infection.

5.3.2 Advantages of using a CAR approach to target HIV

There are several potential benefits of using CAR T cells as therapy versus T cells engineered with an HIV-specific TCR, with the main advantage being that the former is not dependent on recognition of a particular HLA allele. Therefore, the impact of a possible therapeutic strategy will not be restricted only to those individuals with certain HLA alleles. The recognition of the viral antigens by CARs are not affected by Nef-mediated downregulation of HLA class I expression on HIV-infected cells [182]. Additionally, the antibody affinities on which the CAR designs are based tend to be much higher than a TCR (reviewed by [130]). The CAR approach also does not require knock-out of endogenous TCR for preventing incorrect pairing of alpha and beta chains as would be required with approaches using transduced TCR [183]. Furthermore, co-stimulatory and survival signals can be included in the CAR construct to prevent anergy and increase persistence.

Passive immunization with broadly neutralizing antibodies (bNAbs) reduces viral load significantly in mice [184], non-human primates [185, 186], and humans [187]. Potentially, T cells engineered with CARs could have a similar effect as seen in passive immunization studies but they could additionally

provide a longer-lasting response because they can undergo *in-vivo* expansion when encountering their cognate antigen and actively traffic into tissues.

5.3.3 Implications regarding the design of anti-HIV CARs

In our study, we selected antibodies that are cross-reactive against multiple strains of HIV-1 to build a robust CAR construct. Most of the broadly cross-reactive HIV antibodies identified thus far also have the ability to neutralize the virus. However, for our purpose of designing a CAR, these antibodies do not need to be neutralizing because the mechanism that we are trying to take advantage of is the recognition of infected cells that express Env on their surface and not the neutralization of viral particles. Another possibility would be to use non-neutralizing antibodies that target the constant regions of the viral Env. A few of these antibodies have been found to mediate antibody-dependent cellular cytotoxicity (ADCC). However, they are less well characterized for their breadth and some have shown cross-reactivity with human self-antigens (personal communication from Galit Alter's Laboratory at the Ragon Institute). For these reasons, we considered the use of broadly neutralizing antibodies a better option for the design of the extracellular domains of our CAR constructs. Most of these broadly cross-reactive antibodies are highly somatically hypermutated and/or have a very long complementary determining region 3 (CDR3) [8]. As a result, some of these antibodies have unusual tertiary and quaternary structures (reviewed by [188]). Taking this under consideration, the antibodies that we selected for our CAR designs do not have a highly complex structure, so they could conserve their specificity when assembled as an scFv.

First generation CARs used CD3ζ alone, but there is evidence that incorporating co-stimulatory (CD28) and/or survival (CD137) molecules into the CAR design allows for a stronger activation [189] and a longer *in-vivo* half-life [131] of the CAR T cells. Therefore, we decided to include both of these signals in our constructs. Although many CAR T cell studies in cancer use total ($CD4^+$ and $CD8^+$)

T cells for transduction, we decided to only use $CD8^+$ T cells and completely exclude the $CD4^+$ T cells from our approach because of concerns that $CD4^+$ T cells are susceptible to HIV infection. If these $CD4^+$ T cells are expanded *in vivo,* we would likely increase the pool of target cells that HIV could infect, thus contributing to increased viral replication or viral reservoir.

5.3.4 Considerations about safety and limitations of HIV-specific CAR T cells

Safety is an important consideration in any adoptive transfer cell therapy and avoiding auto-reactivity of CAR T cells targeting HIV is one of the main features. Although on-target but off-site effects are seen with some CARs used in cancer (e.g. targeting of non-neoplastic B cells expressing CD19), these effects should not be a problem with HIV-specific CARs since Env is only present on infected cells [128]. However, off-target effects of some HIV-specific CARs could be a concern. Some antibodies targeting the MPER can be cross-reactive with self-antigens since they bind close to the membrane and recognize phospholipids [190]. Therefore, our CAR designs were based on antibodies against the CD4-binding and V2/V3 loop sites of the Env trimer and not the MPER. An alternative conceivable risk would be that the endogenous TCR could cross-react with self-antigens. The expected *in vivo* expansion mediated by the CARs encountering their cognate antigen could exacerbate this problem. Transducing CARs into previously selected T cells whose TCR is also virus-specific will decrease this risk [191, 192].

The risk of malignant transformation of CAR T cells by the transduction process is a relevant aspect to consider. Since retroviruses integrate into the host genome randomly, there is some concern whether it could integrate close to a proto-oncogene causing its over-expression. There have been such cases reported with gene therapy on severe combined immunodeficiency patients using hematopoietic stem cells [193]. Nonetheless, insertional oncogenesis has not been observed when transducing differentiated T cells. The safety of this type of CAR T cells has been evaluated for more than 10 years in patients without the occurrence of malignant transformation [194].

If these HIV-specific CARs were to be taken into human studies, a safety mechanism such as an inducible apoptosis system by activation of the caspase-9 pathway with a commercially available dimerizing agent should be implemented. This system has been proven effective to rapidly deplete transferred cells in allogeneic bone marrow transplants to revert graft versus host disease [195] and does not impair T cell function when co-expressed with CARs [196, 197]. Even though evidence about long-term safety of lentiviruses is not as extensive as with retroviruses, lentiviral vectors are already being safely used in several clinical trials [126, 127, 128, 158].

Arguably, the principal weakness for the CAR T cell approach is that CARs are limited to only target antigens expressed on the membrane of infected cells. Unlike TCRs, CARs cannot detect intracellular protein peptides processed and presented on HLA molecules, the kinetics of which may be advantageous compared to expression of the envelope trimer that would be required for CAR T cell recognition relying on broadly neutralizing antibodies. We showed in Figure 4.1 that the bNAb used as the basis for the design of our CAR constructs are sensitive enough to detect HIV infection in $CD4^+$ T cells, but kinetic studies to define the relationship between targeting and release of infectious virions would be an important next step. Finally, we want to acknowledge that this project is still ongoing. Although we have shown that our CAR T cells bind to multiple HIV strains and that these cells do not become susceptible to infection, we are still in the process of performing experiments to show killing of infected cells and in-vitro viral replication suppression. I will continue to work on these experiments for several weeks after defending my dissertation. Additionally, a post-doctoral fellow and a technician from the Walker laboratory will continue to study these CARs.

5.4 MAIN CONTRIBUTIONS, IMPLICATIONS, AND FUTURE DIRECTIONS

Data from chapter 2 reveal that CTL responses specific for an identical peptide diverge functionally in the context of different presenting HLA molecules, implicating that the HLA allele contributes to the HIV disease-controlling phenotype. Complementary functional data, X-ray crystallography, and molecular dynamics simulations along with free energy perturbation calculations provide a molecular level explanation of how HLA-presentation of QW9 influences TCR interactions with WT and epitope variants. We have reported the first crystal structures of an immunodominant antigenic peptide QW9 derived from HIV Gag p24 loaded on HLA-B*57:01 and B*53:01. The unique observation is that the central peptide residue K7 can assume either a buried conformation in the peptide-binding groove or an exposed one. This dynamic may affect TCR recognition. Comparing the surface representation between HLA-B*57:01 and HLA-B*53:01, we have discussed how these two HLA alleles may contribute differently to host control of HIV-1 infection. This study provides structural and mechanistic insights into T cell-mediated antiviral immunity in a chronic human viral infection.

Chapter 3 presents rare class II-restricted $CD8^+$ T cell responses with potent antiviral properties and clonal expansion in the setting of a natural human viral infection, challenging current paradigms of T cell recognition and restriction. Our findings suggest greater flexibility in $CD8^+$ T cell recognition and restriction, which is likely modulated by TCR cross-reactivity, and which may be important for immunological outcomes. Thus, these data not only enhance our understanding of the basic immunology of TCR-peptide-HLA interactions, but also may be important for future T cell-based vaccine design and immunotherapeutic interventions, where induction of unconventional class II-restricted $CD8^+$ T cells that show antiviral efficacy may be beneficial.

In chapter 4, we observed that using bNAbs as the basis for the design of anti-HIV CAR T cells is a promising approach allowing for HIV-specific recognition of multiple strains and does not make the CAR-bearing cells susceptible to infection. This provides an advantage in terms of future

therapeutic intervention in that it is an HLA-independent mode of recognition, and consistent with evidence in the Fc-mediated effector function field [160, 161, 162, 163, 198], we showed that antibodies binding Env are sensitive enough to detect HIV-infected cells making it a suitable target for CAR-T cells.

Future directions of the CAR project include demonstration of in vitro antiviral function, adaptation to $CD8^+$ T cells from HIV chronic progressors, comparative analysis of additional constructs using both neutralizing and non-neutralizing antibodies, and moving forward to experiments in animal models. HIV-specific $CD8^+$ T cells from chronic progressors are dysfunctional mostly because of overexposure to antigen and exhaustion, and they lack the ability to control viral replication [97, 99, 100].A potentially important question to address is whether a CAR-mediated redirection of specificity of the naïve $CD8^+$ T cells from chronic progressors can allow them to show an effective antiviral profile even when the naturally-induced HIV-specific T cells do not. Given that one of the main limitations of the CAR T cell approach is sensitivity of Env recognition on the surface of infected cells, we also want to look at other antibodies that have higher sensitivity. The J3 llama-derived Env-specific antibody has been shown to be much more sensitive at recognizing infected cells [199]. Its small size and high sensitivity make this an excellent candidate for future experiments. Anti-HIV CARs could potentially also be tested as a strategy for eradication, in combination with latency-reversing agents, or by incorporating chemokine receptors to allow for adequate trafficking of $CD8^+$ T cells to privileged sites of the HIV reservoir where they normally do not have access to, such as the germinal center in secondary lymphoid organs [200, 201, 202]. Testing for *in-vivo* virus control, infection prevention, or even eradication in animal model experiments (humanized mice and/or macaques) would be the next stepping stone before proceeding to human studies.

5.5 CONCLUSSION

Collectively, the detailed studies presented in this thesis demonstrate that HIV-specific CD8+ T cells can contribute to immune control of HIV-1 through multiple modes of recognition. Typically, CD8+ T cell killing of HIV-infected cells is mediated by recognition of HLA class I alleles, which may be 'protective' or 'non-protective', even when presenting an identical peptide. Yet, importantly, we have also demonstrated the existence of HLA class II-restricted CD8+ T cells in a small number of HIV positive individuals, and utilized an HLA-independent mode of recognition in the design of bNAb-based CAR T cells. Our findings reveal substantial flexibility in CD8+ T cell recognition and restriction, which is determined by TCR engagement, or can be modified by genetic engineering of CAR T cells. Thus, these data enhance our understanding of the basic immunology of TCR-peptide-HLA interactions, and are also of major relevance in the design of future vaccines, immunotherapies, and cure strategies against genetically diverse strains of HIV-1.

APPENDIX:

SUPPLEMENTAL INFORMATION

SUPPLEMENTAL MATERIALS FOR CHAPTER 2

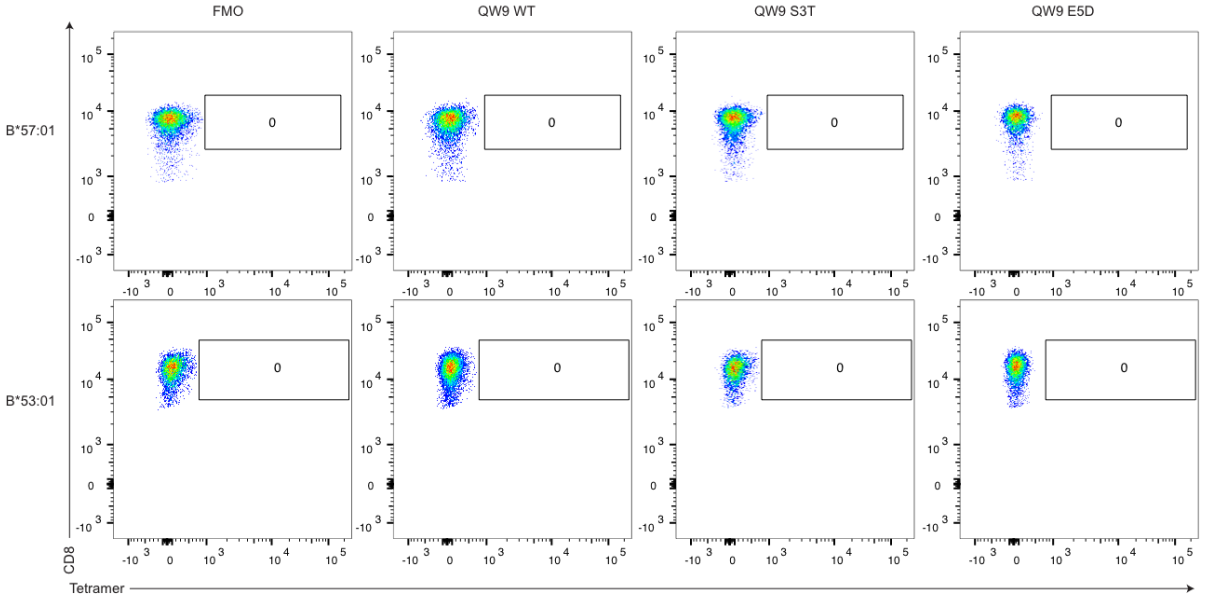

Supplemental Figure S2.1. Validation of QW9 WT and variant tetramers with HIV-negative HLA-matched donors. Flow cytometry plots of representative examples of QW9-tetramer positive cells for either B*53:01 or B*57:01. Gated on CD8+CD3+CD19-CD14-CD56- live lymphocyte singlet cells.

	Sample date	Subject ID	Viral Load (RNA copies/ml) #	CD4 count (cells/uL)	HIV Diagnosis Year	ART	Year of Birth	Gender	Race	HIV Risk
B*57:01	10/22/09	164007	<75	1437	1986	Naïve	1957	Female	African American/Hispanic	IVDU
	8/1/10	970489	493	552	2005	Naïve	1980	Male	Caucasian	MSM
	3/1/05	900837	355	780	1983	Naïve	1956	Male	Caucasian	MSM
	9/13/08	542735	<75	668	1995	Naïve	1965	Male	Unknown	MSM
	4/15/09	264095	184	682	2008	Naïve	1957	Male	Caucasian	MSM
	Sample date	Subject ID	Viral Load (RNA copies/ml) #	CD4 count (cells/uL)	HIV Diagnosis Year	ART	Year of Birth	Gender	Race	HIV Risk
B*53:01	10/21/09	912103	429	501	2000	Naïve	1972	Male	White/Hispanic	MSM
	8/4/11	443552	<50	849	1988	Naïve	1957	Male	African American	IVDU
	7/20/10	187948	<50	1157	2009	Naïve	1987	Female	Hispanic	Heterosexual
	3/31/09	423060	439	706	2000	Off therapy	1959	Male	African American	MSM
	8/8/06	616147	400	772	2000	Naïve	1966	Male	Caucasian	MSM

Supplemental Table S2.1. Clinical characteristics of research subjects.

SUPPLEMENTAL MATERIALS FOR CHAPTER 3

Experimental procedures

Subjects

All study subjects gave informed consent and IRB approval was obtained from the Massachusetts General Hospital institutional regulatory board (IRB). 101 individuals recruited in this study were 'HIV Controllers', defined as HIV infected individuals who spontaneously control HIV infection in the absence of antiretroviral therapy for greater than 1 year. These HIV controllers included 40 'Elite Controllers' with viral loads of below 50 HIV RNA copies/ml for greater than 1 year, and 61 'Viremic Controllers' with viral loads of between >50 <2,000 HIV RNA copies/ml for greater than 1 year. Additionally, 28 treatment-naive HIV progressors with viral loads of greater than 2,000 HIV RNA copies/ml were screened. All subjects were chosen based on delineation of their HLA class II DRB1 alleles (with all individuals selected upon expression of one or more common DRB1 alleles spanning *01:01, *03:01, *04:01, *07:01, *11:01, *13:01 and *15:01 and availability of frozen peripheral blood mononuclear cell (PBMC) samples for HLA-DR CD8 Elispots and further functional characterization (Tables S2.1 and S2.2).

Human leukocyte antigen typing.

High resolution four-digit HLA genotyping was performed by sequence-specific PCR in accordance with standard procedures. Briefly, HLA class I–encoding genes were amplified by PCR with primers spanning exons 2 and 3, and HLA class II DRB1–encoding genes were identified by PCR amplification and sequencing of exon 2. ASSIGN 3.5 software developed by Conexio Genomics was used to interpret the sequencing results.

Peptide synthesis

Overlapping Peptides (OLPs) corresponding to HIV-1 clade B consensus 2001 for Gag protein were synthesized at the MGH Peptide Core Facility on an automated peptide synthesizer using F-moc technology. In addition, N- and C-terminal truncated peptides were synthesized for Gag41.

Elispot with whole PBMC

Screening for class I-restricted HIV-specific $CD8^+$ T cell responses was conducted using a standardized IFN- Elispot assay with whole PBMC, as previously described (Ranasinghe et al., 2012). In brief, whole PBMC was co-cultured individually with 10 µg/mL optimally defined class I epitopes (concordant with HLA class I typing for that individual). Input cell numbers were 100,000 whole PBMC per well and the plates were incubated overnight at 37 °C and 5% CO_2. Responses were regarded as positive if they had at least 3 times the mean background and ≥3 times the standard deviation of the negative control wells; positive responses also had to be at least 50 SFC/10^6 PBMCs.

Epitope fine-mapping

For fine-mapping analysis, $CD8^+$ T cells enriched from whole PBMC by Miltenyi $CD8^+$ MACS MicroBeads were isolated. The IFN- responses of $CD8^+$ T cell populations against serial truncations of Gag41 (YVDRFYKTLRAEQASQEV) restricted by DRB1*11:01 were tested. Each peptide was tested at 20 µM including, with serial truncations from the N and C termini, presented by the restricting HLA-DRB1–expressing L cell lines. Enriched $CD8^+$ T cells were co-cultured at 100,000 cells with 20,000 LCL on a modified 'HLA-DR CD8 Elispot'.

Generation of $CD8^+$ T cell clones

Whole PBMC were thawed and rested for 2 hours, with half of the PBMC then pulsed with the respective peptide of interest for 1 hour at 37 ºC, 5% CO2. After pulsing, the PBMC were washed

to remove free peptide and then cultured in 60 wells of a 96-well round-bottom plate in RPMI 1640 medium containing 50 U/ml of recombinant IL-2. After approximately 2 weeks of culture, the whole PBMC TCL were then tested using the respective HLA class I or II tetramer to ascertain the percentage specificity of the population. Peptide-specific T cells were isolated using an IFN-γ secretion assay (Miltenyi), as per the manufacture's protocol. Isolated IFN-γ-positive T cells were cultured with irradiated allogeneic PBMC and CD3-specific antibody as a T cell proliferation stimulus for approximately 2 weeks and then limited dilution cloning was conducted, as previously described [79]. Developing epitope-specific $CD8^+$ T cell clones were further tested separately by chromium release assays to their respective peptide, and by tetramer staining to confirm their $CD8^+$ T cell specificity. Cloned $CD8^+$ T cells were maintained by restimulation every 14 to 21 days with an anti-CD3 mAb and irradiated allogeneic PBMC in RPMI 1640 medium containing 50 U/ml of recombinant IL-2, as previously described (Ranasinghe et al., 2011) [203]

Generation of autologous targets cells for killing assays

EBV-transformed B cell lines. 10 million frozen PBMC were thawed and resuspended in 1mL of RMPI, 1.5mL of fetal bovine serum (FBS), and 1.5mL of unconcentrated supernatant of Epstein-Barr virus. Cyclosporine A (sigma) was added in a 1 μg/ml concentration. Cell were cultured for 6 to 8 weeks at 37 °C and 5% CO2

Activated CD4+ T cells. CD4+ T cell were isolated from frozen PBMC using CD4 Macs Beads (Miltenyi) and blasted with human T-activator CD3/CD28 dynabeads (ThermoFisher) for three days at 37 °C and 5% CO2

Monocyte-derived macrophages. CD14+ cells were isolated from frozen PBMC using CD14 enrichment EasySep (STEM Cell) and cultured for 6 days at 37 °C and 5% CO2 to differentiate into macrophages (CD14+ CD11b+)

Infection assessment of target cells in killing assays

To assess infectivity, target cells were surface stained with either anti-CD4 or anti-CD11b antibody, and intracellular stained with anti-p24 antibody, KC57-RD1 (Beckman Coulter). The VSV-G pseudotyped HIV NL4-3 was obtained from the NIH AIDS Reagent Program, Division of AIDS, NIAID, NIH: pNL4-3-deltaE-EGFP (Cat# 11100) from Drs. Haili Zhang, Yan Zhou, and Robert Siliciano.

Vital Assay

A modified VITAL assay [204] was conducted with autologous EBV-transformed B cell lines. BCL were stained either with carboxyfluorescein diacetate succinimidyl ester (CFSE; Molecular Probes, Life Technologies, USA) or cell trace violet (CTV; Molecular Probes, Life Technologies) for 7 min at 37°C and then washed. 10 µg/mL of appropriate peptide was added separately to CFSE labeled cells, while CTV labeled cells remained without peptide, for 1 hour at 37 ºC, 5% CO_2. After several washes, 25,000 peptide$^+$ CFSE$^+$ cells were mixed with 25,000 peptide$^-$ CTV$^+$ cells to give a total of 50,000 targets per well. The target cells were then co-cultured with fresh Gag41 Tetramer-sorted CD8$^+$ T cells or bulk CD8$^+$ T cells, at a 1:1 E:T ratio. The co-cultures were incubated for 36 hours at 37 ºC, 5% CO_2. After 36 hours, the co-cultures were surface stained with anti-CD19, -CD3, -CD4, -CD8 antibodies, and a viability marker. Compensation was performed (including CFSE and CTV) and the fixed samples were analyzed on a LSRII flow cytometer (BD Biosciences). Analysis focused on the percentage of viable peptide-loaded CFSE$^+$ cells vs. CTV$^+$ cells, which lacked the cognate peptide.

Viral Sequencing

Genomic DNA was isolated from frozen PBMC as previously described [205]. In brief, genomic DNA was isolated using the Qiagen DNA blood mini kit (Qiagen Inc., Valencia, CA) and HIV-1 Gag was amplified using nested reverse transcriptase PCR (RT-PCR). The primer sequences are available

upon request. PCR products were prepared for sequencing on the 454 Genome Sequencer FLX Titanium (Roche) using standard protocols with modifications as previously described [206].

Single-Cell RNA-seq

Whole Transcriptome amplification (WTA). WTA of single cells in 96 well plates was performed with a modified SMART-Seq2 protocol, as described previously (Trombetta et al., 2014), with Maxima Reverse Transcriptase (Life Technologies) used in place of superscript II. WTA products were then cleaned with Agencourt XP DNA beads (DNA SPRI) and 80% ethanol (Beckman Coulter) and Illumina sequencing libraries were prepared using Nextera XT (Illumina). The 96 samples in each plate were pooled together, and cleaned with two 0.9x DNA SPRIs (Beckman Coulter). Library quality was assessed with a high sensitivity DNA chip (Agilent) and quantified with a high sensitivity dsDNA Quant Kit (Life Technologies). Samples were sequenced on an Illumina NextSeq 500 instrument using either 30bp paired-end reads or 150bp single-end reads.

Single-Cell RNA-Seq Preprocessing. RNA-seq reads were first trimmed using Trimmomatic (Bolger et al.,2014). Trimmed reads were aligned to the RefSeq hg38 genome and transcriptome (GRCh38.2) using TopHat [207] and Bowtie2 [208] respectively. The resulting transcriptome alignments were processed by RSEM to estimate the abundance (TPM) of RefSeq transcripts [209].

Sample Filtering and Normalization. Considering only single-cell libraries in which we could reconstruct a productive TCR alignment (see below), we excluded from further analysis libraries with poor values for total number of reads (< 25000 reads), the percentage of aligned reads (< 10% aligned), or the percentage of detected transcripts (< 20% detected). All transcripts with lower than 10 TPM expression in more than 85% of samples were removed from the analysis, and TPM values were normalized using the “normalize.quantiles” function in the Bioconductor

preprocessCore package [210]. After all filtering steps, 205 cells remained from the 228 cells that had productive TCR alignments with 3274 genes.

Single-Cell gene expression comparisons. Out of the 205 cells with reconstructed TCR sequences, 30 were $CD4^+$ and 175 were $CD8^+$ by Flow Cytometry gating. The expression of CD4, CD8A, and CD8B transcripts between the $CD4^+$ and $CD8^+$ cells was compared using Mann-Whitney-Wilcoxon test in R to determine the independence of CD4, CD8A, and CD8B expression in these populations.

TCR α and β chain sequencing

In order to reconstruct CDR3 sequences from single-cell RNA-sequencing data we developed TrapeS ("TCR Reconstruction Algorithm for Paired-End Single cells"), a software package for reconstruction of TCR sequences using short (~25bp) single cell paired-end RNA-sequencing. 150bp single-end reads were converted to artificial 49 bp read pairs for TrapeS analysis. TrapeS first takes standard genomic alignments as input and identifies the genomic segments that constitute the TCR by selecting the V and J segments expressed in the cell. Next, TrapeS takes the unmapped mates of the reads mapped to the genomic segments of the TCR and reconstructs the CDR3 region using an iterative dynamic programming algorithm. In each iteration the reads are aligned to the V and J segments, allowing only partial alignment to the ends of the segments so the reads "flank" toward the CDR3 region (flank the 3' end of the V segment and the 5' end of the J segment). Our method then extends the V and J regions using the sequence of the aligned reads, and repeats this step iteratively until the reconstructed regions overlap. TrapeS is available upon request.

Preparation of soluble DR11-Gag41

As previously described [211, 212], soluble DR11-Gag41 was expressed as soluble protein in baculovirus infected insect cells with the Gag41 peptide covalently attached via a C-terminal flexible linker to the N-terminus of the DR11 beta chain. A stabilizing C terminal acid-base leucine zipper was added to the C-terminal end of the DR11 alpha and beta chains and a peptide tag for enzymatic biotinylation was added to the c-terminus of the DR11 alpha chain. After purification this tag was biotinylated enzymatically. To prepare fluorescent tetramers, phycoerythrin-coupled streptavidin (PE-SA) was incubated with an excess of the biotinylated DR11-Gag41 or a control mouse IA^b-p3K protein and the fluorescent complex separated from the excess MHCII by size exclusion chromatography.

Preparation of soluble TRAV6-TRBV2 TCR.

As previously described [213, 214], the TRAV6-TRBV2 V domains were expressed separately in bacterial vectors fused to human Cα or Cβ. The separate chains were denatured and solubilized from inclusion bodies, mixed and refolded to form a native TCR.

Surface plasmon resonance (SPR)

SPR studies were performed with a BIAcore 2000 instrument containing a SA biosensor chip. ~2000 resonances units (RU) of biotinylated either DR11-Gag41 or control HLA-DR52c bound to a nickel mimicking peptide were captured in separate flow cells. Various concentrations of the soluble TRAV6 and TRBV2 TCR were injected for 80 seconds at 15 uL/min. Binding affinity was calculated from the association and dissociation curves using BIAEvaluation 4.1 software after subtracting the fluid phase RU signal seen with the control DR52c complex.

Supplemental Table S3.1. Cohort of HIV-infected individuals screened for $CD8^+$ T-cell responses restricted by HLA-DR				
HLA-DRB1 expression	No. of **HIV Controllers** screened by HLA-DRB1 ELISpot	No. of **HIV Controllers** screened by DR11-Gag41 tetramer	No. of **HIV Controllers** screened by DR01-Gag37 tetramer	No. of HIV Controllers with detectable DRB1-restricted CD8+ T cells
DRB1*01:01	25	-	25*	2
DRB1*04:01	18	-	-	0
DRB1*07:01	27	-	-	0
DRB1*11:01	31	68#	-	1
TOTAL	**101**	**68**	**25**	**3**

HLA-DRB1 expression	No. of **HIV Progressors** screened by HLA-DRB1 ELISpot	No. of **HIV Progressors** screened by DR11-Gag41 tetramer	No. of **HIV Progressors** screened by DR01-Gag37 tetramer	No. of HIV Progressors with detectable DRB1-restricted CD8+ T cells
DRB1*01:01	4	-	4*	0
DRB1*03:01	3	-	-	0
DRB1*07:01	7	-	-	0
DRB1*11:01	8	8#	-	0
DRB1*13:01	3	-	-	0
DRB1*15:01	3	-	-	0
TOTAL	**28**	**8**	**4**	**0**

Supplemental Table S3.1. Cohort of HIV-infected individuals screened for $CD8^+$ T-cell responses restricted by HLA-DR. A total of 129 HIV-infected individuals were screened for HLA-DR-restricted $CD8^+$ T-cell responses by IFN-γ Elispot and by flow cytometry using HLA class II tetramers, as depicted in the table. 101 individuals recruited in this study were 'HIV Controllers', defined as HIV infected individuals who spontaneously control HIV infection in the absence of antiretroviral therapy for greater than 1 year. The remaining 28 individual were treatment-naive HIV progressors with viral loads of greater than 2,000 HIV RNA copies/ml. #DRB1*11 subjects screened by tetramer included all DR11 subjects previously screened by HLA-DRB1 Elispot. *DRB1*01 subjects screened by tetramer included all DR01 subjects previously screened by HLA-DRB1 Elispot

Supplemental Table S3.2. Clinical characteristics of study subjects with detected HLA class II-restricted CD8$^+$ T cells.			
Ragon Identifier	474723	270245	388031
HIV status[#]	Viremic Controller	Viremic Controller	Elite Controller
Viral Load (RNA copies/ml) [#]	136	20	<75
CD4 count (cells/uL) [#]	1137	684	1100
HIV Diagnosis Year	1997	1982	2004
Enrolled in the Cohort	2007 until present	2005 until present	2005 until 2013
ART	1997-2003, off therapy 2003-2015, Restarted therapy Jan 2016	1987-2000, off-therapy from 2000 to present	Treatment-naive
Year of Birth	1964	1947	1966
Gender	Male	Male	Male
Race	Black or African American	White	White
HIV Risk	Blood products	MSM	MSM
Known co-infections[#]	HBV	TBD	TBD
HLA class I alleles	A*30:01, A*30:02, B*42:01, B*57:03, Cw17, Cw18	A*02:01, A*03:01, B*08:1, B44*05, Cw*02:02, Cw*07:01	A*11:01, A*32:01, B*27:05, B*27:05, Cw*01:02, Cw*02:02
HLA class II alleles	DRB1*03:02, DRB1*11:01, DPB*01:01, DPB*39:01, DQB*04:02, DQB*05:01,	DRB1*01:01, DRB1*04:03	DRB1*01:01, DRB1*04:01, DPB*04:01, DPB*:04:01, DQB*03:02, DQB*05:01,

Supplemental Table S3.2. Clinical characteristics of study subjects with detected HLA class II-restricted CD8$^+$ T cells. The clinical characteristics for study subjects 474723, 270245, and 388031 with detectable HLA class II-restricted CD8$^+$ T cell responses are depicted in the table. The former two subjects are currently enrolled, however, 388031 left the cohort in 2013 with almost no sample availability remaining. Subject 474723 started antiretroviral therapy in 2016. [#] Information provided for principal date of assays utilizing fresh or frozen PBMC. MSM: Men who have sex with men, HBV: Hepatitis B virus

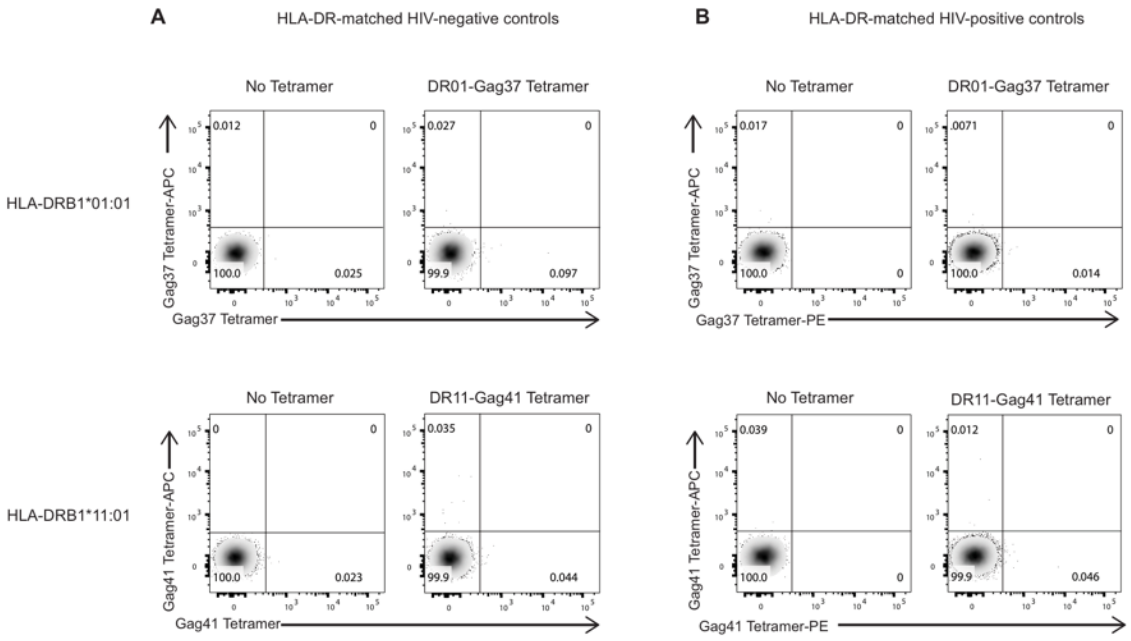

Supplemental Figure S3.1. HLA-DR tetramer validation in HIV-negative and HIV-positive subjects. Representative FACS plot of HLA class II tetramer staining of fresh PBMCs in HLA-matched HIV-negative (**A**) and HIV-positive (**B**) subjects. Populations shown are gated on $CD3^{+}CD8^{+}CD4^{-}CD19^{-}CD14^{-}CD56^{-}$ live lymphocyte singlets. Bulk $CD8^{+}$ T cells are shown in the absence and presence of tetramer.

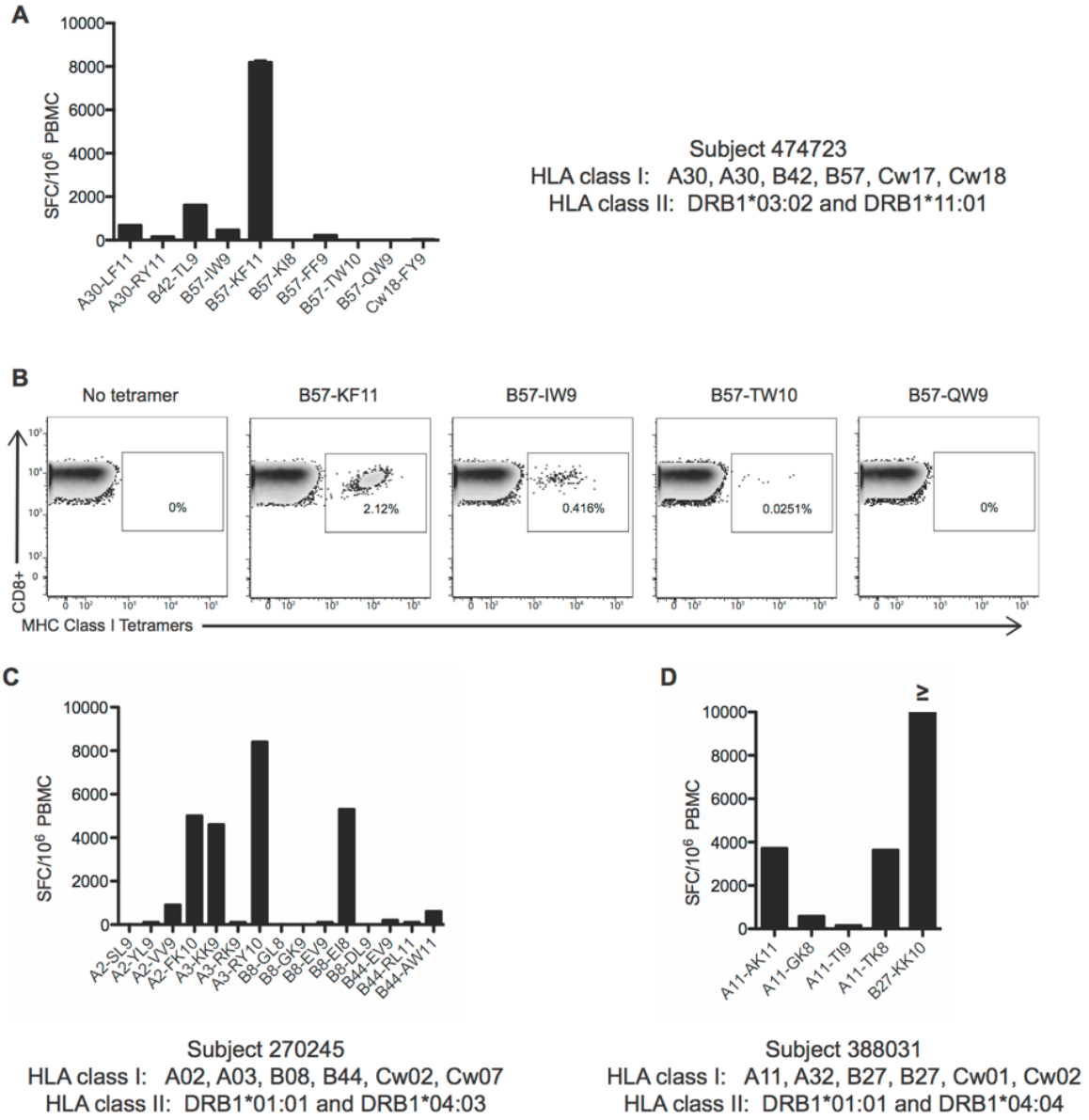

Supplemental Figure S3.2. Epitope-targeting of HLA class I- versus class II-restricted CD8$^+$ T cells. (**A**) Summary graph of HLA class I-restricted Gag-specific CD8$^+$ T cells in subject 474723 as measured in a standard IFN-γ ELISPOT assay. Known optimal peptides matching the subject's HLA class I typing were added to whole PBMC. Error bars with standard deviation (SD) is shown (**B**) Representative FACS plots of ex-vivo tetramer positive CD8$^+$ T cells in subject 474723 to immunodominant HLA-B*57 epitopes KF11, IW9, TW10 and QW9. (**C**) Summary graph of HLA class I-restricted Gag-specific CD8$^+$ T cells in subject 270245 as measured in a standard IFN-γ ELISPOT assay. Known optimal peptides matching the subject's HLA class I were added to whole PBMC. (**D**) Summary graph of HLA class I-restricted Gag-specific CD8$^+$ T cells in subject 388031 as measured in a standard IFN-γ ELISPOT assay. Known optimal peptides matching the subject's HLA class I typing were added to whole PBMC. The B*27-KK10 response was greater than the threshold of accurate detection (9999 SFU/10^6) as represented by "≥".

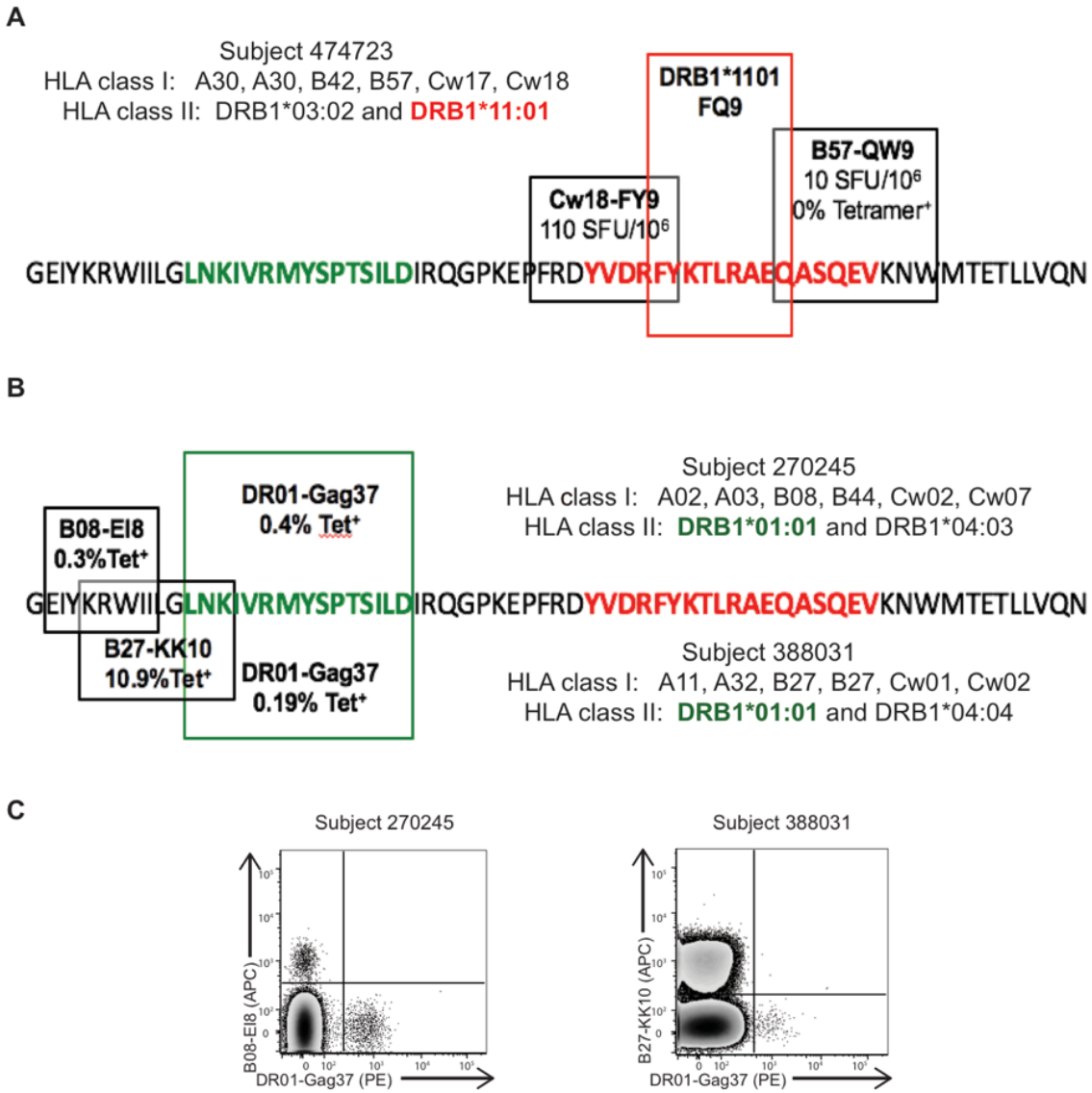

Figure S3.3. Epitope-mapping of class I- versus class II-restricted CD8$^+$ T cells. (**A**) Schematic of a partial Gag p24 sequence highlighting the Gag41 peptide residues in red text and the predicted core peptide FA10 in a red box for subject 473723. HLA class I epitopes B*57-QW9 and Cw*18-FY9 is shown in black boxes, with values corresponding to standard IFN-γ ELISPOT and tetramer staining. (**B**) Schematic of a partial Gag p24 sequence highlighting the Gag37 peptide residues in green text and values corresponding to DR01-Gag37 tetramer staining for subjects 270245 and 388031 in a green box. For subject 270245, values corresponding to B*08-EI8 tetramer staining is shown in a black box. For subject 388031, values corresponding to B*27-KK10 tetramer staining is shown in a black box. For reference, the Gag41 sequence is highlighted in red text. (**C**) Representative FACS plot denoting percentage frequency of ex-vivo tetramer positive CD8$^+$ T cells to DR01-Gag37 and B*08-EI8 in subject 270245, and DR01-Gag37 and B*27-KK10 in subject 388031, as determined by dual staining with HLA class I (APC) and II (PE) tetramers.

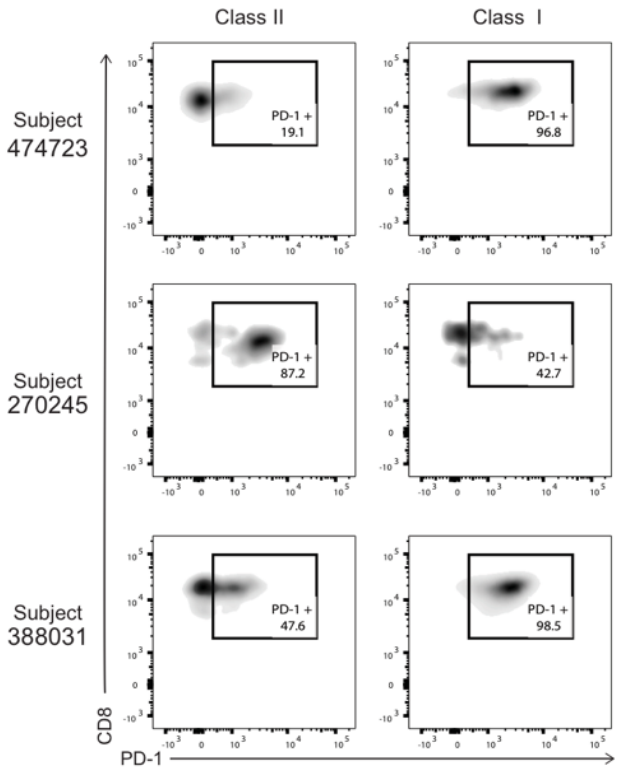

Supplemental Figure S3.4. PD-1 expression on class I- and class II-restricted CD8+ T cells. Representative FACS plots of surface PD-1 expression on tetramer positive HLA class I and class II-restricted CD8+ T cells. Populations shown are gated on Tetramer+ CD3+ CD8+ CD4- CD19- CD14- CD56- live lymphocyte singlets.

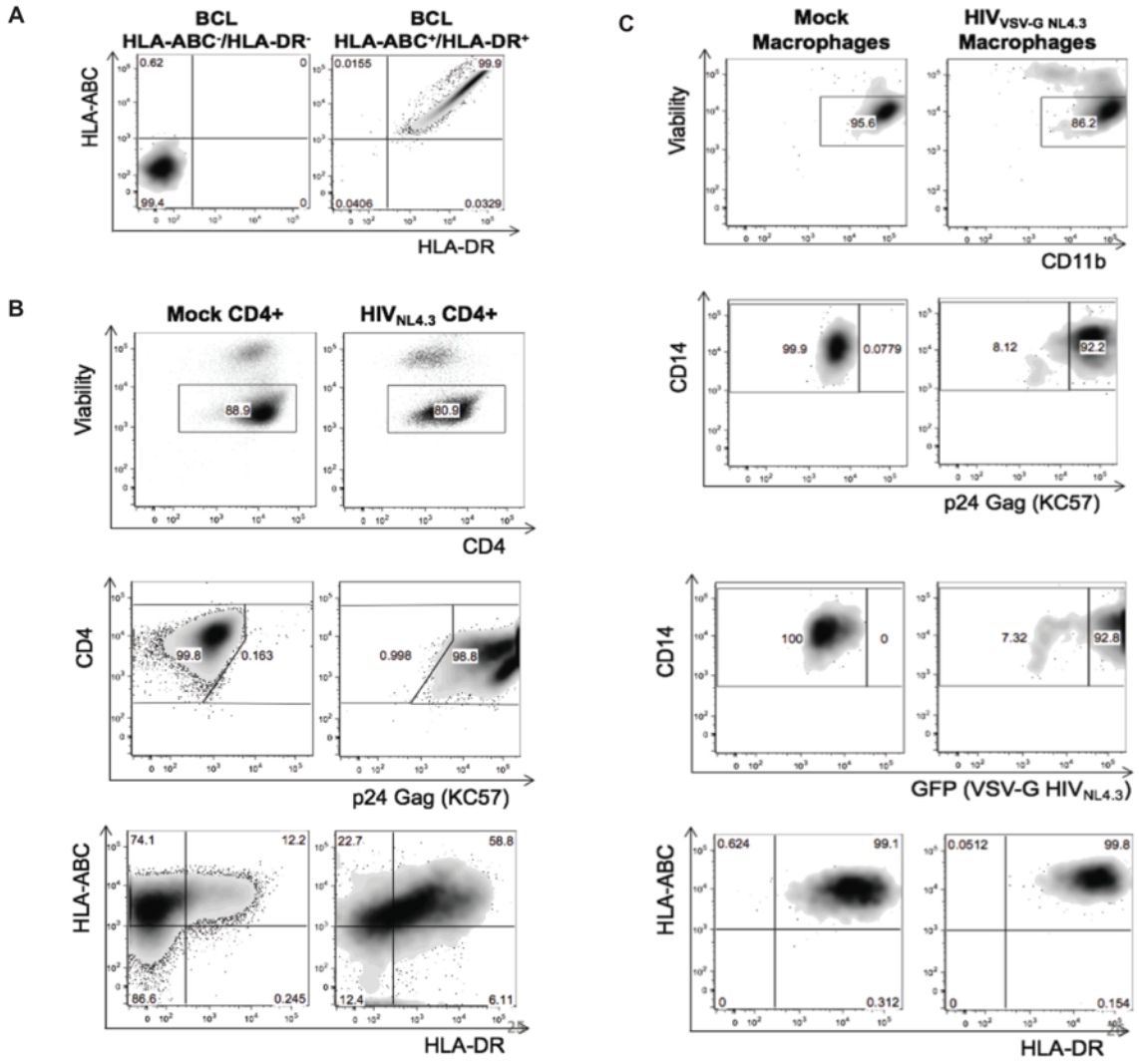

Supplemental Figure S3.5. HIV infection and HLA expression of $CD4^+$ T cells (A), EBV-transformed B cell line (B) and monocyte-derived macrophages (C) from subject 474723. Representative FACS plots denoting surface HLA class I ABC and HLA-DR expression on autologous target cells using W6/32 and L432 antibodies, respectively. The proportion of intracellular Gag p24 positive $CD4^+$ T cells was analyzed by flow cytometry 48 hrs post-infection using KC57 antibody. The $CD4^+$ T cells were blasted with $CD3^+CD28^+$ dynabeads 3 days prior to infection by spinoculation with HIV NL4.3. The proportion of GFP positive and intracellular Gag p24 KC57 antibody positive monocyte derived macrophages ($CD14^+$ $CD11b^+$) was analyzed 48 hrs post-infection with VSV-G psuedotyped HIV NL4.3.

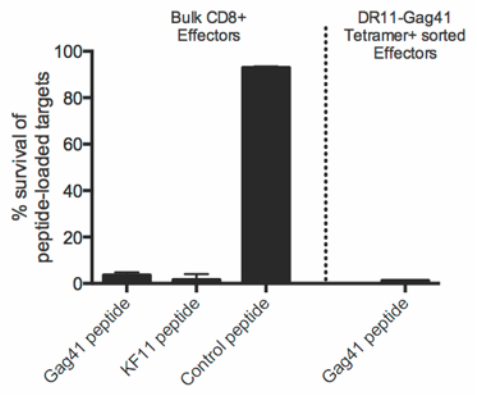

Supplemental Figure S3.6. Specific elimination of peptide-loaded target cells in a modified VITAL assay. Summary graph of ex-vivo bulk $CD8^+$ T cells and tetramer-sorted DR11-Gag41 positive cells from subject 474723 tested in a modified 36 hr VITAL assay. Ex-vivo effector cells were derived from fresh blood; processed and isolated within 12hrs. Bulk $CD8^+$ T cells were isolated using Miltenyi CD8 MACS beads. DR11-Gag41 positive $CD8^+$ T cells were tetramer stained and isolated by FACS. Autologous EBV-transformed BCL were used as target cells, in which half of the autologous BCL were pulsed with peptide and labeled with CFSE (Carboxyfluorescein succinimidyl ester), and the other half remained without peptide and were labeled with CTV (Cell Trace Violet), prior to co-culture with the tetramer sorted effectors in duplicate. After 36 hours, the co-culture was stained and analyzed by flow cytometry. Error bars with standard deviation shows the percentage survival of peptide-loaded cells ($CFSE^+$).

REFERENCES

1. Bertagnolio, S. *et al.* Determinants of HIV drug resistance and public health implications in low- and middle-income countries. *Antivir Ther* **17**, 941-953 (2012).

2. Bertagnolio, S. *et al.* World Health Organization generic protocol to assess drug-resistant HIV among children <18 months of age and newly diagnosed with HIV in resource-limited countries. *Clin Infect Dis* **54 Suppl 4**, S254-260 (2012).

3. Abdool Karim, S.S. Overcoming Impediments to Global Implementation of Early Antiretroviral Therapy. *N Engl J Med* **373**, 875-876 (2015).

4. Padian, N.S. *et al.* HIV prevention transformed: the new prevention research agenda. *Lancet* **378**, 269-278 (2011).

5. Johnston, M.I. & Fauci, A.S. HIV vaccine development--improving on natural immunity. *N Engl J Med* **365**, 873-875 (2011).

6. Simek, M.D. *et al.* Human immunodeficiency virus type 1 elite neutralizers: individuals with broad and potent neutralizing activity identified by using a high-throughput neutralization assay together with an analytical selection algorithm. *J Virol* **83**, 7337-7348 (2009).

7. Liao, H.X. *et al.* Co-evolution of a broadly neutralizing HIV-1 antibody and founder virus. *Nature* **496**, 469-476 (2013).

8. Klein, F. *et al.* Somatic mutations of the immunoglobulin framework are generally required for broad and potent HIV-1 neutralization. *Cell* **153**, 126-138 (2013).

9. Rerks-Ngarm, S. *et al.* Vaccination with ALVAC and AIDSVAX to prevent HIV-1 infection in Thailand. *N Engl J Med* **361**, 2209-2220 (2009).

10. Richman, D.D. *et al.* The challenge of finding a cure for HIV infection. *Science* **323**, 1304-1307 (2009).

11. Chun, T.W. *et al.* Presence of an inducible HIV-1 latent reservoir during highly active antiretroviral therapy. *Proc Natl Acad Sci U S A* **94**, 13193-13197 (1997).

12. Finzi, D. *et al.* Identification of a reservoir for HIV-1 in patients on highly active antiretroviral therapy. *Science* **278**, 1295-1300 (1997).

13. Massanella, M. & Richman, D.D. Measuring the latent reservoir in vivo. *J Clin Invest* **126**, 464-472 (2016).

14. Wong, J.K. *et al.* Recovery of replication-competent HIV despite prolonged suppression of plasma viremia. *Science* **278**, 1291-1295 (1997).

15. Davey, R.T., Jr. *et al.* HIV-1 and T cell dynamics after interruption of highly active antiretroviral therapy (HAART) in patients with a history of sustained viral suppression. *Proc Natl Acad Sci U S A* **96**, 15109-15114 (1999).

16. Bruner, K.M., Hosmane, N.N. & Siliciano, R.F. Towards an HIV-1 cure: measuring the latent reservoir. *Trends Microbiol* **23**, 192-203 (2015).

17. Ho, Y.C. *et al.* Replication-competent noninduced proviruses in the latent reservoir increase barrier to HIV-1 cure. *Cell* **155**, 540-551 (2013).

18. Chun, T.W. *et al.* Early establishment of a pool of latently infected, resting CD4(+) T cells during primary HIV-1 infection. *Proc Natl Acad Sci U S A* **95**, 8869-8873 (1998).

19. Laird, G.M. *et al.* Ex vivo analysis identifies effective HIV-1 latency-reversing drug combinations. *J Clin Invest* **125**, 1901-1912 (2015).

20. Archin, N.M. & Margolis, D.M. Emerging strategies to deplete the HIV reservoir. *Curr Opin Infect Dis* **27**, 29-35 (2014).

21. Siliciano, J.D. & Siliciano, R.F. HIV-1 eradication strategies: design and assessment. *Curr Opin HIV AIDS* **8**, 318-325 (2013).

22. Massanella, M., Martinez-Picado, J. & Blanco, J. Attacking the HIV reservoir from the immune and viral perspective. *Curr HIV/AIDS Rep* **10**, 33-41 (2013).

23. Katlama, C. *et al.* Barriers to a cure for HIV: new ways to target and eradicate HIV-1 reservoirs. *The Lancet* **381**, 2109-2117 (2013).

24. Mates, J.M. *et al.* A Novel Histone Deacetylase Inhibitor, AR-42, Reactivates HIV-1 from Chronically and Latently Infected CD4+ T-cells. *Retrovirology (Auckl)* **7**, 1-5 (2015).

25. Stoszko, M. *et al.* Small Molecule Inhibitors of BAF; A Promising Family of Compounds in HIV-1 Latency Reversal. *EBioMedicine* **3**, 108-121 (2016).

26. Rasmussen, T.A. *et al.* Panobinostat, a histone deacetylase inhibitor, for latent-virus reactivation in HIV-infected patients on suppressive antiretroviral therapy: a phase 1/2, single group, clinical trial. *Lancet HIV* **1**, e13-21 (2014).

27. Barton, K. *et al.* Broad activation of latent HIV-1 in vivo. *Nat Commun* **7**, 12731 (2016).

28. Shen, M. *et al.* The chromatin remodeling factor CSB recruits histone acetyltransferase PCAF to rRNA gene promoters in active state for transcription initiation. *PLoS One* **8**, e62668 (2013).

29. Shan, L. *et al.* Stimulation of HIV-1-specific cytolytic T lymphocytes facilitates elimination of latent viral reservoir after virus reactivation. *Immunity* **36**, 491-501 (2012).

30. Deng, K. *et al.* Broad CTL response is required to clear latent HIV-1 due to dominance of escape mutations. *Nature* **517**, 381-385 (2015).

31. Deeks, S.G. & Walker, B.D. Human immunodeficiency virus controllers: mechanisms of durable virus control in the absence of antiretroviral therapy. *Immunity* **27**, 406-416 (2007).

32. Carrington, M. & Walker, B.D. Immunogenetics of spontaneous control of HIV. *Annu Rev Med* **63**, 131-145 (2012).

33. Walker, B.D. & Yu, X.G. Unravelling the mechanisms of durable control of HIV-1. *Nat Rev Immunol* **13**, 487-498 (2013).

34. Buzon, M.J. *et al.* Susceptibility to CD8 T-cell-mediated killing influences the reservoir of latently HIV-1-infected CD4 T cells. *J Acquir Immune Defic Syndr* **65**, 1-9 (2014).

35. Barouch, D.H. & Deeks, S.G. Immunologic strategies for HIV-1 remission and eradication. *Science* **345**, 169-174 (2014).

36. Migueles, S.A. *et al.* CD8+ T-cell Cytotoxic Capacity Associated with Human Immunodeficiency Virus-1 Control Can Be Mediated through Various Epitopes and Human Leukocyte Antigen Types. *EBioMedicine* **2**, 46-58 (2015).

37. Migueles, S.A. *et al.* Lytic granule loading of CD8+ T cells is required for HIV-infected cell elimination associated with immune control. *Immunity* **29**, 1009-1021 (2008).

38. Siliciano, J.D. & Siliciano, R.F. Recent developments in the effort to cure HIV infection: going beyond N = 1. *J Clin Invest* **126**, 409-414 (2016).

39. Lyles, R.H. *et al.* Natural history of human immunodeficiency virus type 1 viremia after seroconversion and proximal to AIDS in a large cohort of homosexual men. Multicenter AIDS Cohort Study. *J Infect Dis* **181**, 872-880 (2000).

40. Arnaout, R.A. *et al.* A simple relationship between viral load and survival time in HIV-1 infection. *Proc Natl Acad Sci U S A* **96**, 11549-11553 (1999).

41. Quinn, T.C. *et al.* Viral load and heterosexual transmission of human immunodeficiency virus type 1. Rakai Project Study Group. *N Engl J Med* **342**, 921-929 (2000).

42. Gallo, R.C. *et al.* Frequent detection and isolation of cytopathic retroviruses (HTLV-III) from patients with AIDS and at risk for AIDS. *Science* **224**, 500-503 (1984).

43. Popovic, M., Sarngadharan, M.G., Read, E. & Gallo, R.C. Detection, isolation, and continuous production of cytopathic retroviruses (HTLV-III) from patients with AIDS and pre-AIDS. *Science* **224**, 497-500 (1984).

44. Sarngadharan, M.G., Popovic, M., Bruch, L., Schupbach, J. & Gallo, R.C. Antibodies reactive with human T-lymphotropic retroviruses (HTLV-III) in the serum of patients with AIDS. *Science* **224**, 506-508 (1984).

45. Schupbach, J. *et al.* Serological analysis of a subgroup of human T-lymphotropic retroviruses (HTLV-III) associated with AIDS. *Science* **224**, 503-505 (1984).

46. Barre-Sinoussi, F. *et al.* Isolation of a T-lymphotropic retrovirus from a patient at risk for acquired immune deficiency syndrome (AIDS). *Science* **220**, 868-871 (1983).

47. Brun-Vezinet, F. *et al.* Prevalence of antibodies to lymphadenopathy-associated retrovirus in African patients with AIDS. *Science* **226**, 453-456 (1984).

48. Goodsell, D.S. Illustrations of the HIV life cycle. *Curr Top Microbiol Immunol* **389**, 243-252 (2015).

49. Douek, D.C. *et al.* HIV preferentially infects HIV-specific CD4+ T cells. *Nature* **417**, 95-98 (2002).

50. Fauci, A.S., Pantaleo, G., Stanley, S. & Weissman, D. Immunopathogenic mechanisms of HIV infection. *Ann Intern Med* **124**, 654-663 (1996).

51. McMichael, A.J., Borrow, P., Tomaras, G.D., Goonetilleke, N. & Haynes, B.F. The immune response during acute HIV-1 infection: clues for vaccine development. *Nat Rev Immunol* **10**, 11-23 (2010).

52. Brenchley, J.M. *et al.* CD4+ T cell depletion during all stages of HIV disease occurs predominantly in the gastrointestinal tract. *J Exp Med* **200**, 749-759 (2004).

53. Ndhlovu, Z.M. *et al.* Magnitude and Kinetics of CD8+ T Cell Activation during Hyperacute HIV Infection Impact Viral Set Point. *Immunity* **43**, 591-604 (2015).

54. Robb, M.L. *et al.* Prospective Study of Acute HIV-1 Infection in Adults in East Africa and Thailand. *N Engl J Med* **374**, 2120-2130 (2016).

55. Rodriguez, B. *et al.* Predictive value of plasma HIV RNA level on rate of CD4 T-cell decline in untreated HIV infection. *Jama* **296**, 1498-1506 (2006).

56. Buchbinder, S.P., Katz, M.H., Hessol, N.A., O'Malley, P.M. & Holmberg, S.D. Long-term HIV-1 infection without immunologic progression. *AIDS* **8**, 1123-1128 (1994).

57. Hubert, J.B. *et al.* Natural history of serum HIV-1 RNA levels in 330 patients with a known date of infection. The SEROCO Study Group. *AIDS* **14**, 123-131 (2000).

58. Neefjes, J., Jongsma, M.L., Paul, P. & Bakke, O. Towards a systems understanding of MHC class I and MHC class II antigen presentation. *Nat Rev Immunol* **11**, 823-836 (2011).

59. Schmitz, J.E. *et al.* Control of viremia in simian immunodeficiency virus infection by CD8+ lymphocytes. *Science* **283**, 857-860 (1999).

60. Jin, X. *et al.* Dramatic rise in plasma viremia after CD8(+) T cell depletion in simian immunodeficiency virus-infected macaques. *J Exp Med* **189**, 991-998 (1999).

61. Migueles, S.A. *et al.* HIV-specific CD8+ T cell proliferation is coupled to perforin expression and is maintained in nonprogressors. *Nat Immunol* **3**, 1061-1068 (2002).

62. Ndhlovu, Z.M. *et al.* High-dimensional immunomonitoring models of HIV-1-specific CD8 T-cell responses accurately identify subjects achieving spontaneous viral control. *Blood* **121**, 801-811 (2013).

63. Altfeld, M. *et al.* HLA Alleles Associated with Delayed Progression to AIDS Contribute Strongly to the Initial CD8(+) T Cell Response against HIV-1. *PLoS Med* **3**, e403 (2006).

64. Edwards, B.H. *et al.* Magnitude of functional CD8+ T-cell responses to the gag protein of human immunodeficiency virus type 1 correlates inversely with viral load in plasma. *J Virol* **76**, 2298-2305 (2002).

65. Davenport, M.P. & Petravic, J. CD8+ T cell control of HIV--a known unknown. *PLoS Pathog* **6**, e1000728 (2010).

66. Kiepiela, P. *et al.* Dominant influence of HLA-B in mediating the potential co-evolution of HIV and HLA. *Nature* **432**, 769-775 (2004).

67. Kiepiela, P. *et al.* CD8+ T-cell responses to different HIV proteins have discordant associations with viral load. *Nat Med* **13**, 46-53 (2007).

68. Migueles, S.A. *et al.* HLA B*5701 is highly associated with restriction of virus replication in a subgroup of HIV-infected long term nonprogressors. *Proc Natl Acad Sci U S A* **97**, 2709-2714 (2000).

69. Kaslow, R.A. *et al.* Influence of combinations of human major histocompatibility complex genes on the course of HIV-1 infection. *Nat Med* **2**, 405-411 (1996).

70. Pereyra, F. *et al.* The major genetic determinants of HIV-1 control affect HLA class I peptide presentation. *Science* **330**, 1551-1557 (2010).

71. Fellay, J. *et al.* A whole-genome association study of major determinants for host control of HIV-1. *Science* **317**, 944-947 (2007).

72. Emu, B. *et al.* HLA class I-restricted T-cell responses may contribute to the control of human immunodeficiency virus infection, but such responses are not always necessary for long-term virus control. *J Virol* **82**, 5398-5407 (2008).

73. Riou, C. *et al.* Differential impact of magnitude, polyfunctional capacity, and specificity of HIV-specific CD8+ T cell responses on HIV set point. *J Virol* **88**, 1819-1824 (2014).

74. Almeida, J.R. *et al.* Superior control of HIV-1 replication by CD8+ T cells is reflected by their avidity, polyfunctionality, and clonal turnover. *J Exp Med* **204**, 2473-2485 (2007).

75. Betts, M.R. *et al.* HIV nonprogressors preferentially maintain highly functional HIV-specific CD8+ T cells. *Blood* **107**, 4781-4789 (2006).

76. Almeida, J.R. *et al.* Antigen sensitivity is a major determinant of CD8+ T-cell polyfunctionality and HIV-suppressive activity. *Blood* **113**, 6351-6360 (2009).

77. Chen, H. *et al.* Differential neutralization of human immunodeficiency virus (HIV) replication in autologous CD4 T cells by HIV-specific cytotoxic T lymphocytes. *J Virol* **83**, 3138-3149 (2009).

78. Day, C.L. *et al.* Proliferative capacity of epitope-specific CD8 T-cell responses is inversely related to viral load in chronic human immunodeficiency virus type 1 infection. *J Virol* **81**, 434-438 (2007).

79. Chen, H. *et al.* TCR clonotypes modulate the protective effect of HLA class I molecules in HIV-1 infection. *Nat Immunol* **13**, 691-700 (2012).

80. Ladell, K. *et al.* A molecular basis for the control of preimmune escape variants by HIV-specific CD8+ T cells. *Immunity* **38**, 425-436 (2013).

81. Goulder, P.J. & Walker, B.D. HIV and HLA class I: an evolving relationship. *Immunity* **37**, 426-440 (2012).

82. Miura, T. *et al.* HLA-B57/B*5801 human immunodeficiency virus type 1 elite controllers select for rare gag variants associated with reduced viral replication capacity and strong cytotoxic T-lymphocyte [corrected] recognition. *J Virol* **83**, 2743-2755 (2009).

83. Miura, T. *et al.* HLA-associated alterations in replication capacity of chimeric NL4-3 viruses carrying gag-protease from elite controllers of human immunodeficiency virus type 1. *J Virol* **83**, 140-149 (2009).

84. Miura, T. *et al.* Impaired replication capacity of acute/early viruses in persons who become HIV controllers. *J Virol* **84**, 7581-7591 (2010).

85. Lassen, K.G. *et al.* Elite suppressor-derived HIV-1 envelope glycoproteins exhibit reduced entry efficiency and kinetics. *PLoS Pathog* **5**, e1000377 (2009).

86. Troyer, R.M. *et al.* Variable fitness impact of HIV-1 escape mutations to cytotoxic T lymphocyte (CTL) response. *PLoS Pathog* **5**, e1000365 (2009).

87. Robinson, J. *et al.* The IMGT/HLA database. *Nucleic Acids Res* **39**, D1171-1176 (2011).

88. Addo, M.M. *et al.* Comprehensive epitope analysis of human immunodeficiency virus type 1 (HIV-1)-specific T-cell responses directed against the entire expressed HIV-1 genome demonstrate broadly directed responses, but no correlation to viral load. *J Virol* **77**, 2081-2092 (2003).

89. Betts, M.R. *et al.* Analysis of total human immunodeficiency virus (HIV)-specific CD4(+) and CD8(+) T-cell responses: relationship to viral load in untreated HIV infection. *J Virol* **75**, 11983-11991 (2001).

90. Harari, A. *et al.* Skewed association of polyfunctional antigen-specific CD8 T cell populations with HLA-B genotype. *Proc Natl Acad Sci U S A* **104**, 16233-16238 (2007).

91. Allen, T.M. *et al.* Selective escape from CD8+ T-cell responses represents a major driving force of human immunodeficiency virus type 1 (HIV-1) sequence diversity and reveals constraints on HIV-1 evolution. *J Virol* **79**, 13239-13249 (2005).

92. Allen, T.M. *et al.* De novo generation of escape variant-specific CD8+ T-cell responses following cytotoxic T-lymphocyte escape in chronic human immunodeficiency virus type 1 infection. *J Virol* **79**, 12952-12960 (2005).

93. Iglesias, M.C. *et al.* Escape from highly effective public CD8+ T-cell clonotypes by HIV. *Blood* **118**, 2138-2149 (2011).

94. Koibuchi, T. *et al.* Limited sequence evolution within persistently targeted CD8 epitopes in chronic human immunodeficiency virus type 1 infection. *J Virol* **79**, 8171-8181 (2005).

95. Schwartz, J.A. *et al.* Tim-3 is a Marker of Plasmacytoid Dendritic Cell Dysfunction during HIV Infection and Is Associated with the Recruitment of IRF7 and p85 into Lysosomes and with the Submembrane Displacement of TLR9. *J Immunol* **198**, 3181-3194 (2017).

96. Tian, X. *et al.* The upregulation of LAG-3 on T cells defines a subpopulation with functional exhaustion and correlates with disease progression in HIV-infected subjects. *J Immunol* **194**, 3873-3882 (2015).

97. Day, C.L. *et al.* PD-1 expression on HIV-specific T cells is associated with T-cell exhaustion and disease progression. *Nature* **443**, 350-354 (2006).

98. Kaufmann, D.E. *et al.* Upregulation of CTLA-4 by HIV-specific CD4+ T cells correlates with disease progression and defines a reversible immune dysfunction. *Nat Immunol* **8**, 1246-1254 (2007).

99. Trautmann, L. *et al.* Upregulation of PD-1 expression on HIV-specific CD8+ T cells leads to reversible immune dysfunction. *Nat Med* **12**, 1198-1202 (2006).

100. Petrovas, C. *et al.* PD-1 is a regulator of virus-specific CD8+ T cell survival in HIV infection. *J Exp Med* **203**, 2281-2292 (2006).

101. Arumugham, V.B. & Baldari, C.T. cAMP: a multifaceted modulator of immune synapse assembly and T cell activation. *J Leukoc Biol* (2017).

102. Zhou, F. Perforin: more than just a pore-forming protein. *Int Rev Immunol* **29**, 56-76 (2010).

103. Shastri, N., Cardinaud, S., Schwab, S.R., Serwold, T. & Kunisawa, J. All the peptides that fit: the beginning, the middle, and the end of the MHC class I antigen-processing pathway. *Immunol Rev* **207**, 31-41 (2005).

104. Yewdell, J.W., Reits, E. & Neefjes, J. Making sense of mass destruction: quantitating MHC class I antigen presentation. *Nat Rev Immunol* **3**, 952-961 (2003).

105. Reeves, E. & James, E. Antigen processing and immune regulation in the response to tumours. *Immunology* **150**, 16-24 (2017).

106. Emmerich, N.P. *et al.* The human 26 S and 20 S proteasomes generate overlapping but different sets of peptide fragments from a model protein substrate. *J Biol Chem* **275**, 21140-21148 (2000).

107. Zinkernagel, R.M. Cellular immune recognition and the biological role of major transplantation antigens. *Biosci Rep* **17**, 91-111 (1997).

108. Mizuochi, T., Tentori, L., Sharrow, S.O., Kruisbeek, A.M. & Singer, A. Differentiation of Ia-reactive CD8+ murine T cells does not require Ia engagement. Implications for the role of CD4 and CD8 accessory molecules in T cell differentiation. *J Exp Med* **168**, 437-442 (1988).

109. Matechak, E.O., Killeen, N., Hedrick, S.M. & Fowlkes, B.J. MHC class II-specific T cells can develop in the CD8 lineage when CD4 is absent. *Immunity* **4**, 337-347 (1996).

110. Shimizu, T. & Takeda, S. CD8 T cells from major histocompatibility complex class II-deficient mice respond vigorously to class II molecules in a primary mixed lymphocyte reaction. *Eur J Immunol* **27**, 500-508 (1997).

111. Pearce, E.L., Shedlock, D.J. & Shen, H. Functional characterization of MHC class II-restricted CD8+CD4- and CD8-CD4- T cell responses to infection in CD4-/- mice. *J Immunol* **173**, 2494-2499 (2004).

112. Tyznik, A.J., Sun, J.C. & Bevan, M.J. The CD8 population in CD4-deficient mice is heavily contaminated with MHC class II-restricted T cells. *J Exp Med* **199**, 559-565 (2004).

113. Suzuki, H. *et al.* Origin of a T cell clone with a mismatched combination of MHC restriction and coreceptor expression. *J Immunol* **153**, 4496-4507 (1994).

114. Hirosawa, T. *et al.* Mismatched human leukocyte antigen class II-restricted CD8(+) cytotoxic T cells may mediate selective graft-versus-leukemia effects following allogeneic hematopoietic cell transplantation. *Cancer Sci* **102**, 1281-1286 (2011).

115. Rist, M., Smith, C., Bell, M.J., Burrows, S.R. & Khanna, R. Cross-recognition of HLA DR4 alloantigen by virus-specific CD8+ T cells: a new paradigm for self-/nonself-recognition. *Blood* **114**, 2244-2253 (2009).

116. Heemskerk, M.H. *et al.* Dual HLA class I and class II restricted recognition of alloreactive T lymphocytes mediated by a single T cell receptor complex. *Proc Natl Acad Sci U S A* **98**, 6806-6811 (2001).

117. Hansen, S.G. *et al.* Cytomegalovirus vectors violate CD8+ T cell epitope recognition paradigms. *Science* **340**, 1237874 (2013).

118. Hansen, S.G. *et al.* Broadly targeted CD8(+) T cell responses restricted by major histocompatibility complex E. *Science* **351**, 714-720 (2016).

119. Hansen, S.G. *et al.* Profound early control of highly pathogenic SIV by an effector memory T-cell vaccine. *Nature* **473**, 523-527 (2011).

120. Ranasinghe, S. & Walker, B.D. Programming CMV for vaccine vector design. *Nat Biotechnol* **31**, 811-812 (2013).

121. Yang, O.O. *et al.* Lysis of HIV-1-infected cells and inhibition of viral replication by universal receptor T cells. *Proc Natl Acad Sci U S A* **94**, 11478-11483 (1997).

122. Checkley, M.A., Luttge, B.G. & Freed, E.O. HIV-1 envelope glycoprotein biosynthesis, trafficking, and incorporation. *J Mol Biol* **410**, 582-608 (2011).

123. Mitsuyasu, R.T. *et al.* Prolonged survival and tissue trafficking following adoptive transfer of CD4zeta gene-modified autologous CD4(+) and CD8(+) T cells in human immunodeficiency virus-infected subjects. *Blood* **96**, 785-793 (2000).

124. Haynes, B.F. *et al.* Immune-correlates analysis of an HIV-1 vaccine efficacy trial. *N Engl J Med* **366**, 1275-1286 (2012).

125. Ali, A. *et al.* HIV-1-Specific Chimeric Antigen Receptors Based on Broadly Neutralizing Antibodies. *J Virol* **90**, 6999-7006 (2016).

126. Grupp, S.A. *et al.* Chimeric antigen receptor-modified T cells for acute lymphoid leukemia. *N Engl J Med* **368**, 1509-1518 (2013).

127. Kalos, M. *et al.* T cells with chimeric antigen receptors have potent antitumor effects and can establish memory in patients with advanced leukemia. *Sci Transl Med* **3**, 95ra73 (2011).

128. Porter, D.L., Levine, B.L., Kalos, M., Bagg, A. & June, C.H. Chimeric antigen receptor-modified T cells in chronic lymphoid leukemia. *N Engl J Med* **365**, 725-733 (2011).

129. Jena, B., Dotti, G. & Cooper, L.J. Redirecting T-cell specificity by introducing a tumor-specific chimeric antigen receptor. *Blood* **116**, 1035-1044 (2010).

130. Chmielewski, M., Hombach, A.A. & Abken, H. Antigen-Specific T-Cell Activation Independently of the MHC: Chimeric Antigen Receptor-Redirected T Cells. *Front Immunol* **4**, 371 (2013).

131. Milone, M.C. *et al.* Chimeric receptors containing CD137 signal transduction domains mediate enhanced survival of T cells and increased antileukemic efficacy in vivo. *Mol Ther* **17**, 1453-1464 (2009).

132. Dorrell, L. *et al.* Cytotoxic T lymphocytes recognize structurally diverse, clade-specific and cross-reactive peptides in human immunodeficiency virus type-1 gag through HLA-B53. *Eur J Immunol* **31**, 1747-1756 (2001).

133. Gao, F. *et al.* Molecular characterization of a highly divergent HIV type 1 isolate obtained early in the AIDS epidemic from the Democratic Republic of Congo. *AIDS Res Hum Retroviruses* **17**, 1217-1222 (2001).

134. Horton, H. *et al.* Preservation of T cell proliferation restricted by protective HLA alleles is critical for immune control of HIV-1 infection. *J Immunol* **177**, 7406-7415 (2006).

135. Gillespie, G.M. *et al.* Cross-reactive cytotoxic T lymphocytes against a HIV-1 p24 epitope in slow progressors with B*57. *AIDS* **16**, 961-972 (2002).

136. Lecuroux, C. *et al.* Both HLA-B*57 and plasma HIV RNA levels contribute to the HIV-specific CD8+ T cell response in HIV controllers. *J Virol* **88**, 176-187 (2014).

137. Kim, A.Y. *et al.* Spontaneous control of HCV is associated with expression of HLA-B 57 and preservation of targeted epitopes. *Gastroenterology* **140**, 686-696 e681 (2011).

138. Elahi, S. & Horton, H. Association of HLA-alleles with the immune regulation of chronic viral infections. *Int J Biochem Cell Biol* **44**, 1361-1365 (2012).

139. Feng, B.J. *et al.* Multiple Loci within the major histocompatibility complex confer risk of psoriasis. *PLoS Genet* **5**, e1000606 (2009).

140. Monshi, M.M. *et al.* Human leukocyte antigen (HLA)-B*57:01-restricted activation of drug-specific T cells provides the immunological basis for flucloxacillin-induced liver injury. *Hepatology* **57**, 727-739 (2013).

141. Elahi, S. *et al.* Protective HIV-specific CD8+ T cells evade Treg cell suppression. *Nat Med* **17**, 989-995 (2011).

142. Xia, Z. *et al.* The complex and specific pMHC interactions with diverse HIV-1 TCR clonotypes reveal a structural basis for alterations in CTL function. *Sci Rep* **4**, 4087 (2014).

143. Pereyra, F. *et al.* Genetic and immunologic heterogeneity among persons who control HIV infection in the absence of therapy. *J Infect Dis* **197**, 563-571 (2008).

144. Stewart-Jones, G.B., McMichael, A.J., Bell, J.I., Stuart, D.I. & Jones, E.Y. A structural basis for immunodominant human T cell receptor recognition. *Nat Immunol* **4**, 657-663 (2003).

145. Otwinowski, Z. & Minor, W. Processing of X-ray diffraction data collected in oscillation mode. *Methods Enzymol* **276**, 307-326 (1997).

146. Southwood, S. *et al.* Several common HLA-DR types share largely overlapping peptide binding repertoires. *J Immunol* **160**, 3363-3373 (1998).

147. Ranasinghe, S. *et al.* Association of HLA-DRB1-restricted CD4(+) T cell responses with HIV immune control. *Nat Med* **19**, 930-933 (2013).

148. Ranasinghe, S. *et al.* HIV-specific CD4 T cell responses to different viral proteins have discordant associations with viral load and clinical outcome. *J Virol* **86**, 277-283 (2012).

149. Scriba, T.J. *et al.* Ultrasensitive detection and phenotyping of CD4+ T cells with optimized HLA class II tetramer staining. *J Immunol* **175**, 6334-6343 (2005).

150. van der Merwe, P.A. & Davis, S.J. Molecular interactions mediating T cell antigen recognition. *Annu Rev Immunol* **21**, 659-684 (2003).

151. Mason, D. Allelic exclusion of alpha chains in TCRs. *Int Immunol* **6**, 881-885 (1994).

152. Leisner, C. *et al.* One-pot, mix-and-read peptide-MHC tetramers. *PLoS One* **3**, e1678 (2008).

153. Trombetta, J.J. *et al.* Preparation of Single-Cell RNA-Seq Libraries for Next Generation Sequencing. *Curr Protoc Mol Biol* **107**, 4 22 21-17 (2014).

154. Bolger, A.M., Lohse, M. & Usadel, B. Trimmomatic: a flexible trimmer for Illumina sequence data. *Bioinformatics* **30**, 2114-2120 (2014).

155. White, J., Kappler, J. & Marrack, P. Production and characterization of T cell hybridomas. *Methods Mol Biol* **134**, 185-193 (2000).

156. Volkel, T., Korn, T., Bach, M., Muller, R. & Kontermann, R.E. Optimized linker sequences for the expression of monomeric and dimeric bispecific single-chain diabodies. *Protein Eng* **14**, 815-823 (2001).

157. Severino, M.E., Sarkis, P.T.N., Walker, B.D. & Yang, O.O. Chimeric immune receptor T cells bypass class I requirements and recognize multiple cell types relevant in HIV-1 infection. *Virology* **306**, 371-375 (2003).

158. Barrett, D.M., Singh, N., Porter, D.L., Grupp, S.A. & June, C.H. Chimeric antigen receptor therapy for cancer. *Annu Rev Med* **65**, 333-347 (2014).

159. Lam, S. & Bollard, C. T-cell therapies for HIV. *Immunotherapy* **5**, 407-414 (2013).

160. Ackerman, M.E. *et al.* Polyfunctional HIV-Specific Antibody Responses Are Associated with Spontaneous HIV Control. *PLoS Pathog* **12**, e1005315 (2016).

161. Chung, A.W. *et al.* Immune escape from HIV-specific antibody-dependent cellular cytotoxicity (ADCC) pressure. *Proc Natl Acad Sci U S A* **108**, 7505-7510 (2011).

162. Lambotte, O. *et al.* Heterogeneous neutralizing antibody and antibody-dependent cell cytotoxicity responses in HIV-1 elite controllers. *AIDS* **23**, 897-906 (2009).

163. Lambotte, O. *et al.* High antibody-dependent cellular cytotoxicity responses are correlated with strong CD8 T cell viral suppressive activity but not with B57 status in HIV-1 elite controllers. *PLoS One* **8**, e74855 (2013).

164. Deeks, S.G. *et al.* A phase II randomized study of HIV-specific T-cell gene therapy in subjects with undetectable plasma viremia on combination antiretroviral therapy. *Mol Ther* **5**, 788-797 (2002).

165. Jones, R.B. & Walker, B.D. HIV-specific CD8(+) T cells and HIV eradication. *J Clin Invest* **126**, 455-463 (2016).

166. Sahu, G.K. *et al.* Anti-HIV designer T cells progressively eradicate a latently infected cell line by sequentially inducing HIV reactivation then killing the newly gp120-positive cells. *Virology* **446**, 268-275 (2013).

167. Liu, L. *et al.* Novel CD4-Based Bispecific Chimeric Antigen Receptor Designed for Enhanced Anti-HIV Potency and Absence of HIV Entry Receptor Activity. *J Virol* **89**, 6685-6694 (2015).

168. Zhen, A. *et al.* HIV-specific Immunity Derived From Chimeric Antigen Receptor-engineered Stem Cells. *Mol Ther* **23**, 1358-1367 (2015).

169. Hale, M. *et al.* Engineering HIV-Resistant, Anti-HIV Chimeric Antigen Receptor T Cells. *Mol Ther* **25**, 570-579 (2017).

170. Liu, B. *et al.* Chimeric Antigen Receptor T Cells Guided by the Single-Chain Fv of a Broadly Neutralizing Antibody Specifically and Effectively Eradicate Virus Reactivated from Latency in CD4+ T Lymphocytes Isolated from HIV-1-Infected Individuals Receiving Suppressive Combined Antiretroviral Therapy. *J Virol* **90**, 9712-9724 (2016).

171. West, A.P., Jr., Galimidi, R.P., Gnanapragasam, P.N. & Bjorkman, P.J. Single-chain Fv-based anti-HIV proteins: potential and limitations. *J Virol* **86**, 195-202 (2012).

172. Falkowska, E. *et al.* PGV04, an HIV-1 gp120 CD4 binding site antibody, is broad and potent in neutralization but does not induce conformational changes characteristic of CD4. *J Virol* **86**, 4394-4403 (2012).

173. Tran, E.E. *et al.* Structural mechanism of trimeric HIV-1 envelope glycoprotein activation. *PLoS Pathog* **8**, e1002797 (2012).

174. Dropulic, B. Lentiviral vectors: their molecular design, safety, and use in laboratory and preclinical research. *Hum Gene Ther* **22**, 649-657 (2011).

175. Migueles, S.A. & Connors, M. Success and failure of the cellular immune response against HIV-1. *Nat Immunol* **16**, 563-570 (2015).

176. Kosmrlj, A. *et al.* Effects of thymic selection of the T-cell repertoire on HLA class I-associated control of HIV infection. *Nature* **465**, 350-354 (2010).

177. Yin, Y. & Mariuzza, R.A. The multiple mechanisms of T cell receptor cross-reactivity. *Immunity* **31**, 849-851 (2009).

178. Kloverpris, H.N. *et al.* HLA-specific intracellular epitope processing shapes an immunodominance pattern for HLA-B*57 that is distinct from HLA-B*58:01. *J Virol* **87**, 10889-10894 (2013).

179. Navis, M. *et al.* Viral replication capacity as a correlate of HLA B57/B5801-associated nonprogressive HIV-1 infection. *J Immunol* **179**, 3133-3143 (2007).

180. Mendoza, D. *et al.* HLA B*5701-positive long-term nonprogressors/elite controllers are not distinguished from progressors by the clonal composition of HIV-specific CD8+ T cells. *J Virol* **86**, 4014-4018 (2012).

181. Benati, D. *et al.* Public T cell receptors confer high-avidity CD4 responses to HIV controllers. *J Clin Invest* **126**, 2093-2108 (2016).

182. Schwartz, O., Marechal, V., Le Gall, S., Lemonnier, F. & Heard, J.M. Endocytosis of major histocompatibility complex class I molecules is induced by the HIV-1 Nef protein. *Nat Med* **2**, 338-342 (1996).

183. Flerin, N.C. *et al.* T-Cell Receptor (TCR) Clonotype-Specific Differences in Inhibitory Activity of HIV-1 Cytotoxic T-Cell Clones Is Not Mediated by TCR Alone. *J Virol* **91** (2017).

184. Bournazos, S. *et al.* Broadly neutralizing anti-HIV-1 antibodies require Fc effector functions for in vivo activity. *Cell* **158**, 1243-1253 (2014).

185. Barouch, D.H. *et al.* Therapeutic efficacy of potent neutralizing HIV-1-specific monoclonal antibodies in SHIV-infected rhesus monkeys. *Nature* **503**, 224-228 (2013).

186. Fuchs, S.P. *et al.* AAV-Delivered Antibody Mediates Significant Protective Effects against SIVmac239 Challenge in the Absence of Neutralizing Activity. *PLoS Pathog* **11**, e1005090 (2015).

187. Bar, K.J. *et al.* Effect of HIV Antibody VRC01 on Viral Rebound after Treatment Interruption. *N Engl J Med* **375**, 2037-2050 (2016).

188. Kwong, P.D. & Mascola, J.R. Human antibodies that neutralize HIV-1: identification, structures, and B cell ontogenies. *Immunity* **37**, 412-425 (2012).

189. Loskog, A. *et al.* Addition of the CD28 signaling domain to chimeric T-cell receptors enhances chimeric T-cell resistance to T regulatory cells. *Leukemia* **20**, 1819-1828 (2006).

190. Huang, J. *et al.* Broad and potent neutralization of HIV-1 by a gp41-specific human antibody. *Nature* **491**, 406-412 (2012).

191. Micklethwaite, K.P. *et al.* Derivation of human T lymphocytes from cord blood and peripheral blood with antiviral and antileukemic specificity from a single culture as protection against infection and relapse after stem cell transplantation. *Blood* **115**, 2695-2703 (2010).

192. Yee, C. & Greenberg, P. Modulating T-cell immunity to tumours: new strategies for monitoring T-cell responses. *Nat Rev Cancer* **2**, 409-419 (2002).

193. Hacein-Bey-Abina, S. *et al.* Insertional oncogenesis in 4 patients after retrovirus-mediated gene therapy of SCID-X1. *J Clin Invest* **118**, 3132-3142 (2008).

194. Scholler, J. *et al.* Decade-long safety and function of retroviral-modified chimeric antigen receptor T cells. *Sci Transl Med* **4**, 132ra153 (2012).

195. Di Stasi, A. *et al.* Inducible apoptosis as a safety switch for adoptive cell therapy. *N Engl J Med* **365**, 1673-1683 (2011).

196. Casucci, M. & Bondanza, A. Suicide gene therapy to increase the safety of chimeric antigen receptor-redirected T lymphocytes. *J Cancer* **2**, 378-382 (2011).

197. Straathof, K.C. *et al.* An inducible caspase 9 safety switch for T-cell therapy. *Blood* **105**, 4247-4254 (2005).

198. Chung, A.W. *et al.* Activation of NK cells by ADCC responses during early HIV infection. *Viral Immunol* **24**, 171-175 (2011).

199. McCoy, L.E. *et al.* Potent and broad neutralization of HIV-1 by a llama antibody elicited by immunization. *J Exp Med* **209**, 1091-1103 (2012).

200. Perreau, M. *et al.* Follicular helper T cells serve as the major CD4 T cell compartment for HIV-1 infection, replication, and production. *J Exp Med* **210**, 143-156 (2013).

201. Fukazawa, Y. *et al.* Lymph node T cell responses predict the efficacy of live attenuated SIV vaccines. *Nat Med* (2012).

202. Lindqvist, M. *et al.* Expansion of HIV-specific T follicular helper cells in chronic HIV infection. *J Clin Invest* **122**, 3271-3280 (2012).

203. Jones, R.B. *et al.* HERV-K-specific T cells eliminate diverse HIV-1/2 and SIV primary isolates. *J Clin Invest* **122**, 4473-4489 (2012).

204. Hermans, I.F. *et al.* The VITAL assay: a versatile fluorometric technique for assessing CTL- and NKT-mediated cytotoxicity against multiple targets in vitro and in vivo. *J Immunol Methods* **285**, 25-40 (2004).

205. Miura, T. *et al.* Genetic characterization of human immunodeficiency virus type 1 in elite controllers: lack of gross genetic defects or common amino acid changes. *J Virol* **82**, 8422-8430 (2008).

206. Henn, M.R. *et al.* Whole genome deep sequencing of HIV-1 reveals the impact of early minor variants upon immune recognition during acute infection. *PLoS Pathog* **8**, e1002529 (2012).

207. Trapnell, C., Pachter, L. & Salzberg, S.L. TopHat: discovering splice junctions with RNA-Seq. *Bioinformatics* **25**, 1105-1111 (2009).

208. Langmead, B. & Salzberg, S.L. Fast gapped-read alignment with Bowtie 2. *Nat Methods* **9**, 357-359 (2012).

209. Li, B. & Dewey, C.N. RSEM: accurate transcript quantification from RNA-Seq data with or without a reference genome. *BMC Bioinformatics* **12**, 323 (2011).

210. Bolstad, B.M. preprocessCore: A collection of pre-processing functions. R package version 1.32.0. (2011).

211. Crawford, F. *et al.* Use of baculovirus MHC/peptide display libraries to characterize T-cell receptor ligands. *Immunol Rev* **210**, 156-170 (2006).

212. Crawford, F., Kozono, H., White, J., Marrack, P. & Kappler, J. Detection of antigen-specific T cells with multivalent soluble class II MHC covalent peptide complexes. *Immunity* **8**, 675-682 (1998).

213. Dai, S. *et al.* Crossreactive T Cells spotlight the germline rules for alphabeta T cell-receptor interactions with MHC molecules. *Immunity* **28**, 324-334 (2008).

214. Tynan, F.E. *et al.* High resolution structures of highly bulged viral epitopes bound to major histocompatibility complex class I. Implications for T-cell receptor engagement and T-cell immunodominance. *J Biol Chem* **280**, 23900-23909 (2005).